

NON-EQUILIBRIUM DISSOCIATING
FLOWS OVER CURVED SURFACES

by

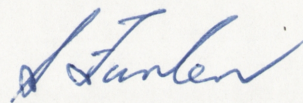
STUART MURRAY FURLER

Thesis submitted for the degree of
Master of Science
at the Australian National University

April 1973



The content of this thesis, except as described in the Acknowledgement, and where credit is indicated by a reference is entirely my own work.

A handwritten signature in blue ink, appearing to read 'S. Furler', with a stylized flourish at the end.

(Stuart Murray Furler)

Canberra.

CONTENTS

ACKNOWLEDGEMENT	iv
ABSTRACT	v
1. INTRODUCTION	1
2. THEORETICAL ANALYSIS	7
2.1 Basic equations	7
2.2 The constant pressure case	12
2.3 An order of magnitude approach and a discussion of the approximations made by Freeman	19
2.4 The case with a pressure gradient	21
2.5 Comparison of the expected behaviour with exact numerical computations	29
2.6 A condition that the recombination rate may be ignored	33
2.7 An application of results to a scaling problem	33
2.8 An application of results to a stand-off distance correlation	36
3. EXPERIMENT	38
3.1 Description of facility	38
3.2 Flow over a wedge with a sharp expansion corner	40
3.3 Flow over a curved wedge	41
3.4 Flow over a circular cylinder	43
3.4.1 A numerical investigation of streamline positions	43
3.4.2 Experimental results	45
4. CONCLUSION	48
5. REFERENCES	50

ACKNOWLEDGEMENT

I wish to express my appreciation for guidance and assistance given to me by Dr. H. G. Hornung, Dr. R. J. Stalker and Mr. R. P. French of the Australian National University, which has been invaluable in the execution and preparation of this work.

The experimental work to obtain interferograms of nitrogen flows over circular cylinders, which have been analysed in this thesis, was performed entirely by Dr. H. G. Hornung and Mr. R. P. French.

ABSTRACT

The problem considered was that of the behaviour of a non-equilibrium flow behind a shock wave supported by a convex curved body in a hypervelocity freestream. A simple gas model was assumed, taking into account the dissociation only of a symmetrical diatomic molecule, whilst the temperature in the shock layer was assumed to be small compared with the characteristic temperature of dissociation. The curvature of the streamlines produces a negative pressure gradient along a streamline and the effect of this pressure gradient upon the reaction was studied.

An approximate analytic solution was obtained, which shows that properties along a streamline are consistent with the assumption that the reaction proceeds independently of the pressure gradient initially, and after a short distance the gas may be considered non-reacting and the properties given by perfect gas relationships.

The result was verified both with exact numerical integration of the relevant equations, and with some experimental results from a hypervelocity nitrogen flow over a circular cylinder.

1. INTRODUCTION

In recent years attention has been paid to the flows of a real gas over aerodynamic bodies, (as distinct from treating the gas as obeying the perfect gas relationships). This has resulted from an interest in hypersonic flows of sufficient total enthalpy, such that the temperatures behind the shock waves caused by the body produce reactions (e.g. chemical, vibrational) in the gas. One may loosely define a "reaction time" as the time taken for a fluid element to effectively reach equilibrium, after a sudden change in its physical properties, such as would be caused by its passage through a shock. Also a characteristic flow time may be defined as the time such a fluid element remains in the vicinity of the body (i.e. a characteristic body scale divided by the fluid element velocity). If these two characteristic times are of the same order then the associated aerodynamic problem is known as a non-equilibrium flow problem, and the gas is said to relax along a streamline.

Of the real gas effects that are considered, chemical reactions may disturb the aerodynamic problem to the greatest extent. Research into non-equilibrium chemically reacting flows could be considered as divided into three related fields.

- (i) Experimental research to study the reactions of gases under controlled conditions in order to determine the laws by which a gas (or systems of gases) will relax. The work done by Appleton et al.⁵ to investigate nitrogen dissociation is an example of such work.
- (ii) Investigations of numerical methods required to compute the inviscid flowfield around an aerodynamic body, once a reliable gas model has been established. Hayes and Probstein¹ discuss numerical methods in considerable detail.
- (iii) Experimental research into flows over models in test facilities capable of producing the necessary high enthalpy freestream conditions in

order to verify the predictions of (i) and (ii). Such a facility has been described by Stalker⁷.

However such an idealized formal approach to the subject leaves much to be desired, particularly in regard to interpretation of computed results. That is, results of a numerical calculation involving many parameters, leaves one largely ignorant of the relative importance of each of the parameters, and also gives no physical insight into the problem being considered. For this reason, approaches which yield approximate results and are of limited applicability, but do provide a greater insight are sometimes to be preferred. Such an approximate method is that considered by Freeman² in his investigation of chemically reacting flows around blunt bodies. The gas model he used was the "ideal dissociating gas" introduced by Lighthill¹³. This model was obtained by putting to a constant value, the product of a temperature function and the partition functions in the law of mass action for a diatomic gas. This procedure was found to yield a good approximation when compared with computed values for the function. The model was derived for equilibrium conditions by Lighthill. It was extended by Freeman to include the non-equilibrium case, by the derivation, based largely on physical arguments, of a form for the forward and reverse dissociation rates. (The gas model has also been used by Capioux and Washington³ in their numerical calculations of reacting flows over straight wedges.)

Freeman's numerical scheme for the blunt body problem was based on the assumption that the ratio of the density in the shock layer to that in the freestream was large compared with unity. One important simplification that arises from this assumption is that the enthalpy along a streamline may be considered constant. This result is discussed further in section 2.3.

The problem that is considered herein is that of the behaviour of the non-equilibrium gas considered by Freeman in a two dimensional flow over a curved body in a hypervelocity freestream. Whereas Freeman obtained

a numerical method for solving the reacting flow in the vicinity of the stagnation region of a blunt body, the present analysis is more concerned with the flowfield considered over distances typical of the body scale, either for a curved wedge (with the angle of incidence decreasing as distance measured away from the tip); with an attached shock, or for blunt body flows away from the stagnation streamline. The approach taken was not one enabling a computation of the flowfield to be made, but rather that of an approximate analysis of flow properties along a streamline, giving a physical insight into the effect of various parameters upon such a flow. In particular the effect of a prescribed negative pressure gradient (i.e. pressure decreasing along a streamline away from the shock) was examined. Such a pressure gradient will tend to reduce the temperature of a fluid element as it moves along a streamline, and thus reduce the forward dissociation rate. The problem was studied in order to determine the consequences of this effect on the reaction.

This approach to the problem is valid because it has been found theoretically and experimentally that real gas effects alter the pressure distribution along a streamline to a small extent only, thus allowing a pressure distribution to be assumed. For example Lick¹⁵ has carried out numerical calculations using an inverse method of assuming a catenary shock shape and integrating to the body. The gas model assumed was that of a pure diatomic gas simulating a mixture of oxygen and nitrogen in the same ratio as atmospheric air. Temperatures considered in the shock layer were such that the only significant dissociation reaction was that of oxygen. The finite relaxation rates were found to have little affect on the pressure distributions obtained.

Spurk, Gerber and Sedney¹⁴ have investigated the inviscid hypersonic flowfields of a reacting mixture of gases around pointed bodies with attached shocks (wedges and cones of angle of attack in the range 30-45°) using the method of characteristics. They assumed a mixture of N_2 , O_2 , NO , N and O with vibrational excitation in local equilibrium, and found

that the variation in pressure along a streamline was small.

The experimental pressure distribution measured by Stalker⁷ on the surface of a re-entry glider model, was also found to be insensitive to real gas effects, and approximated closely a simple Newtonian pressure distribution.

That these results are reasonable may be seen from the following qualitative arguments (refer to figure A1). Freeman has shown that in the vicinity of the stagnation region the pressure distribution is given to a good approximation by the Newton-Buseman pressure law. This result depends only on the assumption that the density ratio across the shock is large, and is insensitive to details of the flow within the shock layer. As the angle of inclination of the shock to the freestream decreases, the approximation of large density ratio tends to break down, although it is still expected to influence the resultant pressure distribution. However one other effect is also operating. Most reaction rates (and in particular the rate considered here) are extremely temperature sensitive, and thus the initial rate of reaction behind a shock is extremely sensitive to the local inclination of the shock to the freestream. Consequently there will exist a so called "cut-off" streamline, along which the effects of the reaction are negligible over a distance comparable to the body scale. Streamlines entering the shock layer where the local angle of inclination of the shock is less than that of the cut-off streamline will also be non-reacting and the gas behaviour may be considered to be that of a perfect gas with composition frozen at the freestream value. Therefore under these circumstances the reacting streamlines are confined to a region close to the body. Referring again to figure A1 consider the determination of the pressure at the point A. Formally, the pressure at this point is determined from the pressure immediately behind the shock at point B and the application of the momentum equation (3) (section 2.1), where the integration is carried out along the path AB, which is the line normal to the streamlines passing through the point A. If the reacting streamlines lie close to the body then they will not radically alter the position of the shock or the non-reacting

shock layer geometry. Furthermore the reacting streamlines will play only a small part in the evaluation of the integral (3) and thus the total effect of the reaction on the pressure distribution along the reacting streamlines (and non-reacting streamlines) will be small. The effect of the reaction on the pressure distribution around the blunt bodies used in the experimental section of this work are examined numerically in section 3.4.1.

The theoretical analysis was carried out by firstly assuming a constant pressure distribution. Certain restrictions were placed on the magnitudes of terms arising from the Freeman rate equation enabling approximate analytic expressions to be obtained for flow parameters along a streamline. The form of these expressions was examined and it was found that they included a sudden displacement in the values of the flow parameters in a small region close to the shock, followed by a more gradual displacement over the remainder of the body scale. An order of magnitude analysis suggested that the sudden displacement near the shock would be unaffected by the presence of a pressure gradient. This result was then checked more rigorously with the assumption of a constant unit pressure gradient along the streamline. A solution to the problem was then postulated, including a short spatial regime behind the shock in which most of the reaction was confined and which was unaffected by the presence of a pressure gradient along the streamline. This was followed by a region in which reaction effects could be neglected, with the gas behaving as a perfect gas whose properties are influenced only by the presence of a pressure gradient. The model was then checked by comparing it with numerical solutions of the relevant equations to determine its accuracy and the limits of its applicability.

The model was also compared with the density distribution in the shock layer of aerodynamic models placed in a hypervelocity nitrogen freestream. It was found that with the experimental facility used (discussed in section 3.1) significant reaction effects were observed only with blunt body flows.

The gas model used in the analysis (the ideal dissociating gas) assumes that the vibrational energy of the molecule is half excited, whereas experimentally it would be more usual for vibrational states to be in equilibrium in the shock layer. The analysis was carried out retaining the vibrational half excitation, and relevant results for the equilibrium case are quoted where necessary. In general the difference in the value of flow parameters predicted under the two assumptions is small.

2. THEORETICAL ANALYSIS

2.1 Basic equations

The relevant two-dimensional equations of motion in the shock layer may be written as

$$\text{Continuity} \quad \frac{\partial(\rho'q')}{\partial x'} + \rho'q' \frac{\partial\theta}{\partial n'} = 0 \quad (1)$$

$$\text{Momentum} \quad \rho'q' \frac{\partial q'}{\partial x'} + \frac{\partial p'}{\partial x'} = 0 \quad (2)$$

$$\rho'q'^2 \frac{\partial\theta}{\partial x'} + \frac{\partial p'}{\partial n'} = 0, \quad (3)$$

where a primed variable is dimensioned and

ρ = density

p = pressure

q = velocity along a streamline

θ = inclination of streamline to the freestream

x = distance measured along a streamline

n = distance measured normal to a streamline.

The co-ordinate system is illustrated in figure A1.

The equation of conservation of energy can be written in several equivalent ways.

$$\rho' \left(\frac{Dh'}{Dt} \right) - \frac{Dp'}{Dt} = 0 \quad (4)$$

$$\frac{D}{Dt} \left(h' + \frac{q'^2}{2} \right) = 0, \quad (5)$$

where h = specific enthalpy

D/Dt = convective derivative.

The equations that are used in this analysis are (2), (4) and (5).

Considering first the ideal dissociating gas

$$e' = 3RT' + \alpha D,$$

- where e = specific internal energy
 R = gas constant defined as the universal gas constant divided by the molecular weight of the molecular species
 α = degree of dissociation defined as the mass of dissociated atoms divided by the total mass of the gas
 D = dissociation energy per unit mass.

Then the specific enthalpy is defined as

$$h' \equiv e' + p'/\rho' ,$$

i.e.
$$h' = (4 + \alpha)RT' + \alpha D . \quad (6)$$

For the case of vibrational excitation in equilibrium

$$e' = (3.5 - \alpha/2)RT' + \alpha D ,$$

and
$$h' = (4.5 + \alpha/2)RT' + \alpha D . \quad (7)$$

Equations (6) and (7) were obtained using the equation of state which may be written as

$$p' = \rho'RT'(1 + \alpha) . \quad (8)$$

(4) and (6) may be combined to yield

$$(4 + \alpha) \frac{d(RT')}{dx'} + (D + RT') \frac{d\alpha'}{dx'} - \frac{1}{\rho'} \frac{dp'}{dx'} = 0 . \quad (9)$$

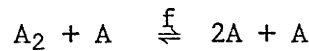
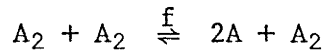
A chemical rate law applicable to this situation is taken as that given by Freeman²

$$\frac{d\alpha}{dt} = C T'^{\eta} \rho' \left\{ (1 - \alpha) \exp(-D/RT') - \frac{\rho'}{\rho_D} \alpha^2 \right\} , \quad (10)$$

- where ρ_D = constant
 C = constant
 η = constant.

A discussion of this reaction rate is given by Vincenti and Kruger⁴ (p.232).

The main approximation in expressing the reaction rate in this form lies in the assumption that C is a constant. In general there are two distinct reactions occurring



both of which have a forward reaction rate which may be expressed as

$$\left\{ \frac{d[A_2]}{dt} \right\}_f = -k_f [A_2] [M] ,$$

where M is the second body involved in the reaction (either A or A₂) and

$$k_f = C_f T^{n_f} \exp(-D/RT) .$$

Thus a more general expression for the forward rate would be

$$\left(\frac{d\alpha}{dt} \right)_f = \left\{ k_{f1} \alpha + k_{f2} \frac{1-\alpha}{2} \right\} \frac{\rho'}{M_A} (1-\alpha) ,$$

where subscript f refers to the forward rate and subscripts 1,2 refer to the reaction with A and A₂ as the second body respectively. M_A is the molecular weight of species A. Thus the approximation involved in (10) is that k_{f1} and k_{f2} have the same temperature dependence and that the expression in brackets { } in the last equation is independent of α.

Variables are non-dimensioned in the following manner, where unprimed variables are dimensionless

$$T = \frac{RT'}{U_\infty'^2 \epsilon} \quad q = \frac{q'}{U_\infty'}$$

$$\rho = \frac{\rho' \epsilon}{\rho_\infty'} \quad x = \frac{x'}{A}$$

$$p = \frac{p'}{\rho_\infty' U_\infty'^2} ,$$

where U_∞' = freestream velocity
 ϵ = density ratio across the shock = $\frac{\rho_\infty'}{\rho_0'}$
 A = typical body dimension.

Subscript ∞ refers to freestream conditions. Subscript 0 refers to conditions immediately behind the shock as given by the shock jump conditions before any dissociation takes place. The variables have been non-dimensional in this manner so that in general variables (except α) will be of order one behind the shock wave. Specifically for the hypersonic shock conditions,

$$p_0 \sim 0(\sin^2\phi)$$

$$T_0 \sim 0(\sin^2\phi)$$

$$\alpha_0 \equiv \alpha_\infty$$

$$\rho_0 \equiv 1$$

$$q_0 \sim 0(\cos\phi) ,$$

where ϕ is the angle of the shock to the freestream at which the streamline under consideration intersects the shock.

Equations (2), (9), (8) and (10) written in non-dimensional form become

$$\frac{d(\frac{1}{2}q^2)}{dx} = -\epsilon/\rho \frac{dp}{dx} \quad (11)$$

$$(4 + \alpha) \frac{dT}{dx} + \left[T + \frac{D}{U'^2 \epsilon} \right] \frac{d\alpha}{dx} - \frac{1}{\rho} \frac{dp}{dx} = 0 \quad (12)$$

$$p = \rho T(1 + \alpha) \quad (13)$$

$$\frac{d\alpha}{dx} = C \left(\frac{T_0 U_\infty'^2 \epsilon}{R} \right)^\eta \frac{\rho_\infty' A}{\epsilon q_0 U_\infty'} \rho \left(\frac{T}{T_0} \right)^\eta \frac{q_0}{q} \left\{ (1 - \alpha) \exp\left(\frac{-D}{U_\infty'^2 \epsilon T} \right) - \frac{\rho_\infty'}{\rho_D} \frac{\rho}{\epsilon} \alpha^2 \right\} . \quad (14)$$

Two groupings of constants which are used frequently are denoted as

$$a \equiv \frac{D}{U_\infty'^2 \epsilon}$$

$$\Lambda \equiv C \left(\frac{T_0 U_\infty'^2 \epsilon}{R} \right)^\eta \frac{\rho_\infty' A}{\epsilon q_0 U_\infty'} .$$

Equations (12) and (14) then become

$$(4 + \alpha) \frac{dT}{dx} + (T + a) \frac{d\alpha}{dx} - \frac{1}{\rho} \frac{dp}{dx} = 0 \quad (12a)$$

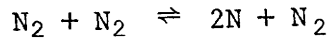
$$\frac{d\alpha}{dx} = \Lambda \rho \left(\frac{T}{T_0} \right)^\eta \frac{q_0}{q} \left\{ (1 - \alpha) \exp -a/T - \frac{\rho_\infty'}{\rho_D} \frac{\rho}{\varepsilon} \alpha^2 \right\} . \quad (14a)$$

The analysis is directed towards the behaviour of the solution to (12a), (14a) in a prescribed pressure gradient.

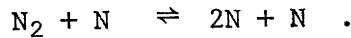
In order to simplify the problem to a state where it is manageable certain assumptions are made. These are

(i) $|\eta|$ is of order one (i.e. $(T/T_0)^\eta$ is not a rapidly varying function of T).

Experimentally the gas that will be considered is nitrogen. For nitrogen, Appleton et al.⁵ give $\eta = -1.6$. Vincenti and Kruger⁴ (p.231) have tabulated data on reaction rates and give $\eta = -0.5$ for the reaction



and $\eta = -1.5$ for the reaction



Furthermore Freeman has shown that variation in flow properties along a streamline is insensitive to the value of η , because of the domination of the exponential term in the rate equation.

For the remainder of the analysis η shall be put equal to zero. It will become evident that this restriction affects the behaviour of the solution to no greater extent than any of the approximations that are made at a later stage. The effect of a non-zero η will be examined numerically in section 2.5 and shown to be small.

(ii) The range of parameters is restricted such that

$$\Lambda \rho^2 \left(\frac{T}{T_0} \right)^\eta \frac{q_0}{q} \frac{\rho_\infty'}{\rho_D \varepsilon} \alpha^2 \ll 1$$

over the range of interest.

That is, the recombination term in the reaction rate equation (14a) is neglected. This is essentially a restriction on the freestream density (and hence the density in the shock layer) requiring it to be low enough so that, over the body dimension, three-body reactions (recombination) have a negligible effect on the gas composition, the only significant variation being due to two-body reactions (dissociation). A sufficient condition that this is the case is derived in section 2.6.

(iii) The parameter $a \equiv D/U_\infty^2 \epsilon$ is required to be large compared to one. It should be noted that

$$\frac{D}{RT'_0} \equiv \frac{a}{T_0},$$

and since T_0 is defined as being of order one, this requirement is that

$D/RT'_0 \gg 1$ (i.e. the thermal energy of the flow is small compared with the dissociation energy). In general the parameter $\epsilon \equiv \rho'_\infty/\rho'_0$ for hypersonic shock conditions is small so that the requirement could also be written as

$$D/(U'_\infty)^2 \geq 0(1).$$

2.2 The constant pressure case

The approach that will be taken is to obtain an approximate solution for (12a), (14a) for the case of constant pressure along a streamline and then to examine the effect of a non-zero pressure gradient on this solution.

Equation (11) yields the result

$$\frac{q_0}{q} \equiv 1.$$

Therefore with the assumptions already made (14a), (12a) may be written

$$\frac{d\alpha_h}{dx} = \Lambda \rho (1 - \alpha) \exp\left(-\frac{a}{T_h}\right),$$

$$\frac{d\alpha_h}{dT_h} = -\frac{4 + \alpha_h}{T_h + a},$$

where subscript h refers to the value of the variable when the specific enthalpy is assumed to be constant (i.e. $dp/dx = 0$).

Hence

$$x = \int_{T_0}^{T_h} \frac{-(4 + \alpha_h) \exp(a/T_h)}{(T_h + a) \Lambda \rho (1 - \alpha)} dT_h.$$

Or, defining a variable $u \equiv a/T_h$, the integral may be expressed as

$$x = \int_{u_0}^u \frac{(4 + \alpha_h) a}{(T_h + a) \Lambda \rho_h (1 - \alpha_h)} \frac{1}{u^2} \exp u du, \quad (15)$$

where the condition $a/T_0 \gg 1$ implies $u_0 \gg 1$ and the effect of the reaction is to decrease T so that $u(x) \gg 1$.

Integrals of the form $\int f(u) \exp u du$ with the condition $u \gg 1$ are examined in order to obtain an approximate solution to equation (15). The integral may be successively integrated by parts to yield the series

$$\int f(u) \exp(u) du = \exp(u) \{f(u) - f'(u) + f''(u) \dots\}.$$

The series may under some circumstances be only semiconvergent, but in general the condition

$$|f'(u)| \ll |f(u)|$$

will enable the approximation

$$\int f(u) \exp(u) du \approx f(u) \exp(u)$$

to be made. That is for 'u' large and for $f(u)$ a slowly varying function of u the exponential term dominates the variation of the whole function. (It is for this reason that putting $\eta = 0$ in equation (14a) has little effect.) As an example of the procedure

$$\int \frac{e^u}{u^2} du = e^u \left\{ \frac{1}{u^2} + \frac{2!}{u^3} + \frac{3!}{u^4} + \dots \right\}$$

i.e.
$$\int \frac{e^u}{u^2} du \approx \frac{e^u}{u^2},$$

with a relative error of $2!/u$.

Similar expressions may be derived for integrals of the form $\int e^u/u$ du and $\int e^u/u^3$ du.

The degree to which the pre-exponential term in equation (15) satisfies the requirement which allows the approximation to be made is discussed below. It will be noted that the relevant condition

$$|f'(u)| \ll |f(u)|$$

may be written

$$\left| \frac{d}{du} \ln f(u) \right| \ll 1$$

and hence if $f(u)$ is a product of terms then the terms of the product may be examined individually.

The variation in the term $\rho_h(1-\alpha_h)$ with temperature may be written (from equations (8) and (12a) as

$$\frac{d}{dT_h} \{\rho_h(1-\alpha_h)\} = p \cdot \left\{ \frac{(4+\alpha_h)}{(T_h+a)} \cdot \frac{2}{(1+\alpha_h)^2} - \frac{1}{T_h^2} \frac{(1-\alpha_h)}{(1+\alpha_h)} \right\}$$

With typical values of the variables the last term in this expression is of order one. The magnitude of the first term depends on the magnitude of the parameter 'a', but with the condition that has been imposed of $a \gg 1$, it will be assumed that it is less than order one. The two terms in the above expression tend to cancel, and if a term $n(T_h)$ is introduced such that $n(T_h) \leq 0(1)$ then,

$$\frac{d}{dT_h} \{\rho_h(1-\alpha_h)\} = -n(T_h)$$

and
$$\frac{d}{du} \{\rho_h(1-\alpha_h)\} = n(T_h) T_h^2/a$$

Since
$$\rho_h(1-\alpha_h) \sim 0(1)$$

then
$$-\frac{d}{du} \ln\{\rho_h(1-\alpha_h)\} \sim 0(n(T_h) \cdot T_h^2/a)$$

Regarding the remaining terms one may write

$$\frac{d}{du} \ln(u^{-2}) = -2/u$$

$$\frac{d}{du} \ln(4 + \alpha_h) = \frac{T_h^2}{a} \frac{1}{(T_h + a)}$$

$$\frac{d}{du} \ln(T_h + a) = -\frac{T_h^2}{a} \frac{1}{(T_h + a)}$$

Hence for the pre-exponential factor $f(u)$ in equation (15)

$$-\frac{d}{du} \ln f(u) \sim 0(2/a) \ll 1$$

from the condition $a \gg 1$.

Thus equation (15) may be approximated to

$$x = \frac{(4 + \alpha_h) \times a}{(T_h + a) \Lambda \rho_h (1 - \alpha_h)} \frac{1}{u^2} \exp u \Bigg|_{u_0}^u \quad (16)$$

This may be inverted to yield

$$a/T_h - \ln G(x)/G(o) = \ln\{\exp(a/T_o) + x G(o)\} \quad (17)$$

Where

$$G(x) = \frac{a}{T_h^2} \frac{(T_h + a)}{(4 + \alpha_h)} \Lambda \rho_h (1 - \alpha_h)$$

(For the case of equilibrium vibration

$$G(x) = \frac{a}{T_h^2} \frac{(T_h + a)}{(4.5 + \alpha_h/2)} \Lambda \rho_h (1 - \alpha_h) \quad .)$$

The relative magnitudes of the two terms on the L.H.S. of equation (17) are considered by the introduction of the function $R(T_h)$ defined as

$$R = \frac{T_h}{a} \ln G(x)/G(o)$$

The function is examined over the range $T_o \leq T < 0$. It is seen that $|R|$ has a maximum value when

$$R = -\frac{T_{hm}^2}{a} \left(\frac{d}{dT_h} \ln G(x[T_h]) \right)_{T_h=T_{hm}}$$

Where T_{hm} is the solution to the equation

$$\ln\{G(x[T_h])/G(o)\} + T_h \frac{d}{dT_h} \ln G(x[T_h]) = 0$$

An order of magnitude analysis, almost identical to that carried out for $f(u)$ in relation to equation (15) shows that

$$-\frac{d}{dT_h} \ln G(x[T_h]) \sim 0(2)$$

and thus from the condition $a \gg 1$, $|R(T_h)| \ll 1$ in the range $T_o \leq T_h < 0$.

(This procedure could perhaps be better understood by considering a specific simple temperature dependence for G . Assume that the variation with T_h in the terms $\rho_h(1-\alpha_h)(T_h+a)/(4+\alpha_h)$ cancel to a large extent, and consider a temperature dependence of G as

$$G \propto T^{-s} \quad \text{where } s \sim 0(2). \text{ Then}$$

$$R = \{s T_h \ln(T_o/T_h)\}/a$$

Examination of this function yields the result that $|R|$ has a maximum value of

$$|R| = \frac{s T_o}{a \exp(1)}$$

which occurs when $T_h = T_o/\exp(1)$.

Consequently the second term in the L.H.S. of equation (17) is small compared with the first and may be ignored with only a small

error introduced. Thus (17) may be written as

$$T_h \approx \frac{a}{\ln\{\exp a/T_0 + G(0)x\}} \quad (17a)$$

(It will be noted that the approximation made here is that of putting

$$G(x) \approx G(0) \quad).$$

α_h can be calculated approximately from the condition of constant enthalpy which may be written as

$$\frac{T_h + a}{T_0 + a} = \frac{4 + \alpha_0}{4 + \alpha_h} \quad (18)$$

For the conditions $T_0 \ll a$ and $(\alpha_h - \alpha_0) \ll 4$ a useful approximation to (18) is

$$(\alpha_h - \alpha_0) = \frac{4 + \alpha_0}{T_0 + a} (T_0 - T_h) \quad (18a)$$

For equilibrium vibration the equations corresponding to (18) and (18a) are

$$\frac{T_h + a}{T_0 + a} = \frac{4.5 + \alpha_0/2}{4.5 + \alpha_h/2}$$

and

$$(\alpha_h - \alpha_0) = \frac{4.5 + \alpha_0/2}{T_0 + a} (T_0 - T_h) .$$

The density distribution may be determined from the equation of state (13).

It should be noted however that the approximation leading to (17a) although expected to give a good approximation for $T_h(x)$ and $\alpha_h(x)$ will give only the order of magnitude for terms of the form $dT_h(x)/dx$ and $d\alpha_h(x)/dx$ since (16) may be written

$$\left(\frac{d\alpha_h}{dx}\right)^{-1} = \frac{a(T_h + a)}{(4 + \alpha_h) T_h} \cdot \left\{ x + \frac{(4 + \alpha_0) T_0^2}{(T_0 + a) a} \left(\frac{d\alpha_h}{dx}\right)^{-1}_{x=0} \right\} .$$

Here it is obvious that putting terms equal to their initial values will introduce errors in the last term of the above equation as a factor of

order $(T_0/T_h)^2$. Nevertheless it is useful to write this equation as

$$\left(\frac{d\alpha_h}{dx}\right)^{-1} \sim 0 \left\{ \left(\frac{d\alpha_h}{dx}\right)^{-1}_{x=0} + x \frac{(T_0+a)}{(4+\alpha_0)} \frac{a}{T_0^2} \right\} \quad (19)$$

and consequently

$$\left(\frac{dT_h}{dx}\right)^{-1} \sim 0 \left\{ \left(\frac{dT_h}{dx}\right)^{-1}_{x=0} - x \frac{a}{T_0^2} \right\} \quad (20)$$

It is useful to consider the form of the solution so far obtained. (17a) can be written

$$\frac{T_h}{T_0} = \left[1 + \frac{T_0}{a} \ln \left\{ 1 + \frac{a}{T_0^2} \left| \frac{dT}{dx} \right|_0 x \right\} \right]^{-1} \quad (17b)$$

If $|dT/dx|_0 \ll 1$ then it is obvious that the variation of T_h in the range $0 < x < 1$ is small. If $|dT/dx|_0 \sim 0(1)$ then

$$\left(\frac{T_h}{T_0}\right)_{x=1} \sim 0 \left\{ 1 + \frac{T_0}{a} \ln \frac{a}{T_0} - \frac{T_0}{a} \ln(T_0) \right\}^{-1}$$

Since $T_0/a \ll 1$ the last term in this expression is small. The condition that the variation in T_h is small compared with one in the range $0 < x < 1$ can therefore be written as

$$\frac{a}{T_0} \gg \ln \left(\frac{a}{T_0} \right)$$

This condition is only slightly more stringent than the condition $a/T_0 \gg 1$ and the former will be assumed to be included in the latter.

It should also be remembered that no special emphasis is placed on the conditions behind the shock and any other initial conditions would suffice as starting values for the integration. In particular (20) shows that for $x > \frac{T_0^2}{a}$, $|dT_h/dx| \lesssim 1$ and hence if the conditions at $x = \frac{T_0^2}{a}$ were used to start the integration then the variation in T_h over the remainder of the body scale would be small.

Thus with the assumptions that have been made the following conclusion may be drawn. If any variation in temperature due to the reaction is to occur then the larger part of that variation will occur

before $x \sim 0(T_0^2/a)$ and the variation of temperature over the remaining body scale will be small. Equations (18), (13) show that the same will be true of α and the density. That is, since the pressure is constant, then for $x \geq T_0^2/a$, the gas is behaving approximately as a perfect gas except that the flow starts from values which are different from those given by the conditions behind the shock. (An assumption of equilibrium vibration does not alter this basic property.)

The remainder of the analysis will be directed towards determining whether this behaviour persists in the presence of a pressure gradient.

2.3 An order of magnitude approach and a discussion of the approximations made by Freeman

The basic approximation made by Freeman² was that of constant enthalpy along a streamline even in the presence of a pressure gradient. This result was derived by Freeman from an order of magnitude analysis of equation (4) which may be written

$$\frac{\partial h'}{\partial x'} - \frac{1}{\rho'} \frac{\partial p'}{\partial x'} = 0 \quad (4)$$

Considering the magnitude of the terms in this equation from shock relations, they can be written

$$h' \sim O(U_\infty'^2) \quad , \quad \rho' \sim (\rho_\infty'/\epsilon) \quad , \quad p' \sim O(\rho_\infty' U_\infty'^2)$$

Thus

$$\frac{1}{\rho'} \frac{\partial p'}{\partial x'} \bigg/ \frac{\partial h'}{\partial x'} \sim O(\epsilon)$$

Freeman considered the case $\epsilon \ll 1$ and made the approximation

$\partial h'/\partial x' \approx 0$. (i.e. the effect of the pressure gradient on the reaction was ignored.) Thus the approximate solutions obtained for T and α assuming zero pressure gradient would also suffice as approximate solutions for the Freeman constant enthalpy case. The density could then be calculated from the equation of state with an assumed pressure distribution. The main objection that can be brought against this analysis when considering the flow along a streamline, where the pressure

can vary considerably, is that the temperature distribution is determined solely by the effect of the reaction, and ignores the effect of the pressure gradient.

Consider equation (12a)

$$(4 + \alpha) \frac{dT}{dx} + (T + a) \frac{d\alpha}{dx} - \frac{1}{\rho} \frac{dp}{dx} = 0 \quad (12a)$$

and confine the discussion to cases where $dp/dx \leq 0(1)$. This is a reasonable assumption to make for a smooth body since the pressure may only vary from one to zero over a body scale. Thus the last term in equation (12a) is of order one. Ignoring this last term is a good approximation provided $d\alpha/dx (T + a) \gg 1$. But it has already been shown that the effects of a reaction (for the gas considered) are confined to a small region close to the shock, and if a situation is reached where $(T + a) d\alpha/dx \ll 1$ then it is this term that can be ignored and the temperature distribution will be determined predominately by the pressure distribution. (There will also exist a region where $(T + a) d\alpha/dx \sim 0(1)$ and in these circumstances all three terms in (12a) are important.)

Thus the expected behaviour of properties along a streamline would be an initial rapid change due to the reaction followed by a slower variation in density and pressure due to the pressure distribution. The question must now be asked as to whether the values which the flow properties assume at the end of the reaction zone, as calculated with no pressure gradient, are effected by the pressure gradient. It has already been shown for the constant pressure case that if $|d\alpha/dx|_0, |dT/dx|_0 \sim 0(1)$ then no significant change occurs in flow properties, and therefore if $|d\alpha/dx|_0, |dT/dx|_0 \gg 1$ then by the time the pressure gradient in (12a) is important no further significant variation of flow parameters due to the reaction would have occurred, even in the absence of the pressure gradient. This would imply that α would rise to a 'plateau' level which is unaffected by the pressure distribution (except in the case where the variation of α would be small anyway) and the temperature would continue to fall due to the pressure gradient.

However this sort of analysis ignores one important feature. That is that at all times there are two factors tending to reduce the temperature; the reaction and the pressure gradient, and the approximate solution for flow variables ignoring the pressure gradient was only obtained by using the fact that the reaction rate considered was extremely sensitive to temperature. (This is the assumption $a/T_0 \gg 1$.) Thus, although the qualitative behaviour of parameters (reaction dominated behaviour over a short distance followed by freezing of the reaction and perfect gas behaviour) is still expected to hold, an order of magnitude analysis as given above may not be sufficiently precise to define the frozen-flow levels.

It is the purpose of the next section to show that conclusions reached with such an analysis are valid. Rather than use the order of magnitude results (19), (20) more exact forms for the variation of parameter gradients must be considered.

2.4 The case with a pressure gradient

A brief description of what shall be attempted in this section is in order. The flow variables are considered as a constant enthalpy term and a correction term. A solution for the correction term is obtained when this term is small. This solution is then used to set up differential equations for the correction, which may be applied over a more general range. These are integrated, and the behaviour of these functions are compared with the expected behaviour of the general solutions, which have been discussed in the previous section.

Consider equations (16) and (12a)

$$\frac{(4 + \alpha_h) T_h^2}{(T_h + a) \Lambda \rho_h (1 - \alpha_h) a} \exp \left[\frac{a}{T_h} \right]_{a/T_0}^{a/T_h} = x \quad (16)$$

$$(4 + \alpha) \frac{dT}{dx} + (T + a) \frac{d\alpha}{dx} - \frac{1}{\rho} \frac{dp}{dx} = 0 \quad (12a)$$

Equation (16) is considered to be a better starting point than the further approximated (17a). A specific form of pressure gradient will be chosen. For simplicity the case $dp/dx = -1$ is considered. This is the largest average pressure gradient that can be sustained over a body length and it is expected that results obtained using such a simple gradient will shed light on the effect of more general pressure gradients encountered along streamlines over a smooth body.

The physical properties of the gas are considered as the sum of two terms, a constant-enthalpy term and a term due to the action of the pressure gradient.

Variables with subscript p are defined as

$$T \equiv T_h + T_p \quad \alpha \equiv \alpha_h + \alpha_p$$

Initially the conditions are imposed that $T_p \ll T_h$ and $\alpha_p \ll \alpha_h$.

Thus from (12a)

$$(4 + \alpha) \frac{dT_h}{dx} + (T + a) \frac{d\alpha_h}{dx} = 0 \quad , \quad (21)$$

$$(4 + \alpha) \frac{dT_p}{dx} + (T + a) \frac{d\alpha_p}{dx} + \frac{1}{\rho} = 0 \quad (22)$$

and

$$\begin{aligned} \frac{d\alpha_p}{dx} &= \frac{d\alpha}{dx} - \frac{d\alpha_h}{dx} \\ &= \Lambda\rho(1 - \alpha) \left\{ \exp\left[-\frac{a}{T_p + T_h}\right] - \exp\left[-\frac{a}{T_h}\right] \right\} \end{aligned}$$

which for $T_p \ll T_h$ implies

$$\frac{d\alpha_p}{dx} = \frac{d\alpha_h}{dx} \left\{ \frac{aT_p}{T_h^2} \right\}$$

Thus from (22)

$$\frac{dT_p}{dx} + \left\{ \frac{(T + a)}{(4 + \alpha)} \frac{a}{T_h^2} \frac{d\alpha_h}{dx} \right\} T_p = -\frac{1}{(4 + \alpha)\rho}$$

Thus, using $d\alpha_h = -(4 + \alpha)/(T + a) dT_h$, the formal solution to the above first order differential equation becomes

$$T_p = - \exp\left(-\frac{a}{T_h}\right) \int_0^x \frac{1}{(4 + \alpha)} \frac{1}{\rho} \exp\left(\frac{a}{T_h}\right) dx \quad (23)$$

Then, using $d\alpha_h/dx = \Lambda\rho(1 - \alpha) \exp(-a/T_h)$, (23) can be written

$$T_p = \exp\left(-\frac{a}{T_h}\right) \int_{T_0}^{T_h} \frac{\exp(2a/T_h)}{(T + a) \Lambda(1 - \alpha) \rho^2} dT_h$$

The integral involved in this relation is of the same form as those considered previously for the constant pressure case. Thus it can be written approximately as

$$T_p = - \exp\left(-\frac{a}{T_h}\right) \left[\frac{1}{2} \frac{T_h^2}{\rho^2} \frac{\exp(2a/T_h)}{a(T + a) \Lambda(1 - \alpha)} \right]_{T_0}^{T_h}$$

provided that $(T + a)(1 - \alpha)\rho^2$ is a slowly varying function of T_h compared with the exponential.

Since the condition $T_p \ll T_h$ has been specified the variation in terms like T_h^2 are small compared with the variation in $\exp(2a/T_h)$ and the above equation may be written

$$T_p = -\frac{1}{2} \cdot \frac{T_h^2}{\rho^2} \frac{1}{a(T + a) \Lambda(1 - \alpha)} \frac{\{(\exp a/T_h)^2 - (\exp(a/T_0))^2\}}{\exp a/T_h} \quad (24)$$

Equation (24) gives the deviation of the temperature from the constant enthalpy solution when this deviation is small. When this is the case all variables in (24) could be put equal to their constant enthalpy values.

It is the purpose of the following to use (24) as a basis for the behaviour of T_p when T_p is not small. Initially however the condition $T_p \ll T_h$ is retained. A change in notation is useful.

A small constant δ is chosen and the point at which

$$T_p = -(\delta/a) T_h^2 \quad (25)$$

is investigated. For this point equation (24) gives

$$\frac{(\exp a/T_h)^2 - (\exp a/T_0)^2}{\exp a/T_h} = 2(T+a) \Lambda \rho^2 (1-\alpha) \delta \quad (26)$$

A variable ζ_h is defined as

$$\zeta_h \equiv \frac{\exp(a/T_h)}{(T+a) \Lambda \rho^2 (1-\alpha)} \quad (27)$$

Then (26) is quadratic in ζ_h and has solution

$$\zeta_h = \delta + \sqrt{\delta^2 + \zeta_0^2} \quad (28)$$

Where

$$\zeta_0 = (\zeta_h)_{x=0}$$

The significance of this equation is as follows. If an initial value of ζ_h is chosen then (28) is a relationship between the departure of the solution due to the pressure gradient and the solution where pressure gradient terms are neglected.

A variable similar to ζ_h may be defined as

$$\zeta \equiv \frac{\exp a/T}{(T+a) \Lambda \rho^2 (1-\alpha)} \quad (29)$$

where from (25)

$$\zeta = \zeta_h \exp \delta \quad (30)$$

The constant enthalpy case has been dealt with previously and (16) may be written as

$$\zeta_h = \zeta_0 + \chi(x) \quad (31)$$

where

$$\chi = \frac{x}{\rho} \frac{a}{T^2} \frac{1}{(4+\alpha)}$$

Consider the following scheme. Behind the shock all variables are known from the shock conditions. Then a value of δ is chosen such that it satisfies the condition $T_p \ll T_0$ through equation (25). A point (1) may then be defined where (28) is satisfied, i.e.

$$(\zeta_h)_1 = \delta + \sqrt{\delta^2 + \zeta_0^2} \quad , \quad (32)$$

and at this point

$$\zeta_1 = (\zeta_h)_1 \exp \delta \quad . \quad (33)$$

However there is nothing unique about the conditions behind the shock. The conditions at point (1) could be used in conjunction with (18) to find a point (2). In principle this local linearization process could be repeated indefinitely.

That is, for a given δ , between two such points equation (31) holds for the constant enthalpy solution between those points, and when (28) is satisfied, the departure from the constant enthalpy solution during this step is given by (30). Consider the behaviour between the points (i) and (i+1).

$$(\zeta_h)_{i+1} = \delta + \sqrt{\delta^2 + \zeta_i^2}$$

and

$$(\zeta_h)_{i+1} = \zeta_i + \chi \Big|_i^{i+1} .$$

Thus

$$\chi \Big|_i^{i+1} = \delta + \sqrt{\delta^2 + \zeta_i^2} - \zeta_i .$$

Also

$$\zeta = (\zeta_h) \exp \delta ,$$

so that

$$\zeta_{i+1} = \{\delta + \sqrt{\delta^2 + \zeta_i^2}\} \exp \delta ;$$

i.e.

$$\chi \Big|_i^{i+1} = \frac{\{\delta + \sqrt{\delta^2 + \zeta_i^2}\} \exp \delta - \zeta_i}{\delta + \sqrt{\delta^2 + \zeta_i^2} - \zeta_i} ,$$

and

$$\begin{aligned} \frac{d\zeta}{d\chi} &= \lim_{\delta \rightarrow 0} \frac{\{\delta + \sqrt{\delta^2 + \zeta^2}\} \exp \delta - \zeta}{\delta + \sqrt{\delta^2 + \zeta^2} - \zeta} \\ &= 1 + \zeta . \end{aligned}$$

This may be integrated to yield

$$\ln \left\{ \frac{1+\zeta}{1+\zeta_0} \right\} = \chi \quad (34)$$

It is this expression which will be used to determine the behaviour of the gas properties when the reaction has slowed down sufficiently for it to be ignored. From the definition of ζ , equation (29), it can be seen that as $d\alpha/dx \rightarrow 0$ then $\zeta \rightarrow \infty$.

Equation (34) is written with the condition $\zeta \gg 1$,

$$\frac{\exp a/T}{(T+a) \Lambda \rho^2 (1-\alpha)} = (1+\zeta_0) \exp \chi,$$

or

$$\frac{a}{T} = \ln(T+a) \Lambda \rho^2 (1+\zeta_0) + \frac{x}{\rho} \frac{a}{T^2} \frac{1}{(4+\alpha)},$$

or in terms of the pressure

$$\frac{a}{T} \left\{ 1 - \frac{x}{p} \frac{(1+\alpha)}{(4+\alpha)} \right\} = \ln(T+a) \Lambda \rho^2 (1-\alpha) (1+\zeta_0) \quad (35)$$

The variation of the log function is small compared with itself, since the argument is large so that variables included in this function may be put equal to their initial values. (A more rigorous derivation of this result can be obtained by a method similar to that in which the approximation $G(x) = G(0)$ was made in section 2.2). Putting $p = p_0 - x$ and expanding in terms of x (35) may be written as

$$T = \frac{\frac{a}{p_0} \left\{ p_0 - x \frac{(1+\alpha)}{4+\alpha} + 0(x^2) \dots \right\}}{\ln(T_0+a) \Lambda (1-\alpha_0) (1+\zeta_0)}$$

But for a non-reacting gas,

$$T = T_f \left(\frac{p}{p_f} \right)^{(1+\alpha/4+\alpha)},$$

where subscript f refers to a reference condition. This result is obtained from equation (12a), with $d\alpha/dx = 0$, and the equation of state (13).

This may also be written for the case of a negative unit pressure gradient as

$$T = \frac{T_f}{P_0} \left(\frac{P_0}{P_f} \right)^{(1+\alpha/4+\alpha)} \left\{ P_0 - \frac{(1+\alpha)}{(4+\alpha)} x + O(x^2) + \dots \right\}.$$

It should be noted that the third and subsequent terms in the above two expressions are not equal. However, considering the approximate nature of (35) an agreement in the first order of x is considered significant.

These two expressions are in agreement to the first order of x if

$$T_f \left(\frac{P_0}{P_f} \right)^{(1+\alpha/4+\alpha)} = \frac{a}{\ln(T_0 + a) \Lambda(1 - \alpha_0)(1 + \zeta_0)}$$

If the conditions denoted by subscript (f) are chosen at $x = 0$, then

$$T_f = \frac{a}{\ln(T_0 + a) \Lambda(1 - \alpha_0)(1 + \zeta_0)} \quad (36)$$

From the definition of ζ , equation (29), this may also be written as

$$T_f = \frac{a}{\ln\{(T_0 + a) \Lambda(1 - \alpha_0) + \exp a/T_0\}}$$

which may be compared with equation (17a). It is seen that T_f corresponds to the constant enthalpy solution at $x \sim (4 + \alpha_0) T_0^2/a$. This is well within the 'plateau' region of the constant pressure solution and thus it could be assumed that the effect of a unit pressure gradient does not alter the height of the plateau despite the extreme sensitivity of the reaction rate to temperature. (In fact it is a consequence of it, since putting the log. expression in (35) equal to its initial value can only be justified if $\ln \Lambda \gg 1$, i.e. $a/T_0 \gg 1$.)

Corresponding to T_f , there exists an α_f given by (18) which is also characteristic of the 'plateau level' obtained in the absence of a pressure gradient.

The following characteristics of the complete solution are therefore postulated:

(i) In the region $0 < x \leq T_0^2/a$ the physical parameters of the gas

are essentially not effected by a pressure gradient and behave in a manner given approximately by equation (17a) and equations derived from it.

(ii) In the region $x \geq T_0^2/a$ the solution will tend to a perfect gas behaviour, as the pressure gradient causes the temperature to drop, thus inhibiting further reaction. In this region α will be nearly constant and given by (18), (36). The behaviour of temperature and density will tend to a perfect gas solution with initial values at $x = 0$ approximated by (36), (18) and the equation of state (13). It is expected that this asymptotic behaviour will be approached quickly (due to the falling temperature stopping any remnant of the reaction) so that in the major portion of the region $T_0^2/a \leq x \leq 1$ the flow will essentially follow perfect gas behaviour.

It is also expected that this behaviour is not dependent upon the form of the pressure gradient assumed, and that in the presence of any pressure gradient for a smooth body of approximately constant curvature, the behaviour just described will be retained.

Two further points also need discussing at this stage.

(i) The parameter Λ found in (36) contains a characteristic length A over which the streamline is examined. In the case of a defined unit pressure gradient therefore, there exists an implied relationship between A and the dimensioned pressure gradient. Therefore, strictly, (36) holds only for a constant pressure gradient where A is defined as the inverse of such a gradient. It should, however, be pointed out that T_f as defined by (36) is extremely insensitive to the value of Λ so that for practical purposes any obvious characteristic body scale would suffice to define Λ .

(ii) The existence of a 'plateau' in the zero pressure gradient solution is essential to the postulated scheme outlined above. There is, however, a case when this feature does not occur, i.e. when $(d\alpha/dx)_0$ is of order one. Under these circumstances there is no rapid change in $d\alpha_h/dx$ and

dT_h/dx as a function of x , and in the presence of a pressure gradient all terms in equation (12a) are equally important. Therefore the resulting solution will depend upon the form of the pressure gradient. However, it has already been shown that in these circumstances $(\alpha_h - \alpha_0)$ is small and $T_h/T_0 \approx 1$ over a body scale. Therefore T_f , ρ_f and α_f defined from (36) would be sufficiently accurate to enable the perfect gas portion of the solution to be constructed. The value of α_f thus obtained would not necessarily correspond to the plateau in the solution of α but would only be an order of magnitude estimate of the value of α along the streamline.

Thus the value of $(\alpha_f - \alpha_0)$ using this scheme may have a large fractional error if $(\alpha_f - \alpha_0)$ is small, but will have a small absolute error. It should also be pointed out that this feature is a result of the sensitivity of the reaction rate to temperature (i.e. the condition that 'a' is large), and would be expected to break down when this condition is relaxed.

2.5 Comparison of expected behaviour with exact numerical computations

In order to verify the conclusions concerning the form of the solution it was necessary to integrate equations (11), (12a), (14a) numerically (with the recombination term deleted) in conjunction with (13) for specified initial conditions and pressure gradient. This was carried out using a standard library subroutine capable of integrating systems of ordinary differential equations. The only modification found necessary was the use of $\ln(x)$ rather than x as the independent variable in order to accommodate the extremely large gradients in state variables which sometimes occurred. The assumption of half excited vibrational energy was retained throughout.

In order to specify initial conditions an angle ϕ for the shock slope was specified, and approximate shock equations were applied. The exact shock conditions for a shock of inclination ϕ may be written

$$\begin{aligned} \rho_{\infty}' U_{\infty}' \sin\phi &= \rho_0' q_{N0}' \\ p_{\infty}' + \rho_{\infty}' U_{\infty}'^2 \sin^2\phi &= p_0' + \rho_0' q_{N0}'^2 \\ U_{\infty}' \cos\phi &= q_{T0}' \\ h_{\infty}' + \frac{1}{2} U_{\infty}'^2 &= h_0' + \frac{1}{2} q_0'^2, \end{aligned}$$

where all variables are dimensioned and q_{T0}' , q_{N0}' are the components of q_0' tangential and normal to the shock respectively. All other variables and subscripts have been introduced previously.

With the non-dimensionalization used and the assumptions that

- (i) $q_{N0}' \ll U_{\infty}'$ (equivalent to $\epsilon \ll 1$),
- (ii) $p_{\infty}' \ll \rho_{\infty}' U_{\infty}'^2 \sin^2\phi$,
- (iii) h is given by equation (6),

these equations may be written

$$\left. \begin{aligned} T_0 &= \sin^2\phi / (1 + \alpha_0) \\ p_0 &= \sin^2\phi \\ \alpha_0 &= \alpha_{\infty} \\ \rho_0 &= 1 \\ q_0 &= \cos\phi \end{aligned} \right\} \quad (37)$$

The aim of the numerical calculations was to examine the mathematical behaviour of the equations so that any consistent set of initial conditions would have sufficed. The approximate shock equations (37) were used to generate the consistent set only as a convenience.

In addition the following were specified: Λ , η , a (relevant to (14a)) and ϵ (relevant to equation (11)). ϵ was specified independently in order to examine the effect of this parameter on q . The two most important parameters were considered to be Λ , and a , and for this reason, for the majority of the cases considered, $\eta = 0$, $\alpha_{\infty} = 0$ and ϵ was

arbitrarily set at a typical value of $1/8$.

Two forms of imposed pressure distribution were considered.

$$p = \sin^2\{\phi(1-x)\} \quad (38)$$

$$p = \frac{\sin^2\phi}{2} \{(1-x)^{10} + (1-x)\} . \quad (39)$$

A constant unit pressure gradient used to derive the results was considered to be an unsuitable choice because of its limited applicability.

Equation (38) was chosen as it is the simple Newtonian pressure law for a circular arc, where the variation of x goes from 0 to 1 as the inclination of the body streamline goes from ϕ to 0. It was assumed that this pressure distribution would be similar to cases likely to be encountered in real situations.

Equation (39) was deliberately chosen as a bad example because the pressure gradient changes rapidly as a function of x , the largest gradients occurring when x is small (i.e. when large gradients also occur in other flow variables due to the reaction). As well as defining the initial pressure and temperature, ϕ also defines the average pressure gradient since the forms of (38) and (39) have been chosen so that p varies from $\sin^2\phi$ to 0, as x varies from 0 to 1. The magnitude of the parameter a/T_0 was varied by defining 'a' separately.

Altogether there were six parameters to which values could be assigned independently. Only the results of ten computations have been included, each being selected to show a specific feature. They are figures 1 - 10.

The parameters used in the computation for figure 1 are such that they fulfill the conditions $a/T_0 \gg 1$, $(d\alpha/dx)_0 \gg 1$, and there is good agreement between the numerical results and the features predicted by (17a), (36) and the related discussion. Both the absolute and relative errors in the prediction for the behaviour of α are small.

Figure 2 is chosen because none of the necessary approximations hold in this case. The agreement between predicted behaviour and computed results is poor.

Figure 3 has $(d\alpha/dx)_0 \ll 1$ and 'f' values are very close to the initial values of variables; the gas behaves almost like a perfect non-reacting gas throughout. In this case there is a large relative discrepancy between the behaviour of α in the presence of a pressure gradient, and that without, but the absolute change in α in all cases is small.

The values of parameters for the figures 4, 5, 6 and 7 are of the order of magnitude of the values expected for nitrogen flows in available experimental facilities. It is seen that the exact solutions are beginning to depart from the predicted behaviour as the value of 'a' is decreased. In particular the following points should be noted.

(i) The agreement in the temperature and density is reasonable, but the departure from the expected behaviour is more noticeable for the extremely nonlinear pressure gradient, equation (39). It would appear that for 'a' of order 5 the analysis is only applicable to 'well-behaved' pressure distributions.

(ii) α begins to show a significant departure from the expected behaviour of $\alpha \approx \alpha_f$ in the region $T_0^2/a \leq x \leq 1$ both with and without a pressure gradient. For the representative cases considered this approximation is only true if an error in α of order 0.05 is considered small. This error may for some cases be significant.

It is concluded that the smallest value of a that could be tolerated with the approximate solution still yielding useful results would be that of $a \sim 5$.

Figures 8 and 9 show the dependence of the solution on η for the case of constant pressure and nonlinear pressure gradient (39)

respectively. Appleton et al.⁵ give the value of η for nitrogen as -1.6 . It is seen that this value of η affects the solutions to a small extent only.

For figure 10 α_0 was put equal to 0.4 and shows that the agreement between expected behaviour and exact solution is no worse than that of $\alpha_0 = 0$ (see figure 7).

Calculations were also carried out for larger values of ϵ up to $\epsilon = 0.4$. This parameter has the least affect on the solutions of all those considered, affecting only the velocity. All other variables are affected only in the fourth significant figure.

2.6 A condition that the recombination rate may be ignored

In the preceding analysis the recombination of dissociated atoms was ignored. A condition which defines the order of magnitude of parameters which allows this approximation to hold may be written in terms of the 'f' values for each of the flow variables.

Consider equation (14a)

$$\frac{d\alpha}{dx} = \Lambda \rho \left(\frac{T}{T_0} \right)^\eta \frac{q_0}{q} \times \left\{ (1 - \alpha) \exp - \frac{a}{T} - \frac{\rho_\infty'}{\rho_D} \frac{\rho}{\epsilon} \alpha^2 \right\}$$

The recombination term may be neglected if

$$\Lambda \rho_f^2 \left(\frac{T_f}{T_0} \right)^\eta \frac{\rho_\infty'}{\rho_D} \frac{\alpha_f^2}{\epsilon} \ll 1$$

2.7 Application of results to a scaling problem

One of the unavoidable features of experimental facilities using a steady nozzle expansion from a high temperature, high pressure reservoir to generate a hypervelocity flow is the onset of chemical freezing in the nozzle. This is due to the large difference between the characteristic

flow time and the characteristic time required for recombination reactions to occur. Thus, in the test section, the chemical composition of the flow is not in equilibrium and for the case of a nitrogen flow the freestream α is that corresponding to an equilibrium condition at a far higher temperature than the freestream translational temperature (see Vincenti and Kruger⁴ p.293). In this section an attempt has been made to derive a scaling law such that a limited dynamic similarity would exist between flow along a streamline with zero freestream α and one in which the freestream α is finite.

Consider a given shock shape and a streamline entering the shock where its angle of inclination to the flow is ϕ . Then, assuming that the pressure distribution along the streamline is independent of reaction rate, the variations in density and α are characterised by ρ_f and α_f . If under two different sets of conditions ρ_f/ϵ and α_f are the same, then except for the thin region close to the shock where reaction dominates, the ratio of specific heats γ will be the same and hence the variation in density over the greater part of the streamline length will be the same. That is, except for the region close to the shock flow geometries will be similar. Conditions are sought which will keep α_f and ρ_f/ϵ constant while allowing other parameters to vary.

Consider two situations, one denoted by subscript 1 in which all conditions are defined and the other denoted by subscript 2 in which two variables U'_∞ and Λ are left undefined. To simplify matters, the approximate shock equations (37) are used as well as the approximation to (18) given by (18a).

Then require the following two equations to hold, in order to reproduce α_f and ρ_f/ϵ ,

$$\frac{T_{01}}{T_{f1}} \frac{(1+\alpha_{01})}{(1+\alpha_{f1})} \times \frac{1}{\epsilon_1} = \frac{T_{02}}{T_{f2}} \frac{(1+\alpha_{02})}{(1+\alpha_{f2})} \times \frac{1}{\epsilon_2}, \quad (40)$$

$$\frac{4+\alpha_{01}}{a_1} (T_{01} - T_{f2}) + \alpha_{01} = \frac{4+\alpha_{02}}{a_2} (T_{02} - T_{f2}) + \alpha_{02}. \quad (41)$$

Solutions are required for Λ_2 and $U_{\infty 2}'$. After much tedious algebra a solution for $U_{\infty 2}'$ may be written

$$\frac{D}{U_{\infty 2}'^2} = \frac{\frac{1}{2} T_{02} (1 + \alpha_{02}) - T_{f1} (4 + \alpha_{02}) \frac{(1 + \alpha_{02})}{(1 + \alpha_{01})} \times \epsilon_1}{\frac{4 + \alpha_{01}}{a_1} (T_{01} - T_{f1}) + (\alpha_{01} - \alpha_{02}) - (4 + \alpha_{02}) \frac{RT_{\infty 2}'}{D}}, \quad (42)$$

and

$$T_{f2} = T_{f1} \frac{(1 + \alpha_{01})}{(1 + \alpha_{02})} \frac{\epsilon_1}{\epsilon_2}. \quad (43)$$

(42) completes the specification of the freestream for case 2 and hence through the shock equations defines ϵ_2 . From its definition T_{f2} defines Λ_2 .

As an example consider the following

$$\begin{aligned} \sin^2 \phi &= 0.8 & \alpha_{01} &= 0.2 \\ \frac{U_{\infty 1}'^2}{D} &= 1 & \frac{RT_{\infty 1}' (1 + \alpha_{01})}{U_{\infty 1}'^2 \sin^2 \phi} &= 0.02 \\ \Lambda &= 10^5 \end{aligned}$$

These conditions are typical of those found in the experimental facility known as T3 at the A.N.U. for a nitrogen flow. Then consider $\alpha_{02} = 0$, $T_{\infty 2} = 0$, $\sin^2 \phi = 0.8$. Then from (42), (43) and related equations

$$\frac{U_{\infty 2}'^2}{U_{\infty 1}'^2} \approx 3 \quad \text{and} \quad \Lambda_2 \approx 2 \times 10^2$$

Experimental facilities are usually designed to produce temperatures in the shock layer of the same magnitude as those in the situation which is being scaled so that U_{∞}' is conserved in the scaling. Also to conserve reaction rates produced behind the shock the product $\rho_{\infty}' A$ is conserved, i.e. Λ is conserved in the scaling.

It would seem that a scaling based on considerations discussed here suffers from two distinct disadvantages. One is that it deals with flow along a specific streamline, and thus could be used only to scale a region of the flow-field. The other is that to scale the flow geometry

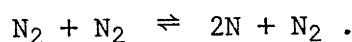
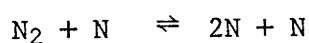
in the region after the reaction has occurred, invalidates the usual scaling requirements for the reacting region itself.

2.8 Application of results to a stand-off distance correlation

The term ϵ/ρ_f is a measure of the overall density ratio, taking into account both the density ratio across the shock and the further density increase due to the reaction. An attempt was made to use this term to correlate stand-off distances for computed nitrogen flows over a cylinder.

It has already been pointed out that the analysis will break down along the stagnation streamline and in the immediate vicinity of it. However the analysis is expected to hold along streamlines other than the stagnation streamline which enter the shock in the subsonic region of the shock layer. Since the stand-off distance depends on the properties of the whole of the stagnation region it was hoped that the quantity ϵ/ρ_f , where ρ_f is calculated from normal shock conditions, would be a sufficiently precise quantity to allow the shock stand-off distance to be correlated, and make unnecessary the computation of the whole flow-field.

Hornung¹² has investigated a nitrogen flow over a cylinder using a modification of the method of Garr and Marronne⁶. This method is an inverse method which uses the full equations of motion and a more general rate equation than that previously considered, taking into account separate rate laws for the reactions,



In order to calculate ρ_f , for the purpose of this study, Λ was taken as $(d\alpha/dx)_0 / (1 - \alpha_0) \exp(-a/T_0)$ and the characteristic scale was taken as the radius (r).

The relevant results of the twelve calculations performed by Hornung were reduced in the manner described above and are presented in figure 11.

The solid line is that given by Hornung for a non-reacting high Mach number flow. In the context of this application it may be interpreted as the case $\rho_f = 1$. It is thus seen that a correlation based on ϵ/ρ_f meets with only limited success. If the solid line were ignored the correlation of the twelve points could be considered reasonable. However if more points were calculated with smaller Λ they would lie between the points shown and the non-reacting solution. The scatter in the correlation is therefore not small.

A large number of points could be computed and a correction term introduced so that all points lie about the line given by the non-reacting gas case but this would only yield a rather complicated empirical correlation. A much simpler correlation has been proposed by Hornung. However it is interesting to observe that ρ_f , calculated from normal shock conditions can be used approximately as a representative density of the shock layer in the stagnation region.

3. EXPERIMENT

3.1 Description of facility

The preceding analysis was directed towards an understanding of the shock layer structure around bodies in nitrogen flows of moderately high velocity (6 km/sec) and density (4×10^{-6} gm/cm³). Such flows may be produced in the experimental facility known as T3 at the A.N.U. This facility has been described in some detail elsewhere (Stalker⁷).

A schematic diagram of T3 showing its main components is included as figure A3. Briefly, the device is conventional in the sense that it is a shock tunnel utilizing the high temperature, high pressure gas produced by a reflected shock wave at the end of a shock tube, as a reservoir for a steady nozzle expansion. Its unorthodox feature is the use of a free piston technique to supply energy to drive the shock tube. The technique involves the storage of energy in compressed air behind a free piston which, when released, isentropically compresses a driver gas between the piston and a diaphragm. The rupturing of this diaphragm produces a strong shock which travels down the shock tube portion of the apparatus. To give an idea of the size of T3, the piston mass is 90 kg, the compression tube is 600 x 30 cm and the shock tube is 600 x 7.6 cm. The test gas is not limited to nitrogen, the most common gases used being air, carbon dioxide and the inert gases argon and helium.

The ambient conditions in the test section are calculated by the nozzle calculations of Lordi et al.⁸ from reservoir conditions which may be determined from the measured shock speed in the shock tube and measured reservoir pressure.

The only diagnostic tool used in the experiments described herein was a Mach-Zehnder interferometer. The principles of operation of a Mach-Zehnder interferometer are described in Liepmann and Roshko¹⁶ (p.165) and shall be discussed only briefly here. A parallel beam of

monochromatic light is passed through a beam splitter (a half silvered mirror) to produce two beams of coherent light. One beam is passed through the test section and the other is used as a reference. The two beams are then recombined, and brought to focus on a screen (or film). If there is a slight angle between the two beams when recombined, and also a uniform distribution of refractive index exists in the test section, then a set of uniformly spaced interference fringes are produced on the screen. A change in the refractive index of the medium in the test section will produce a spatial shift of the fringes displayed on the screen proportional to the change in refractive index. Similarly, a non-uniform refractive index field in the test section (as would be expected for aerodynamic flows around bodies) will produce a fringe pattern such that the relative fringe shift between two points on the image is proportional to the difference of refractive index (spatially integrated across the test section) between those two points. The light source was an exploding wire through which a capacitor was discharged. It provided illumination for about 100 μ secs (the flow in the test section remained steady for the order of 500 μ secs) and was of sufficient intensity to swamp the flow luminosity. A band pass filter of $4330 \pm 100 \text{ \AA}$ was inserted in the optical system to ensure that a large number of fringes of good contrast were produced across the region of interest.

The fringe shift F is related to the density change $\Delta\rho$ by

$$\Delta\rho = \frac{4.16 F\lambda}{L(1 + 0.28 \alpha)} \text{ gm cm}^{-3}, \quad (44)$$

where λ is the wavelength

L is the geometric path.

This expression is derived from the refractivities of molecular and atomic nitrogen given by Alpher and White⁹.

It is seen that if the change in α is not very large then the fringe shift is nearly proportional to the change in density.

The shock tunnel was run with suitable shock driver conditions which were kept constant from shot to shot. Ambient conditions in the test section downstream of the nozzle were altered by changing the quantity of test gas which was introduced into the shock tube. For the driver conditions used nominal freestream conditions are given in table 1 as a function of p_R , the pressure of nitrogen in the shock tube at room temperature before the shot.

TABLE 1

p_R in. Hg	T_∞ °K	p_∞ dyne/cm ²	ρ_∞ gm/cm ³ × 10 ⁶	U_∞ km/sec	M_∞	α_∞
2.0	2382	28960	3.23	6.88	6.27	.266
3.0	2216	29300	3.79	6.35	6.22	.174
4.0	2111	29520	4.15	6.201	6.30	.137
6.0	1833	29080	4.98	5.594	6.36	.073

Henceforth the value of p_R will be used to denote a set of ambient free-stream conditions. It is seen that as p_R decreases the total enthalpy of the flow increases.

Freestream testing conditions may also be changed by altering the nozzle configuration but for these tests it was kept constant.

The flow around three separate classes of models was investigated. In all cases they were plane, of width 6 in., approximating two-dimensional flow. They shall be discussed independently in the following sections. Diagrams of the models and flow regimes around them are included as figure A3.

3.2 Flow over a wedge with a sharp expansion corner

This model examined the flow over a straight wedge at 45° to the flow. At a distance 'd' from the leading edge the angle of incidence of the plate was reduced by 40° through a sharp corner. The model was so

constructed that the parameter 'd' could be varied from 2 mm to 20 mm by attaching rectangular plates to the bottom of the model. The advantage of considering a sudden expansion is that the pressure gradient along different streamlines is a function of the proximity of the streamline to the body. That section of the flow before the expansion is approximately the zero pressure gradient case, so that altering the distance between tip and the corner allows the gas to react to different stages before being subjected to a pressure gradient. In this way the interaction between pressure gradient and reaction rates may be studied with different initial reaction rates.

A typical interferogram with $d = 1.0$ cm and $p_R = 6$ in. Hg., together with the derived fringe shift field is shown as figure 12. Interferograms were taken with p_R equal to 3, 4, 6 in. Hg. In all cases the rise in density along the body streamline of the straight section of the model between the tip and the sharp corner was found to be negligible, and for constant p_R the density field in the expansion fan region was (within experimental error) independent of 'd'. (The body streamline in this context is to be interpreted as meaning the flow just outside the boundary layer, which is easily recognizable on the interferograms.) This implies that the temperature behind a shock of deflection angle equal to 45° is insufficient to produce a reaction fast enough to substantially alter the flow field behind it, with the freestream conditions and body scale which were considered.

Increasing the angle of incidence of the wedge would have caused the shock to have become detached. (This topic will be discussed in the next section.)

3.3 Flow over a curved wedge

This model was a curved plate having a sharp leading edge and a constant radius of curvature of 1 ft. The plate could be tilted to vary the initial angle of incidence. The flowfield was studied with $p_R = 2, 4, 6$ in. Hg with various angles of attack. Here, as with the

previous case, results would only be useful if the shock at the leading edge remained attached. Otherwise the initial conditions immediately behind the shock would be difficult to ascertain.

Figure 13 shows the contours of constant fringe shift derived from a series of shots with $p_R = 6$ in. Hg and the model at three different angles of attack. Close to the body, streamlines may be considered to run parallel to the body. If a reaction were to occur this would manifest itself in an initial density increase (due to the reaction), and a subsequent density decrease (due to pressure gradient effects), measured along a streamline. It is only figure 13(c) which exhibits behaviour that could be interpreted in this way. However the initial angle of attack of the model in this shot is 49.5° and the shock would be expected to be detached.

The accuracy to which the fringe shifts may be measured is of order .1 of a fringe, which would be decreased if the fringe spacing were decreased. In any given situation the spacing of the fringes is a compromise between accuracy, and detail of the flowfield which is being investigated. The fringe spacing chosen for these shots does not allow for good resolution in the region of the model leading edge.

Therefore although (13c) shows evidence of reaction, the reacting streamlines are those close to the body having entered the shock layer through a region of the flowfield which does not lend itself easily to analysis either theoretically or experimentally. The cases of $p_R = 4$ in. Hg and 2 in. Hg exhibit the same form of behaviour.

Thus it may be concluded that for the freestream conditions which were studied no reaction occurs behind an attached shock, of sufficient magnitude to significantly alter the density field from that of a non-reacting flow. Under these circumstances a model with a detached shock which is more easily analysed appears the only alternative. The disadvantage of such a model is that the analysis in the preceding sections is not expected to hold along a body streamline which is the only streamline whose position is known accurately.

3.4 Flow over circular cylinders

3.4.1 A numerical investigation of streamline positions

An experimental investigation of nitrogen flows over circular cylinders was made using the experimental facility T3 by Hornung¹², as part of the work published. The flow fields around these bodies fulfill the requirement of a 'well-behaved' detached shock. The raw data from these experiments was made available for analysis in the context of this work.

Since the expressions derived previously are in terms of the behaviour along a streamline, a determination of the streamline shapes is necessary. The equation of continuity (1) defines the streamline shapes

$$\frac{\partial \theta}{\partial n} = -\frac{1}{\rho q} \frac{\partial \rho q}{\partial x} \quad (1)$$

Consider a given shock shape, a given reaction rate and given freestream conditions. This is sufficient to define the position of a streamline of a particular stream function ψ . If all conditions are left unaltered except that of the reaction rate, a different density field will occur to the shock layer and hence from (1) the position of the streamline ψ will change.

However if the distance during which the reaction dominates is small then from (1) the change in the streamline position due to the change in reaction rate will also be small. When the reaction has stopped and the gas behaves as a perfect gas then the only further difference in the two streamline positions will be due to the difference in the pressure distribution and the effect of a different γ . Both of these effects are considered to be small. That is, the position of the streamlines are insensitive to the reaction rate assumed.

To verify this conclusion figure 14 shows the results of calculations using the inverse method of Garr and Maronne⁶ with the reaction rates of Appleton et al.⁵. The shock shape used was that measured from an

interferogram taken of flow over a 1 in. diameter cylinder with $p_R = 6$ in. Hg. The shock coordinates for this purpose were expressed in terms of x'/d ($d =$ diameter of the cylinder) and d was specified independently. Thus the value of Λ and hence of $(d\alpha/dx)_0$ could be changed by redefining d . Three conditions are shown, with d equal to 20 cm, 1 cm and 0.02 cm corresponding to a fast, moderate and slow reaction rate. Streamlines are identified in the figure by ψ/ψ_d where ψ_d is the value of the stream function at a transverse distance D across the freestream measured from the axis of symmetry.

Figure 14 is a comparison of the pressure and density distributions measured along a streamline for a particular value of 'd', with those where the flow-field is left unaltered but the distributions are measured along streamline shapes calculated for the case $d = 1$ cm superimposed on this flow-field. Figures 14(a) and 14(b) are for a flow-field calculated with $d = 20$ cm while 14(c) and 14(d) are for the case $d = 0.02$ cm. The difference between the distributions shown in each pair of curves is seen to be small.

In order to reduce the experimental data, one has the freestream conditions, the shock shape, and the density field, but the streamline positions are unknown and must be calculated, and superimposed on the density field, to measure the density along a streamline. The purpose of the preceding discussion and figure 14 was to show that the reaction rate used in this calculation is relatively unimportant since the density distribution so measured is insensitive to the variation of streamline position caused by changing the reaction rate. For the reduction of experimental data streamline positions were calculated with the known freestream conditions, shock shapes, and in all cases with $d = 1$ cm.

The experimental points so derived were compared with the solutions for the reacting and frozen reaction solutions derived in earlier sections. For the frozen regime a pressure distribution was required. This was taken as the pressure along a streamline as calculated with $d = 1$ cm.

The magnitude of the errors involved in this approximation are typically of the order of those illustrated by figures 14(b) and 14(d). The difference between the pressure distribution calculated along streamlines, with those measured along the superimposed streamlines calculated for the case $d = 1$ cm, is small in both cases. This shows the insensitivity of the pressure distribution along a streamline (as well as the position of the streamlines relative to the pressure field), to the reaction rate.

3.4.2 Experimental results

Figure 15 shows the experimental fringe shift measured along the computed streamlines for various conditions. Also shown are the corresponding approximate zero pressure gradient solutions derived from (17a) and the expected asymptotic solutions derived from (36). For the purpose of these calculations, and the calculations of initial conditions from shock relations the energy of vibration was assumed to be half excited in the freestream and in equilibrium behind the shock. In order to calculate T_f and related quantities from (36) it was necessary to assume a characteristic body scale. This was taken as the diameter of the cylinder under consideration. The reaction rates of Appleton et al. were used and involve two reactions corresponding to the nitrogen atom and the nitrogen molecule acting as the second body in the dissociation process. The value of Λ was taken as $(d\alpha/dx)_0 / (1 - \alpha_0) \exp(-a/T_0)$.

In order to calculate the final solution (36) the pressure distribution along a streamline was necessary. For the cases with higher freestream enthalpy ($p_R = 4$ in. Hg, 2 in. Hg) the computed pressure distribution became unstable at $x'/d \sim 0.3$ although the computed streamline positions remained stable. For these cases the pressure field before $x'/d = 0.3$ was taken as that computed and for $x'/d > 0.3$ was taken as a $\sin^2\theta$ distribution, where θ was the streamline inclination to the freestream.

The case for $p_R = 6$ in. Hg and $d = 1$ in. was an infinite fringe interferogram and the fringe shift was deduced by interpolation between unit fringe shifts. The error in such a procedure was estimated at

± 0.2 fringe. All other cases were finite fringe pictures, the error in reading being estimated as 0.1 fringe.

The freestream conditions may be investigated experimentally. The use of interferograms of flows over straight wedges, of sufficiently low incidence so that no reaction occurs, yields a value for the freestream density. The shock angle gives a value for the density ratio across the shock, while the fringe shift gives a value of the density difference across the shock; hence the freestream density may be calculated. Pitot pressure measurements may be used to measure the product $\rho_{\infty}'(U_{\infty}')^2$, and hence give a value for U_{∞}' . Values of ρ_{∞}' and U_{∞}' so obtained allow a check to be made on the calculated freestream conditions. Such measurements indicate that ρ_{∞}' and U_{∞}' are known to $\pm 10\%$. No verification has been made at this time of α_{∞} . The curves shown in figure 15 are based on values of flow variables obtained from the calculated freestream, and are therefore subject to the uncertainty associated with these variables.

A further error introduced is that of assuming two-dimensional flow over a three-dimensional model. This will especially exhibit itself in readings close to the shock wave where any sudden change in density will be 'smeared out' due to transverse curvature of the shock. With these considerations and taking into account the small values of (a/T_0) obtained (of order 7), the experimental behaviour as shown in figures 15 (a,b,c,d) agrees reasonably with the predicted behaviour.

Interferograms of flows around models with 2, 1 and $\frac{1}{2}$ in. diameters were studied. The flows around models with 2 in. diameter were similar to the corresponding flows about 1 in. models, as expected from the theory developed. Therefore such cases are not included herein. The flows around $\frac{1}{2}$ in. diameter models however exhibited substantial differences from the 1 in. diameter models in the cases of $p_R = 4$ in. Hg and 2 in. Hg. Figures 15(e) and (f) are of $d = \frac{1}{2}$ in. and $p_R = 4$ in. Hg and show practically no evidence of reaction. Hornung¹² has discussed this phenomenon and found that the apparent reduction in reaction rates for the case of small models is consistent with the induction time effect

suggested by Shui, Appleton and Keck¹⁰. This prediction is based on the theoretical result that significant dissociation occurs only after the electronically excited $\Lambda^3 \Sigma_u^+$ state of the nitrogen molecule is populated. The induction time decreases as the concentration of molecular nitrogen increases in the freestream and no reduction in the amount of dissociation was observed for the case of $p_R = 6$ in. Hg and $d = \frac{1}{2}$ in.

Shown in figures 15 (g,h) are the fringe shift distributions along streamlines over a 1 in. diameter model with $p_R = 2$ in. Hg. It is seen that the experimental behaviour does not approach that which is predicted. One possible explanation is that ionization is occurring to a significant degree causing the electronic component of the gas to lower the refractive index. Kewley¹¹ has studied the flow of nitrogen over a straight wedge using the shock curvature at the tip to deduce the initial reaction rates (i.e. data was obtained which was independent of the refractive index of the gas). Discrepancies were also found in that study for cases where $p_R = 2$ in. Hg.

It should be noted that for the data presented in figure 15(g,h) $a/T_0 \sim 5$ and the analysis is not expected to hold particularly well. However the magnitude of the discrepancy would seem to indicate that some factor other than the inapplicability of the theory is operating. Two possibilities could be incorrect freestream conditions and incorrect reaction rates (or a combination of both). Since the maximum fringe shifts measured are less than or equal to the fringe shifts predicted from the shock equations it seems likely that the calculated freestream conditions are incorrect for this value of p_R .

Examining the results for $p_R = 4$ in. Hg and $d = \frac{1}{2}$ in. would also indicate that the freestream conditions may be slightly incorrect for $p_R = 4$ in. Hg.

4. CONCLUSION

A study was made of the flow properties of an ideal dissociating gas along a streamline in a prescribed negative pressure gradient. Certain restrictions were placed upon the parameters involved including the requirement that the recombination term in the reaction rate was small and could be neglected, and that the ratio of the temperature behind the shock wave to the characteristic temperature of dissociation was small.

A theoretical analysis showed that for the case of constant pressure, the effect of the reaction was confined to a small distance close to the shock, and the variation in properties of the gas away from this region was small; defining a 'plateau' state which could be deduced from initial conditions behind the shock wave. For the case of a constant unit pressure gradient it was found that the flow could be described by assuming that the initial reacting region was unaffected by the pressure gradient and that the gas thereafter behaved as a perfect non-reacting gas with initial conditions given by the 'plateau' conditions of the zero pressure gradient case. It was assumed that this property was not unique to a unit constant pressure gradient and the explicit analytic solutions obtained for the two regions were verified by results obtained by numerical computation of more complicated cases.

The predicted behaviour for the ideal gas was compared with interferograms of flows over circular cylinders in a hypervelocity nitrogen free stream, generated by a free piston shock tube. The behaviour for the lower enthalpy cases showed reasonable agreement with the expected behaviour. There was a large deviation for the high enthalpy cases, and it is thought that the most likely cause was an insufficient knowledge of freestream conditions.

The main advantage of the analysis is that it provides a physical insight into the processes occurring along a streamline, where a single dissociation reaction is taking place, which a computed solution alone would not have

done. It also provides a quantitative measure of the effect of that reaction. This can be applied immediately to the experimental situation encountered with nitrogen flows in T3, to indicate the expected effect of the reaction in a particular experimental arrangement. A more detailed computer study could then be carried out in the light of results from the approximate analysis, if it were thought necessary.

The analysis suffers from two disadvantages. The first is that it does not give a complete description of the flow along a streamline, i.e. it gives only an initial and a final solution. The second is that its accuracy depends on the magnitude of the parameter 'a'. It was found from the computed solutions that $a \sim 0(5)$ defines the lower limit to which the analysis may be reasonably applied. Further work could possibly be done in order to find an intermediate function to match the initial and final solutions and thus overcome the first disadvantage. The second however is fundamental to the whole approach taken and could not easily be rectified. On the experimental side, further work seems necessary in order to define more clearly the cause of the discrepancy between theory and experiment, in the high enthalpy nitrogen runs in T3.

A concept has been developed of a reaction being self-limiting under certain conditions. That is, the reaction itself causes a temperature decrease, thus limiting further reaction, defining a plateau state independent of pressure gradient effects. This could possibly be the basis for the investigation of more complex reactions, however it is unlikely that an analytic solution could be obtained.

5. REFERENCES

1. HAYES, W.D. and PROBSTEIN, R.F. (1966).
Hypersonic flow theory (second edition) Vol. 1 - Inviscid flows.
Academic Press.
2. FREEMAN, N.C. (1958). *Physics of Fluids* 4, 407.
3. CAPIAUX, R. and WASHINGTON, M. (1963).
A.I.A.A. Journal 1, no. 3, 650.
4. VINCENTI, W.G. and KRUGER, C.H. (1965).
Introduction to Physical Gas Dynamics.
John Wiley and Sons, Inc.
5. APPLETON, J.P., STEINBERG, M. and LIQUORNIK, D.J. (1968).
The Journal of Chemical Physics 48, no. 2, 599.
6. GARR, L.J. and MARRONE, P.V. (1963).
Cornell Aeron. Lab. Rep. QM-1626-A-12(II).
7. STALKER, R.J. (1972).
The Aeronautical Journal of the Royal Aeronautical Society, June, 374.
8. LORDI, J.A., MATES, R.E. and MOSELLE, J.R. (1966).
N.A.S.A. Current Report CR-472.
9. ALPHER, R.A. and WHITE, D.R. (1959). *Physics of Fluids*, 2, 162.
10. SHUI, V.H., APPLETON, J.P. and KECK, J.C. (1970).
Journal of Chemical Physics 53, 2547.
11. KEWLEY, D.J. (1971).
Honours Thesis, Australian National University, Canberra.
12. HORNING, H.G. (1972). *Journal of Fluid Mechanics* 53, pt 1, 149.
13. LIGHTHILL, M.J. (1957). *Journal of Fluid Mechanics* 2, pt 1, 1.
14. SPURK, J.H., GERBER, N., SEDNEY, R. (1966).
A.I.A.A. Journal 4, no. 1, 30.
15. LICK, W. (1960). *Journal of Fluid Mechanics* 7, 128.
16. LIEPMANN, H.W. and ROSHKO, A. (1957).
Elements of Gas Dynamics - John Wiley and Sons, Inc.

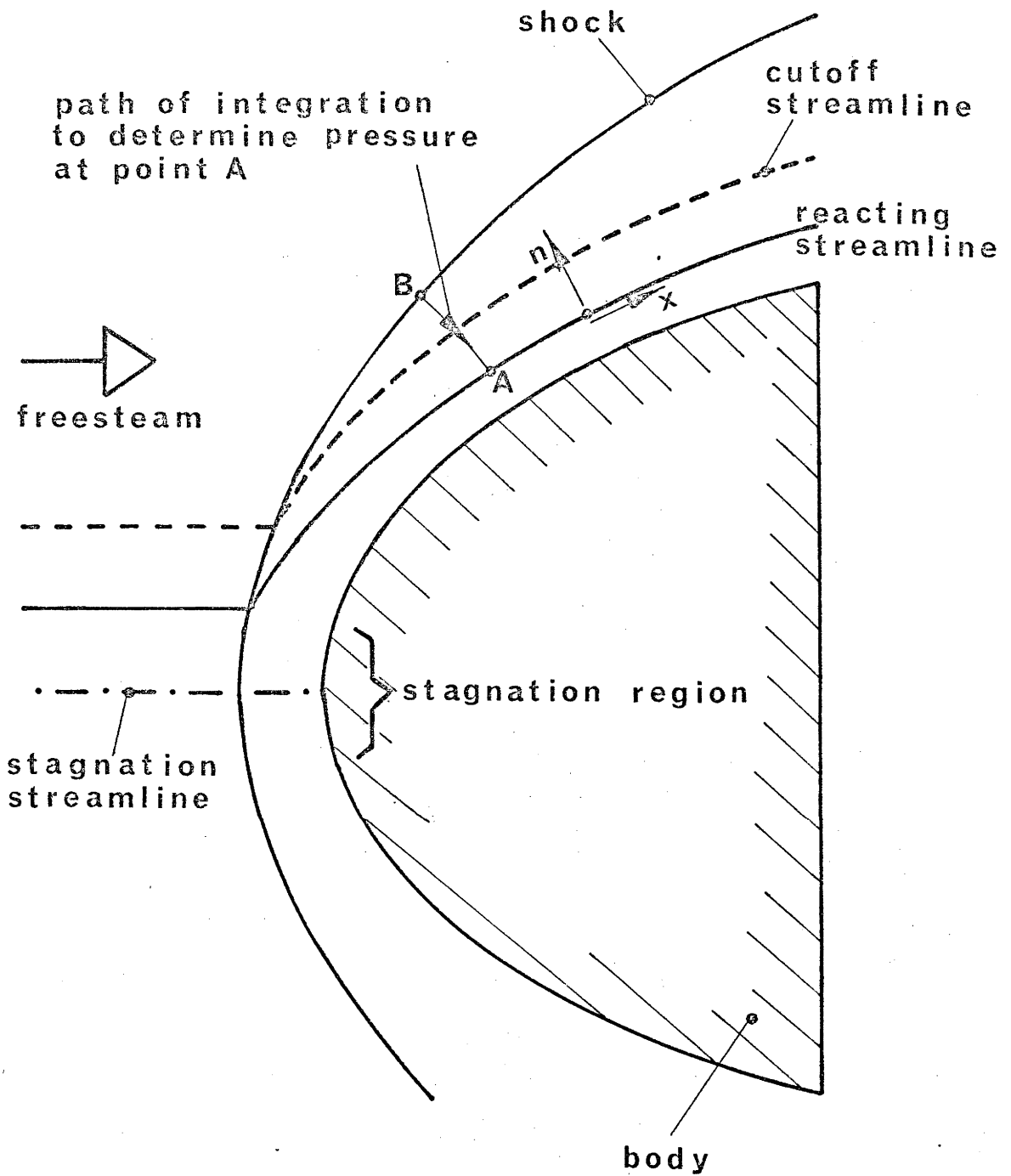


FIGURE A1

Illustration of the main features of the problem considered.

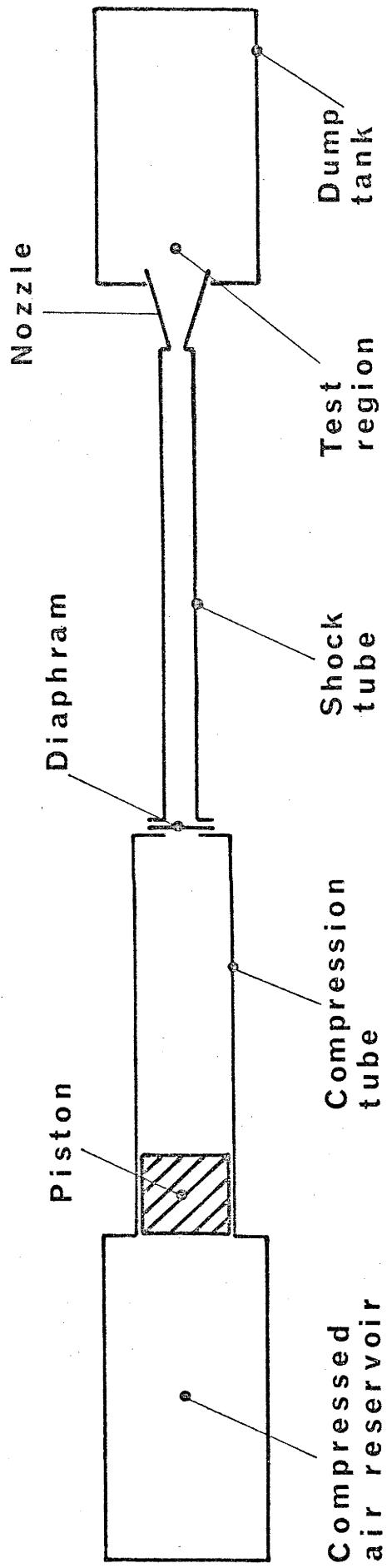
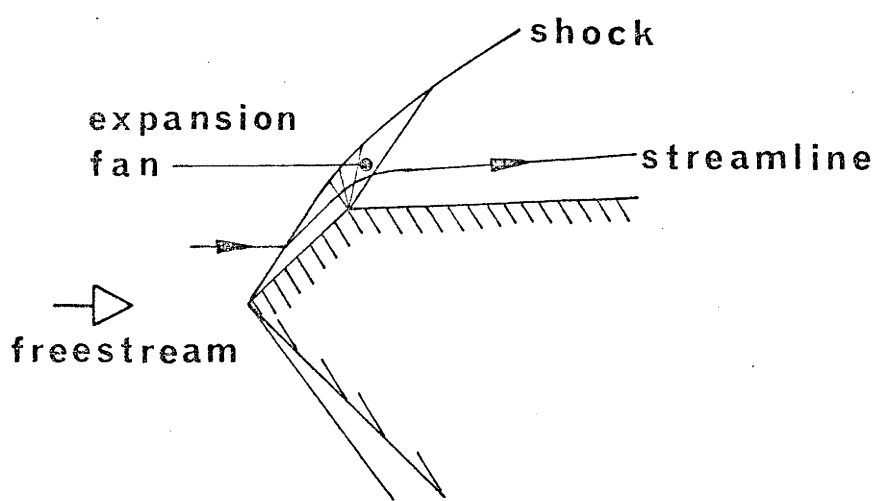
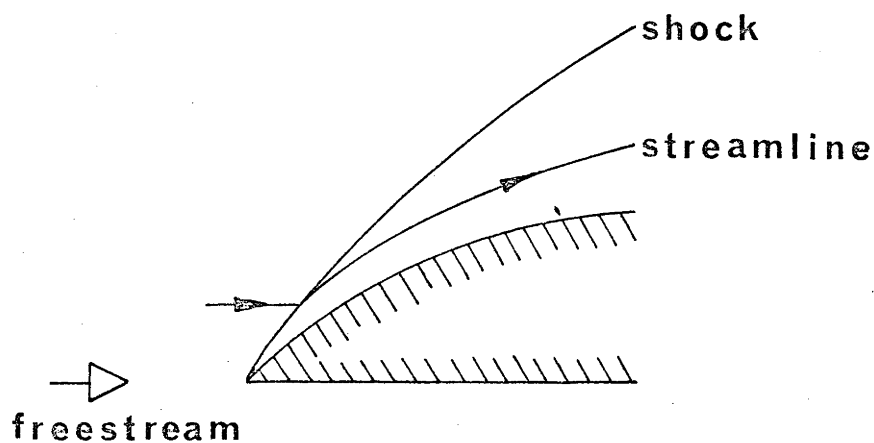


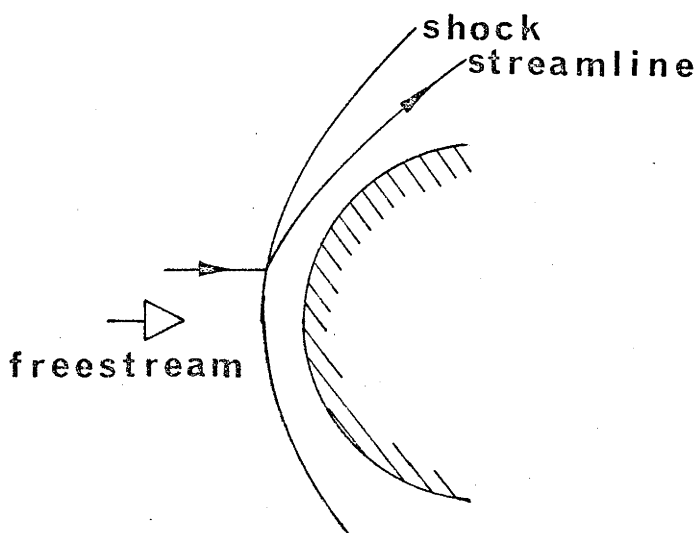
FIGURE A2 Diagram of main components of free piston shock tube T3.



(a) wedge with sharp expansion corner



(b) curved wedge



(c) cylinder

FIGURE A3

Diagrams of models used in experimental investigation.

LEGEND TO FIGURES 1 - 10

showing the comparison between computed solutions of the flow equations with the initial and final solutions derived in sections 2.2 and 2.4.

- Computed solution.
- Zero pressure gradient approximation, and initial solution for the case with a pressure gradient.
- Analytic approximations to the final solutions, in the presence of a pressure gradient.
- A Denotes zero pressure gradient.
- B Denotes an imposed pressure gradient given by equation (38).
- C Denotes an imposed pressure gradient given by equation (39).

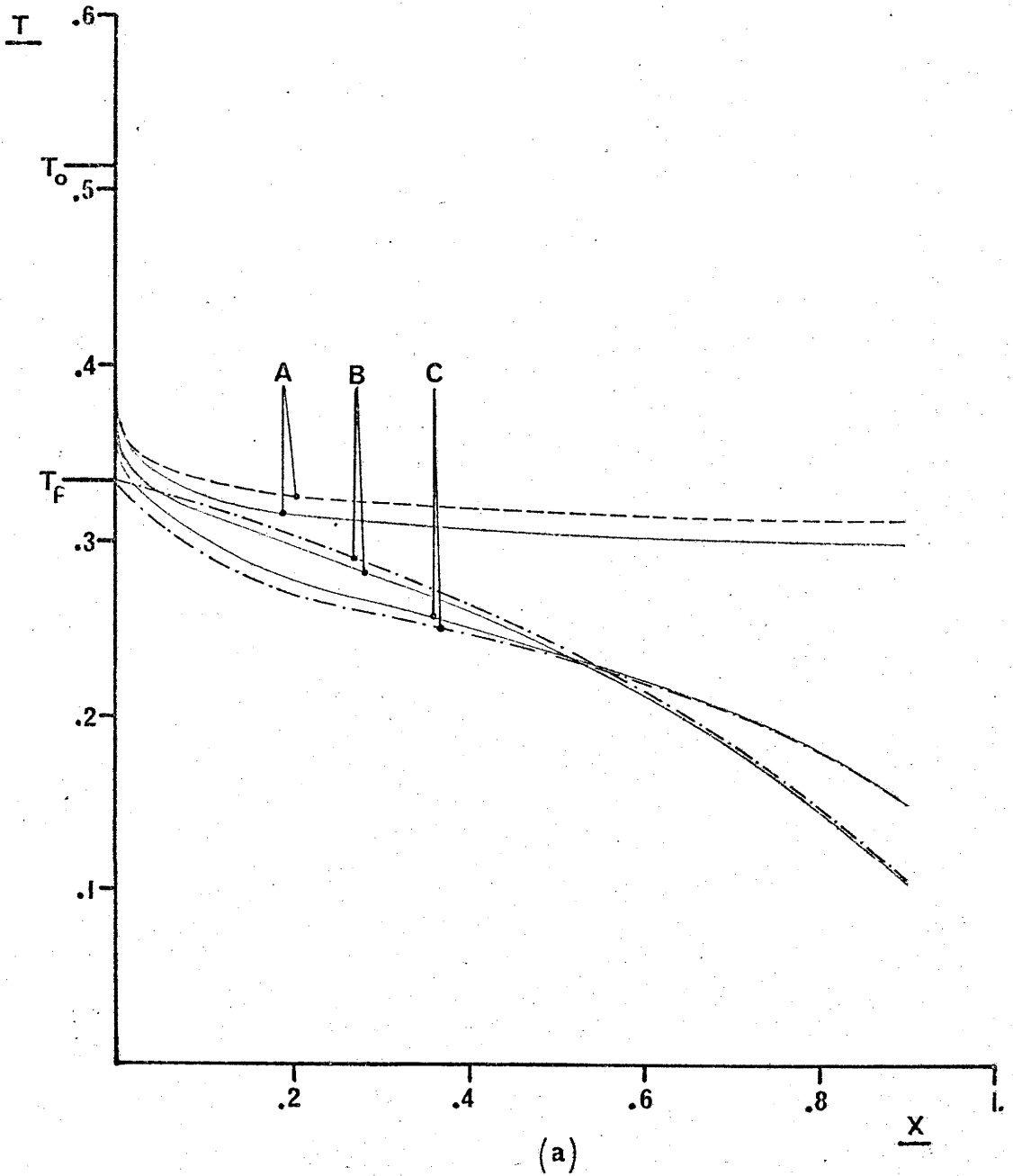


FIGURE 1

$\Lambda = 10^{12}$
 $\Phi = .8$
 $\alpha_0 = 0$
 $\eta = 0$
 $\varepsilon = 1/8$
 $a = 10$

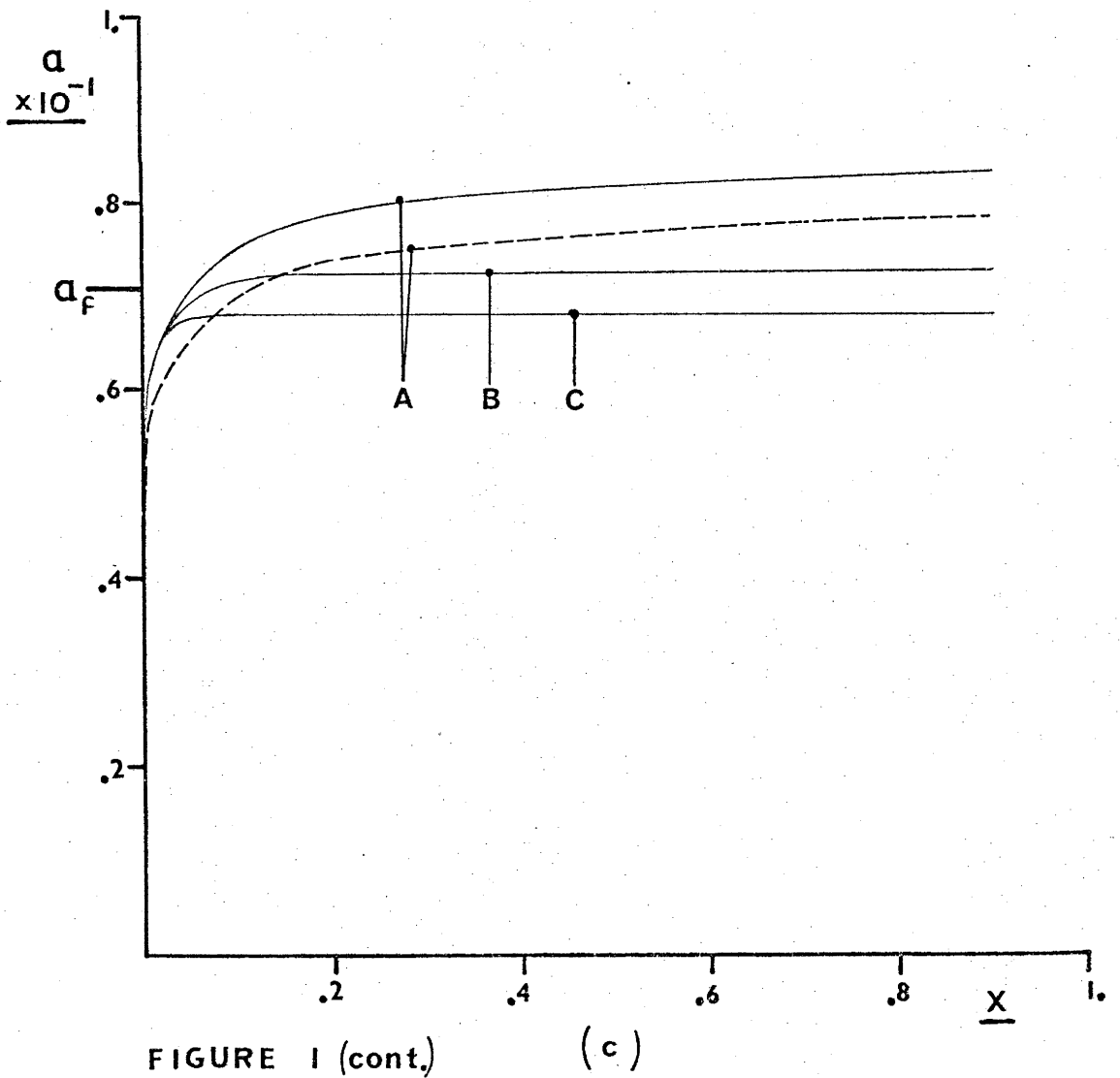
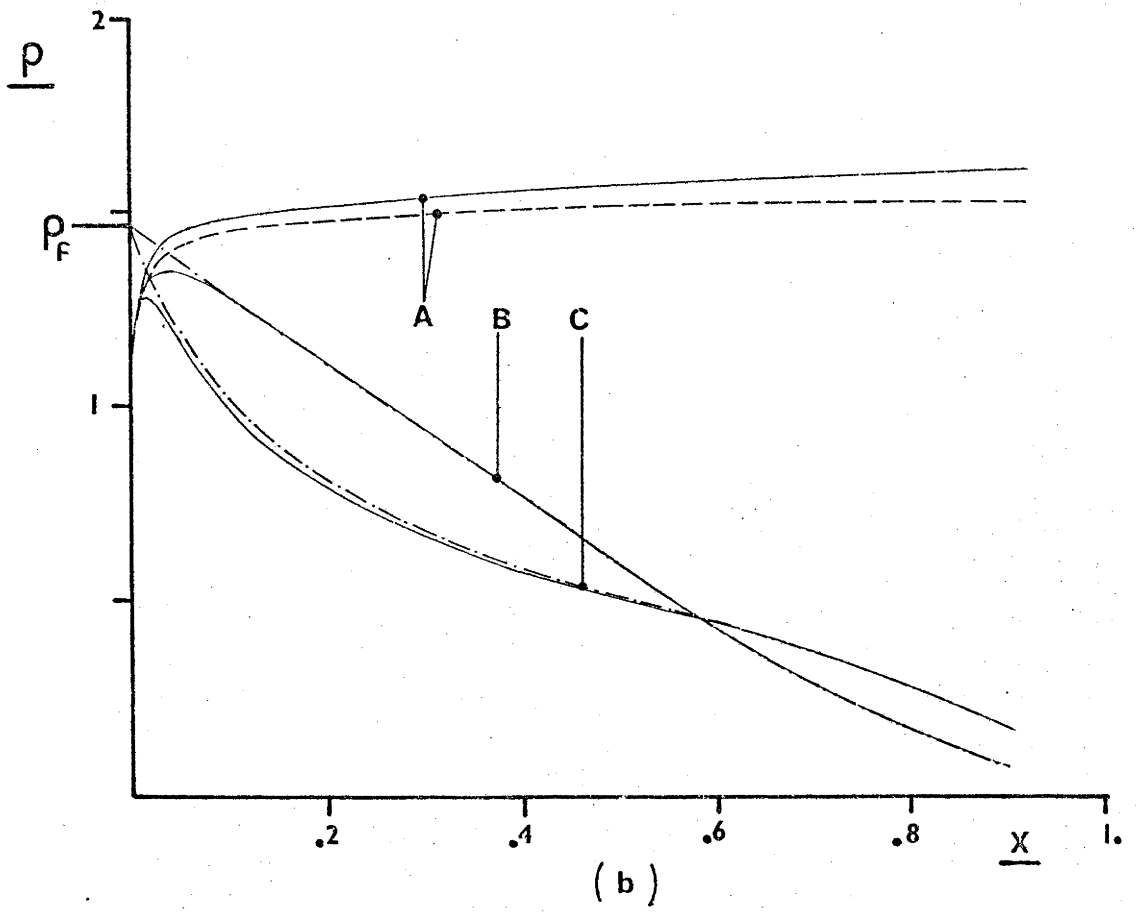
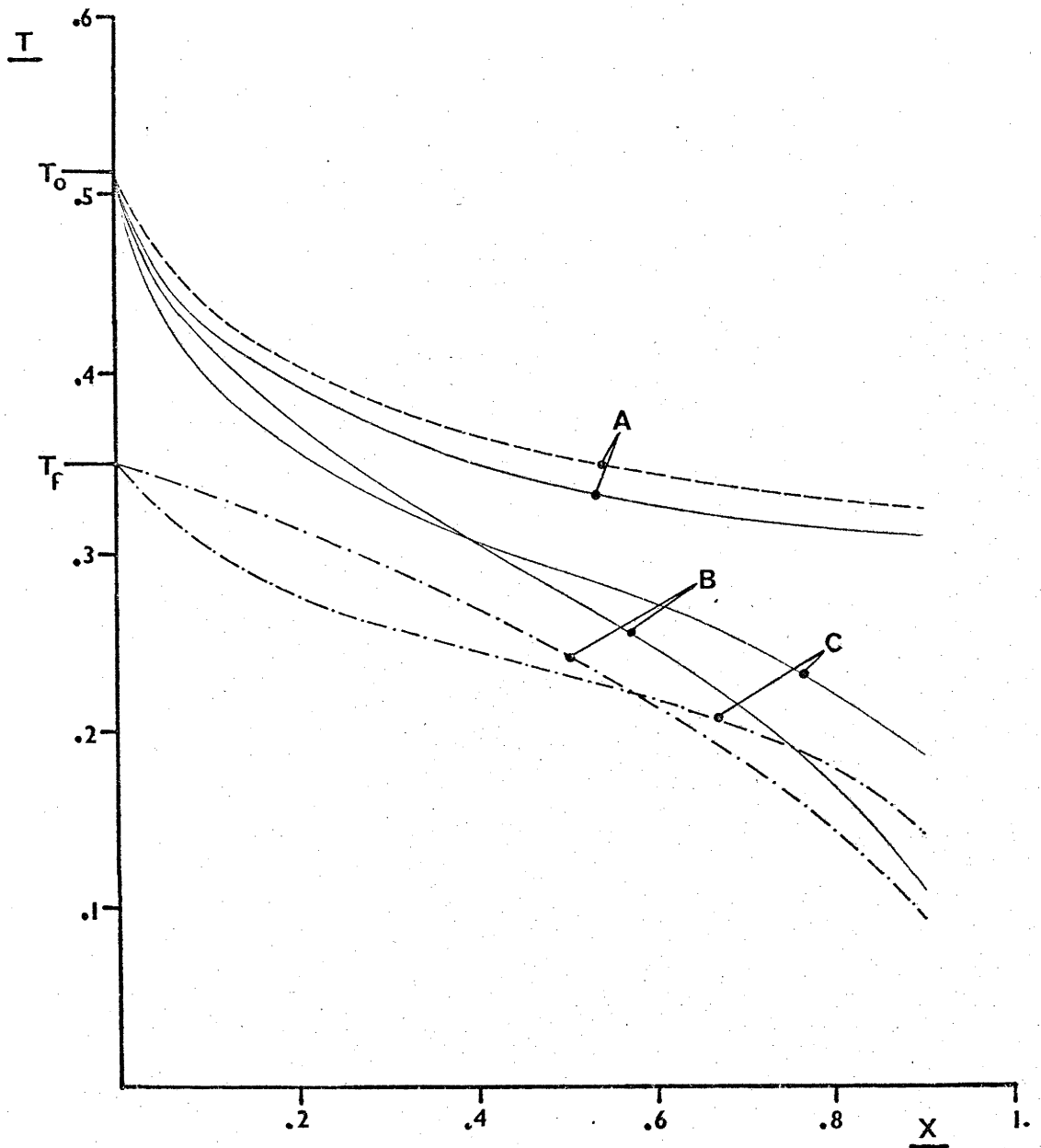


FIGURE 1 (cont.)



(a)

FIGURE 2

$$\Lambda = 10^2$$

$$\Phi = .8$$

$$\alpha_0 = 0$$

$$\eta = 0$$

$$\varepsilon = 1/8$$

$$a = 2$$

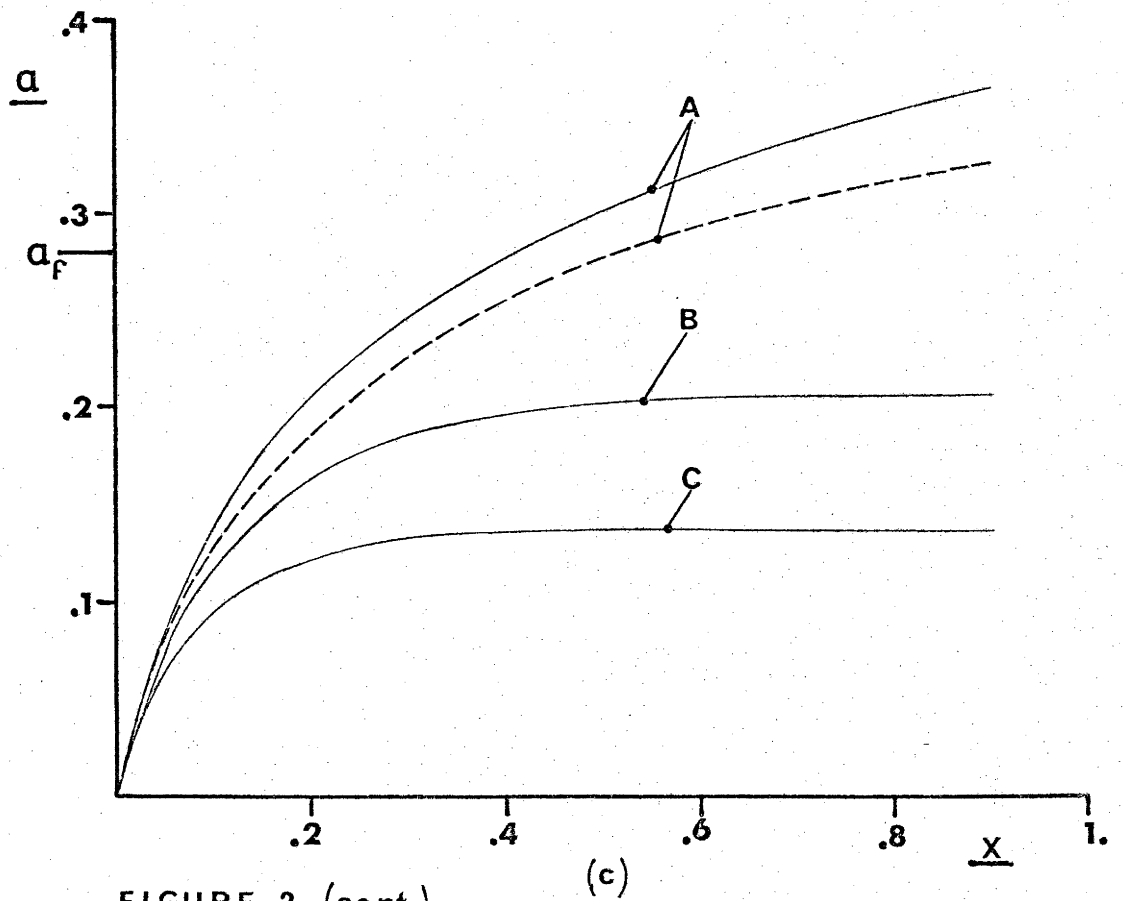
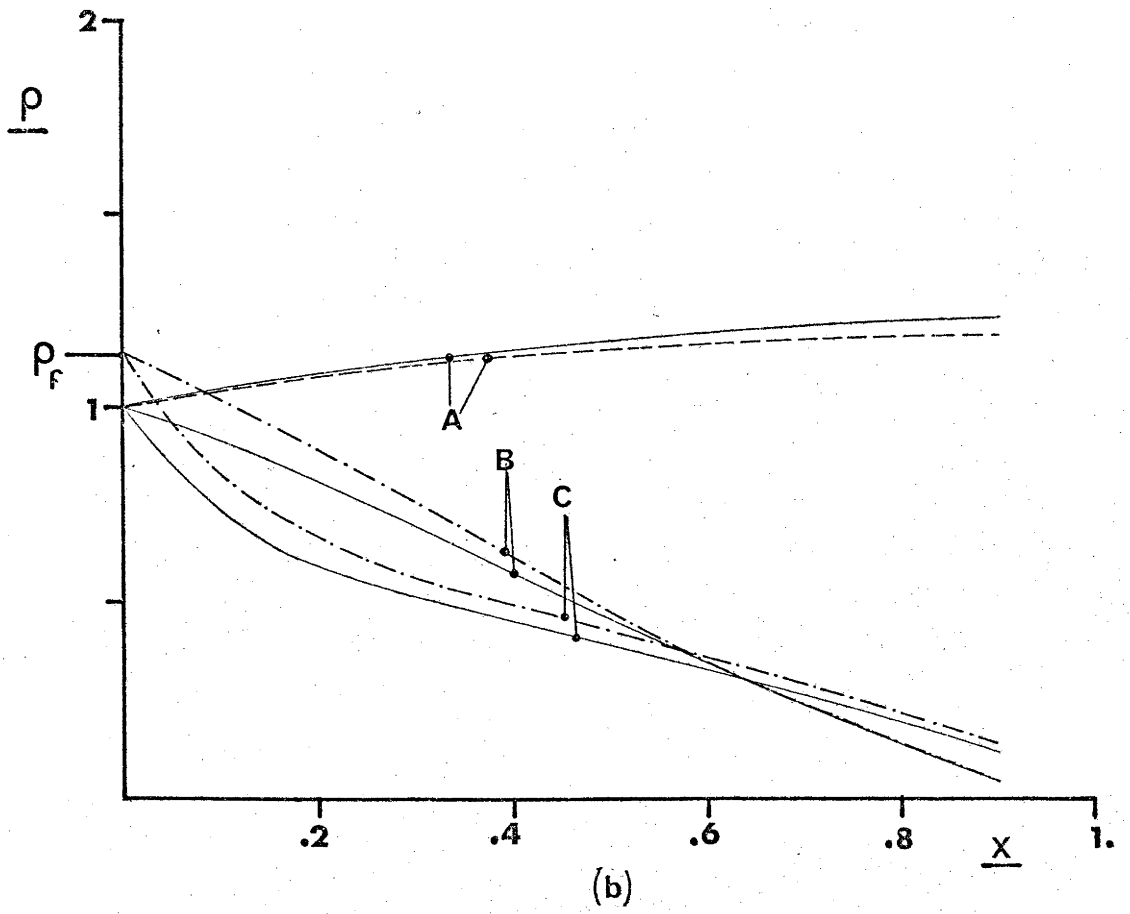


FIGURE 2 (cont.)

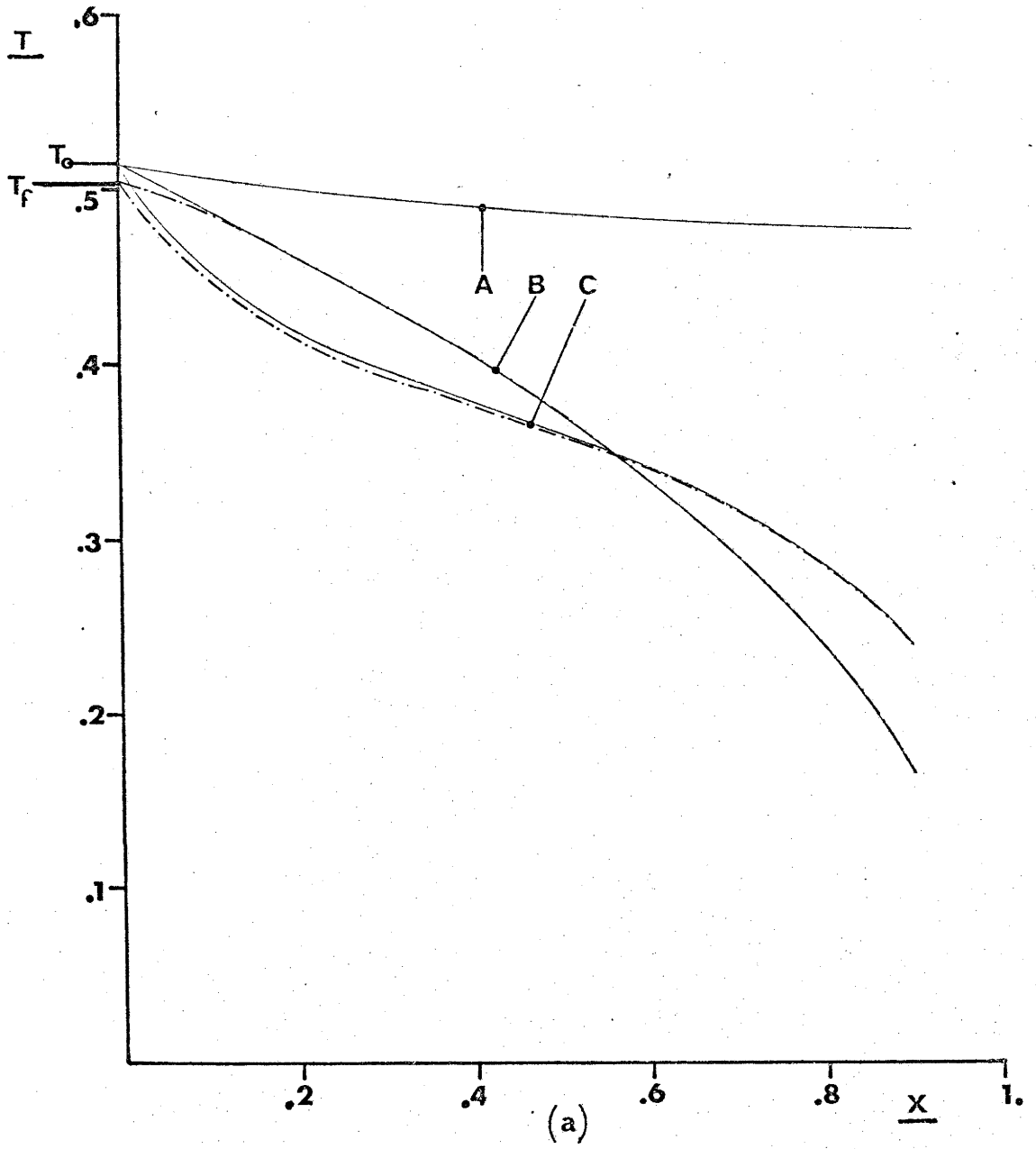


FIGURE 3

$\Lambda = 10^7$
 $\Phi = .8$
 $\alpha_0 = 0$
 $\eta = 0$
 $\epsilon = 1/8$
 $a = 10$

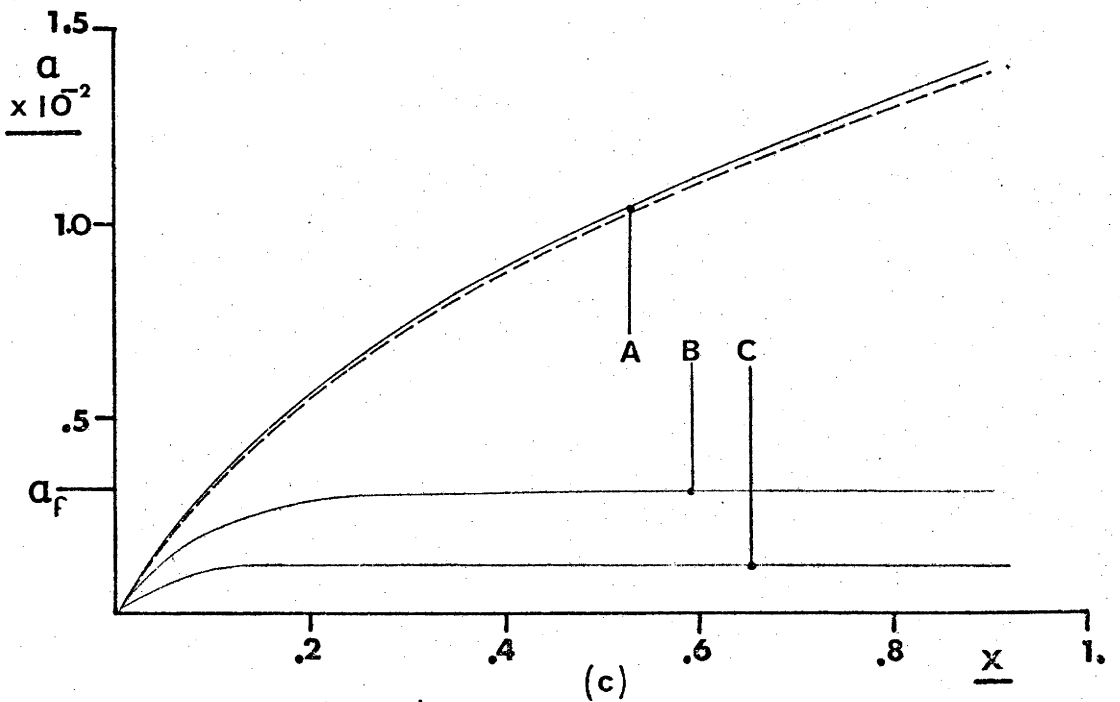
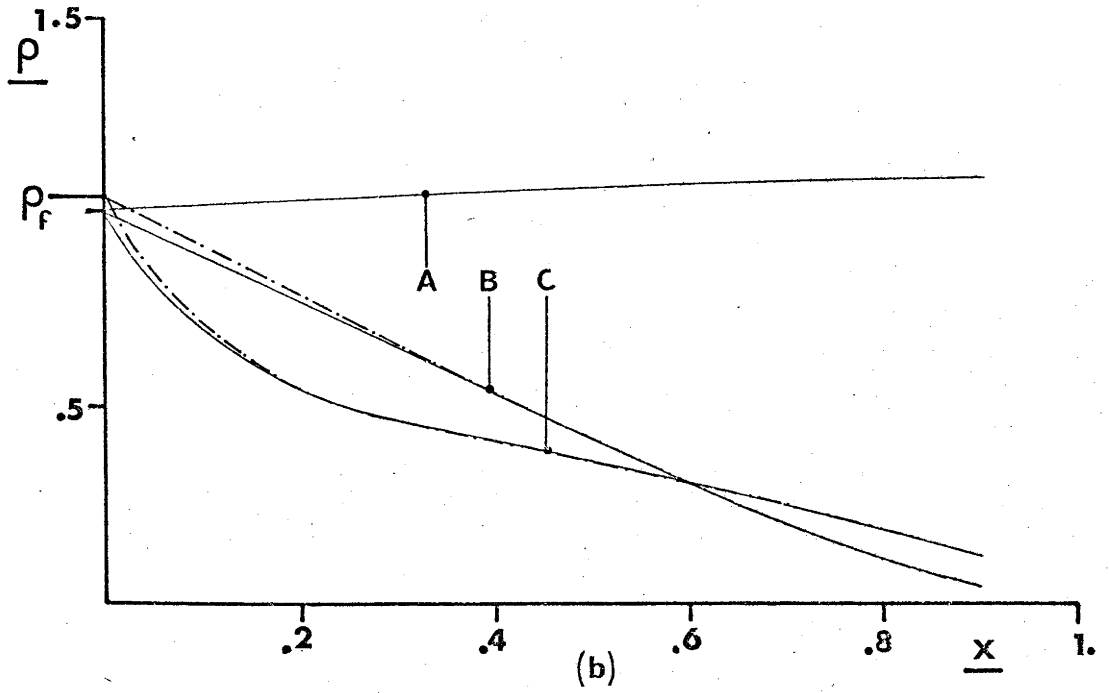


FIGURE 3 (cont.)

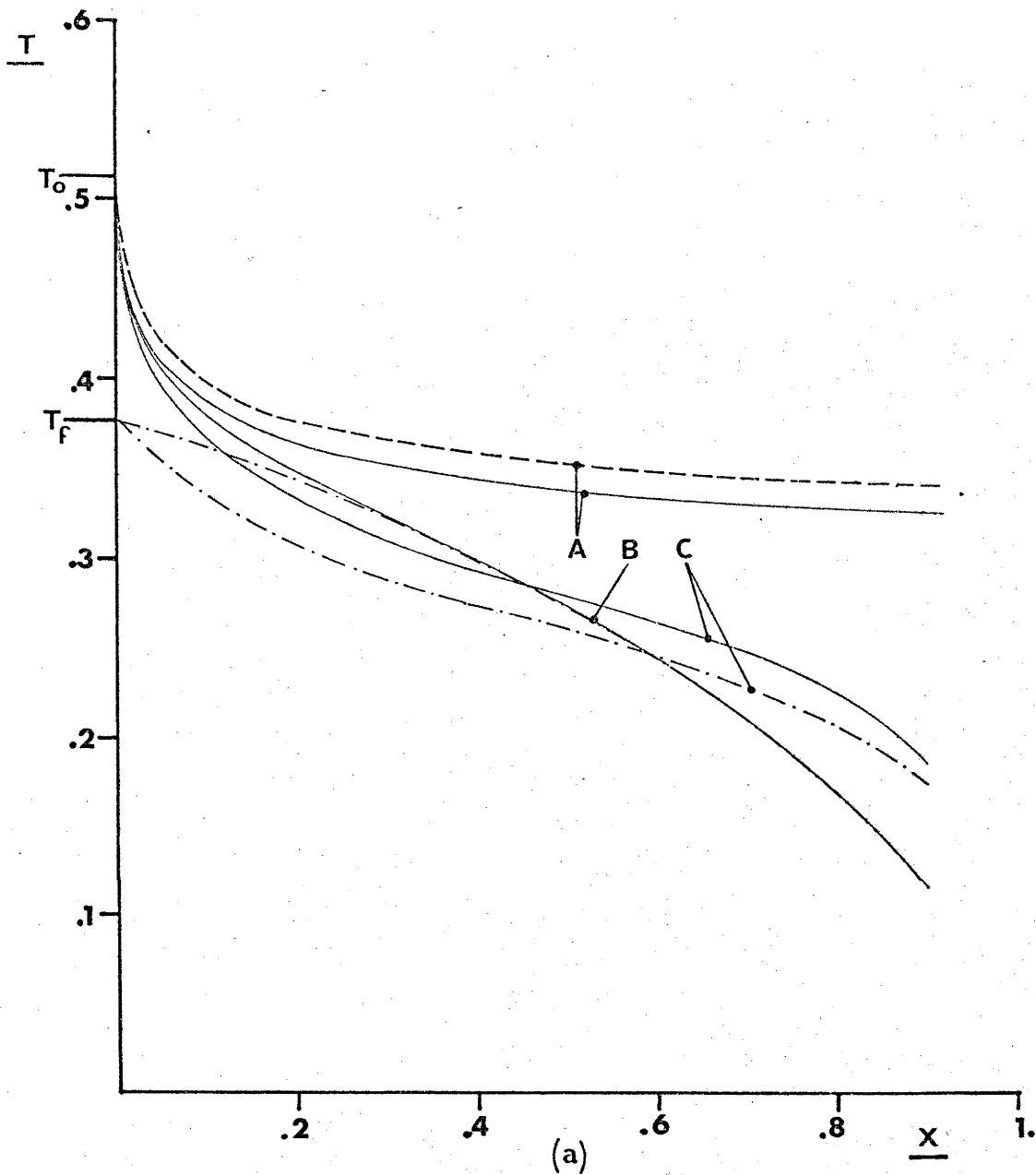


FIGURE 4

$$\Lambda = 10^5$$

$$\Phi = .8$$

$$\alpha_0 = 0$$

$$\eta = 0$$

$$\epsilon = 1/8$$

$$a = 5$$

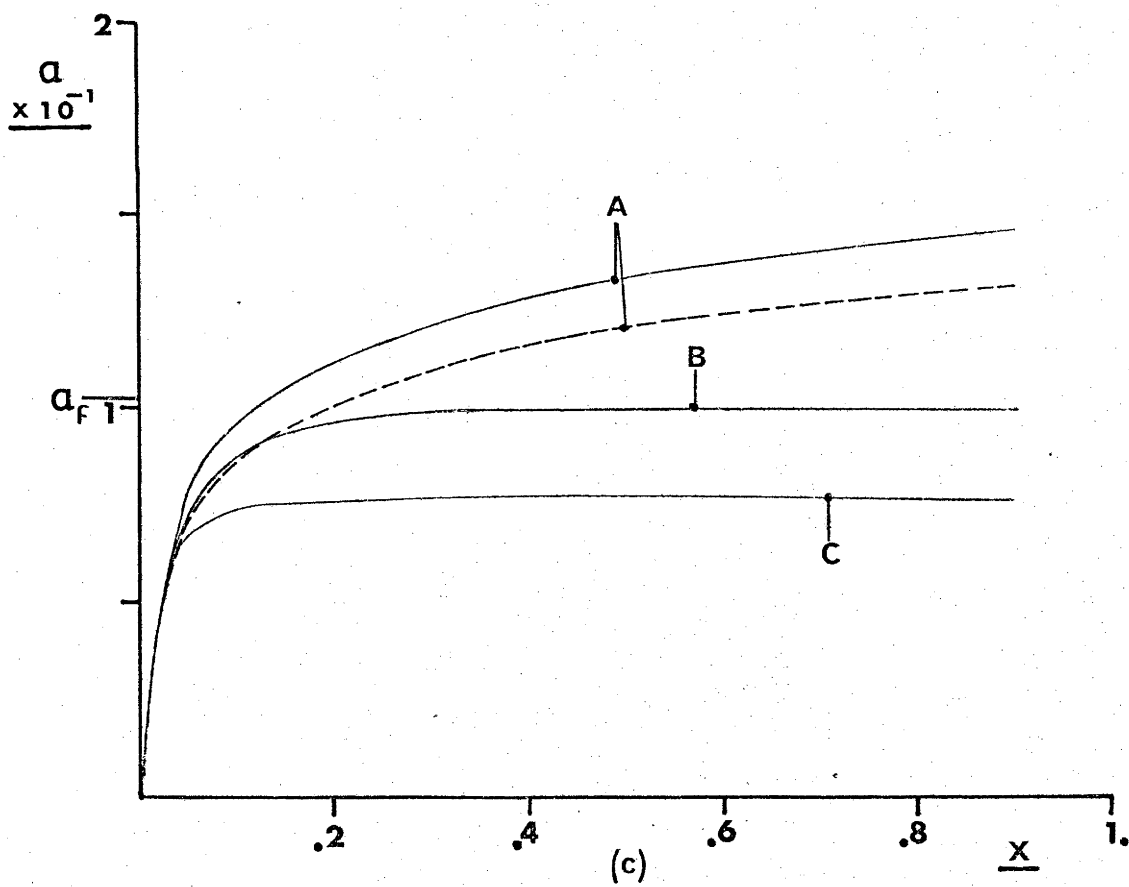
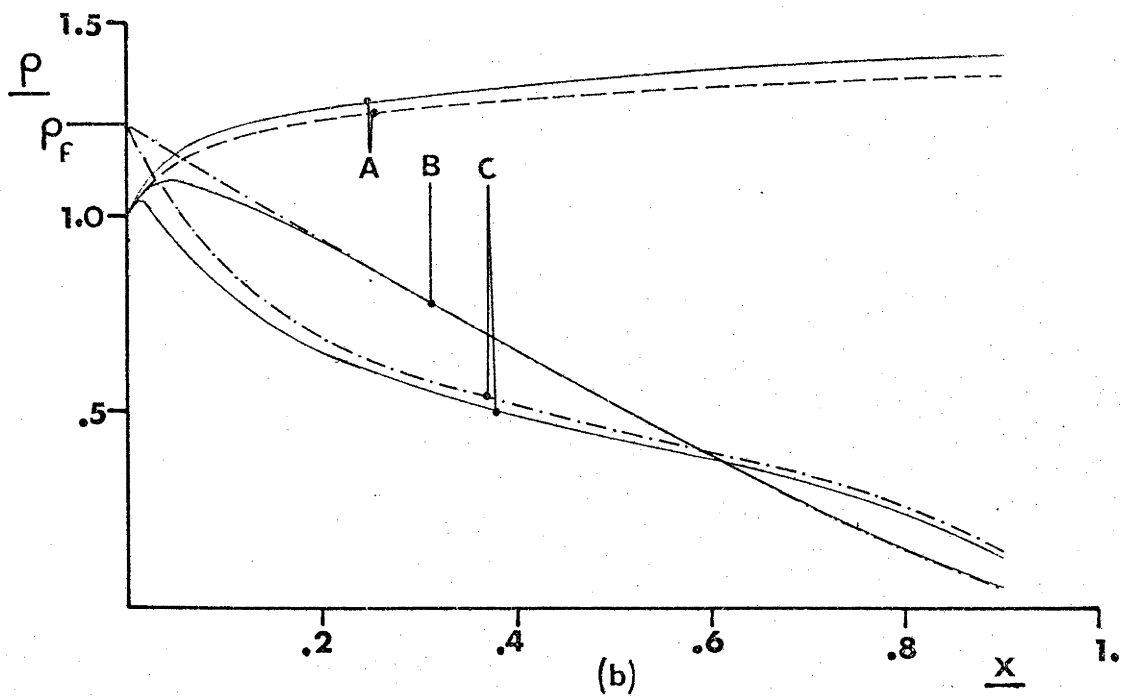


FIGURE 4 (cont.)

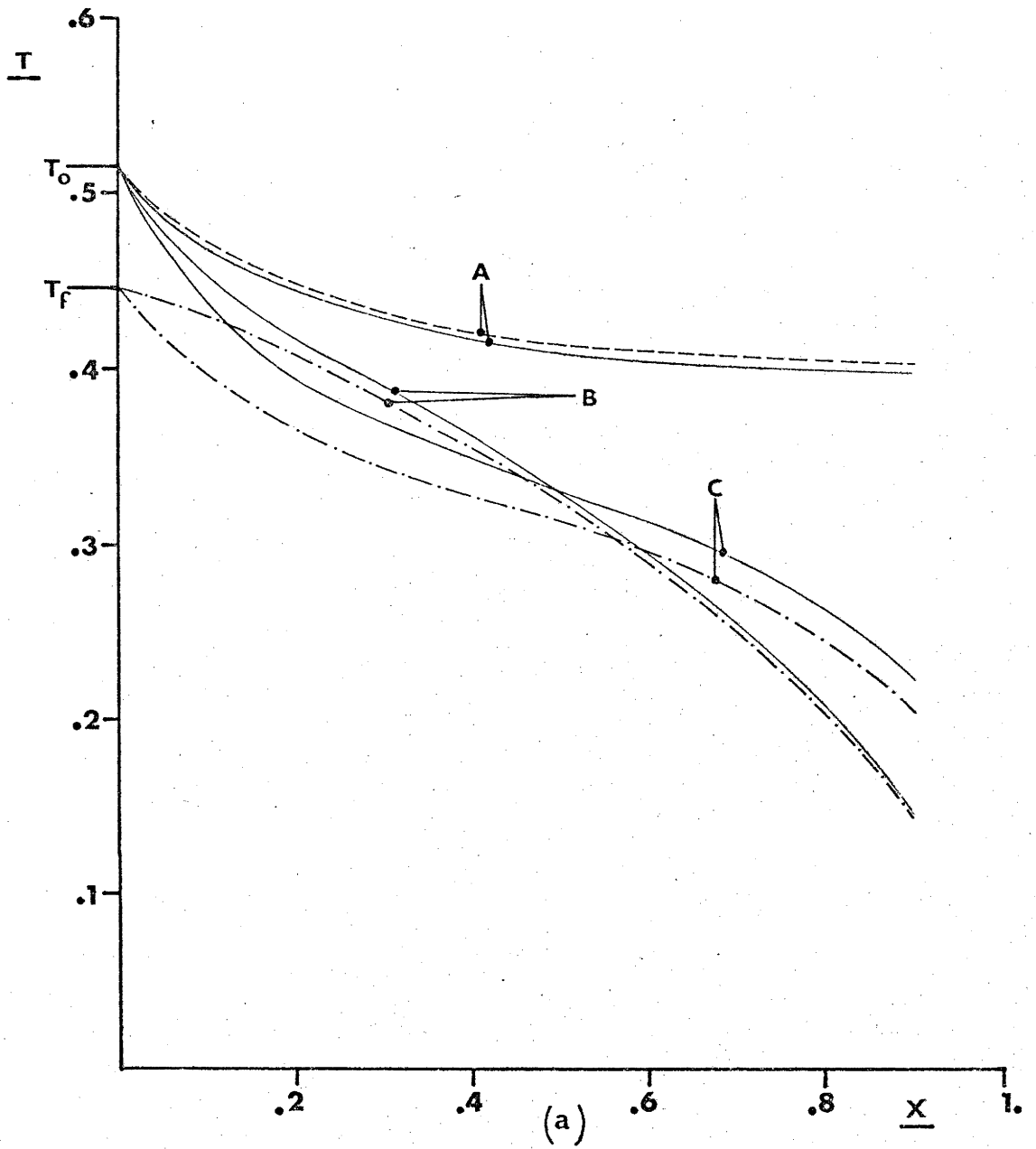


FIGURE 5

$\Lambda = 10^4$
 $\Phi = .8$
 $Q_0 = 0$
 $\eta = 0$
 $\varepsilon = 1/8$
 $a = 5$

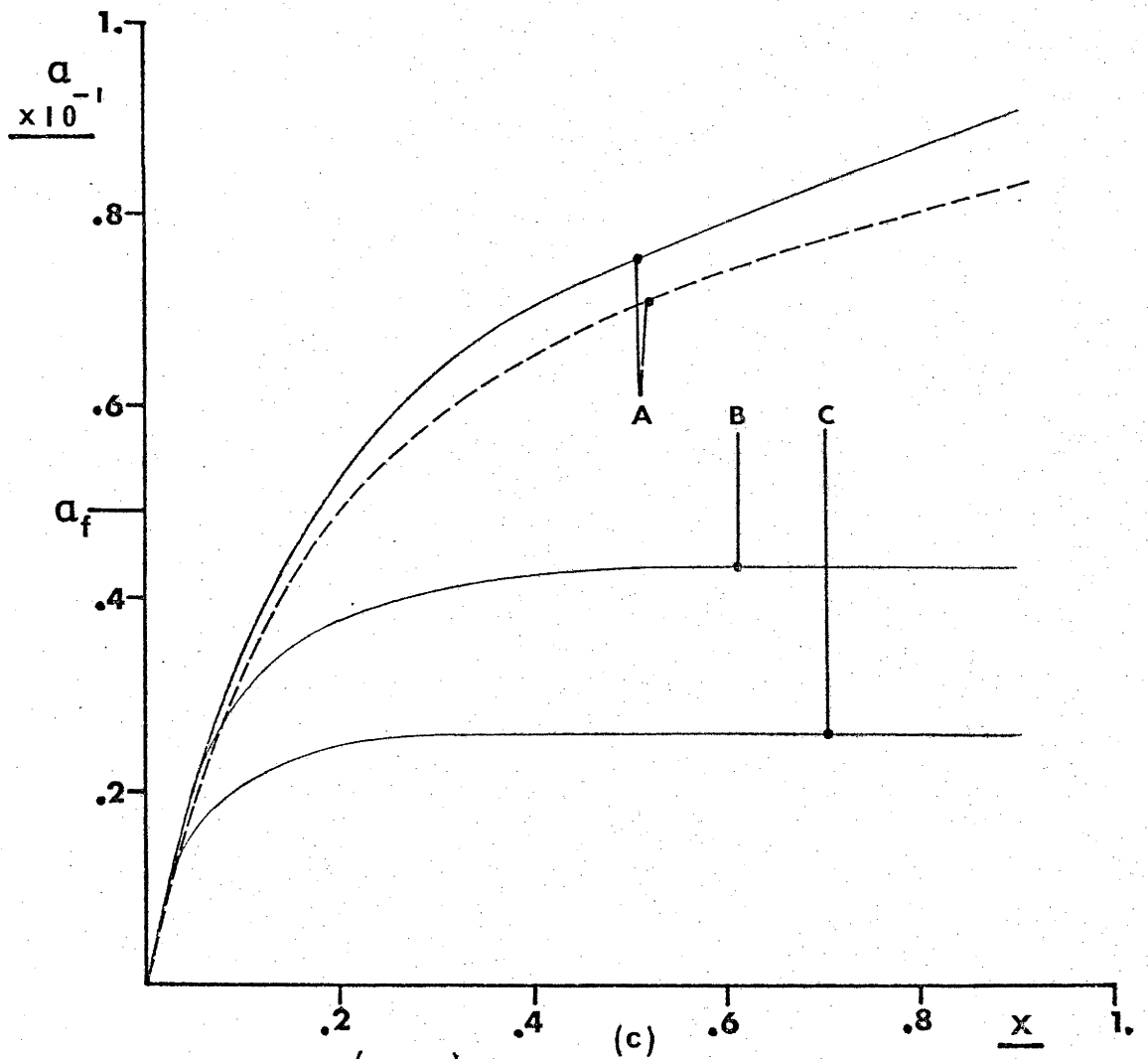
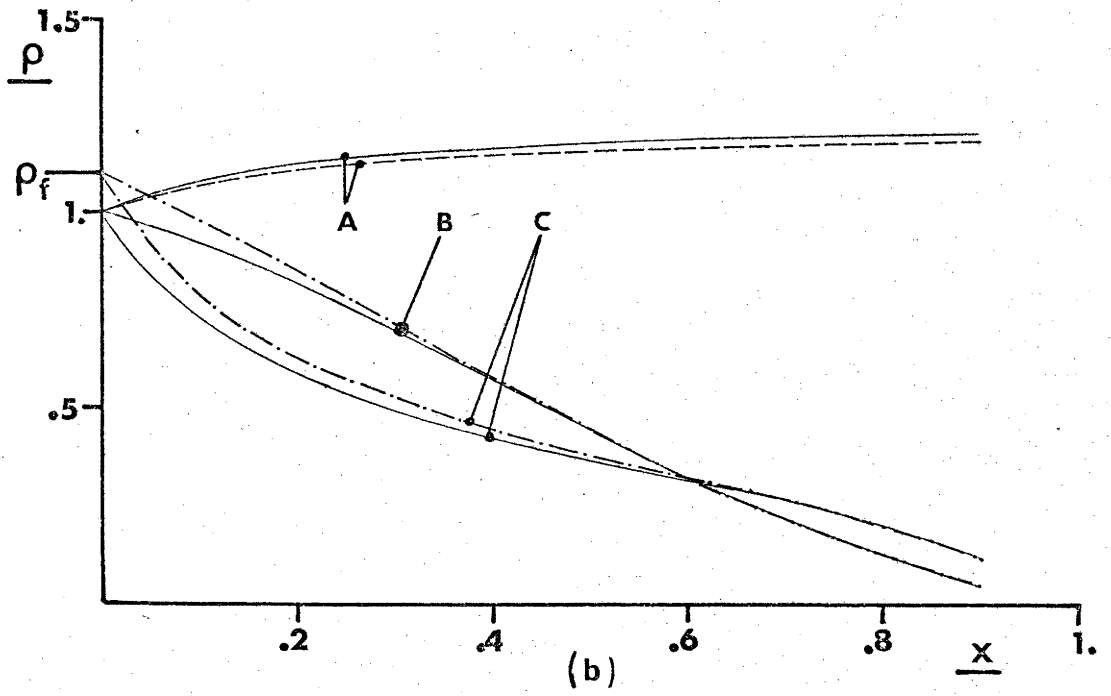


FIGURE 5 (cont.)

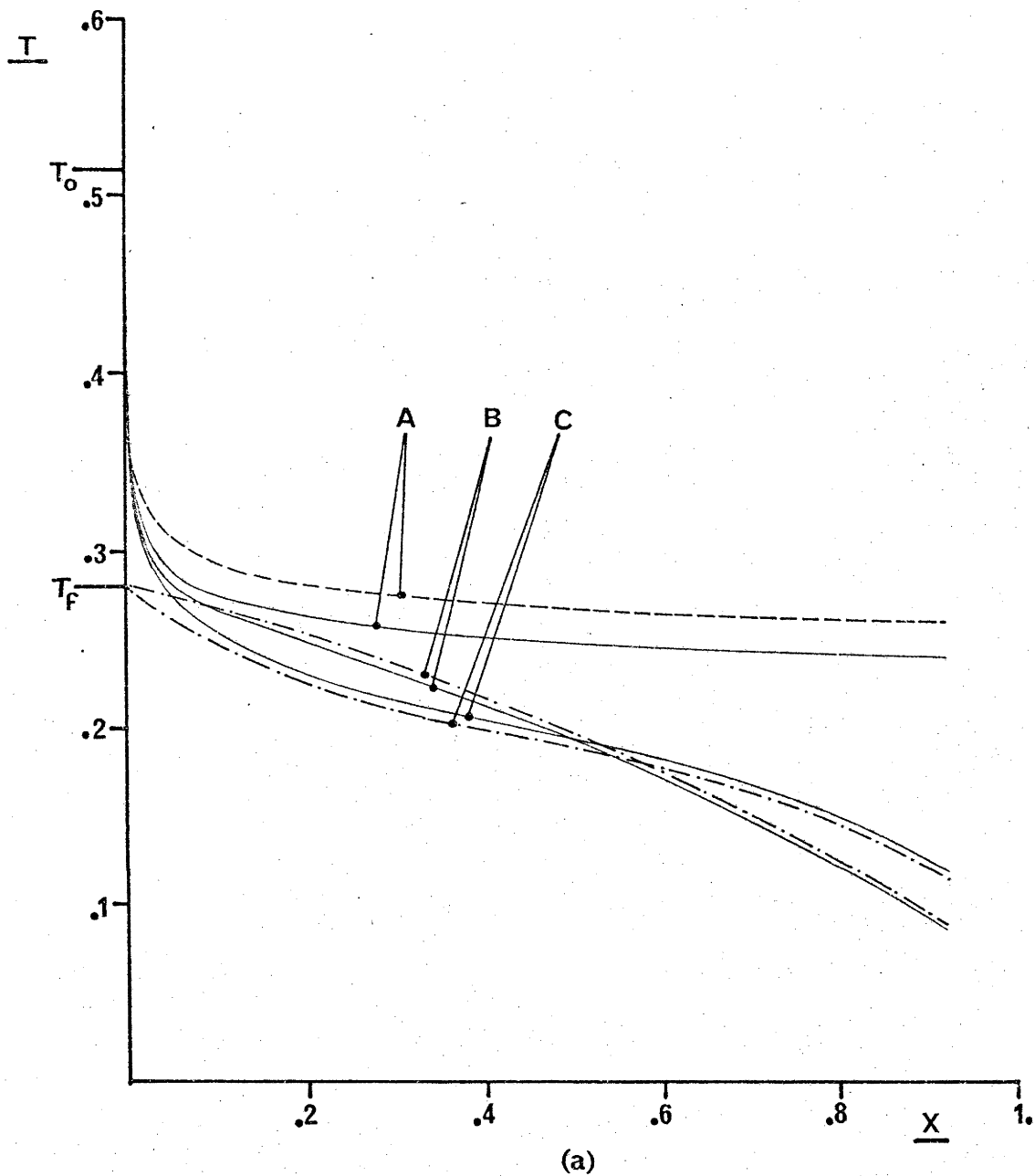


FIGURE 6

$$\Lambda = 10^7$$

$$\Phi = .8$$

$$\alpha_0 = 0$$

$$\eta = 0$$

$$\epsilon = 1/8$$

$$a = 5$$

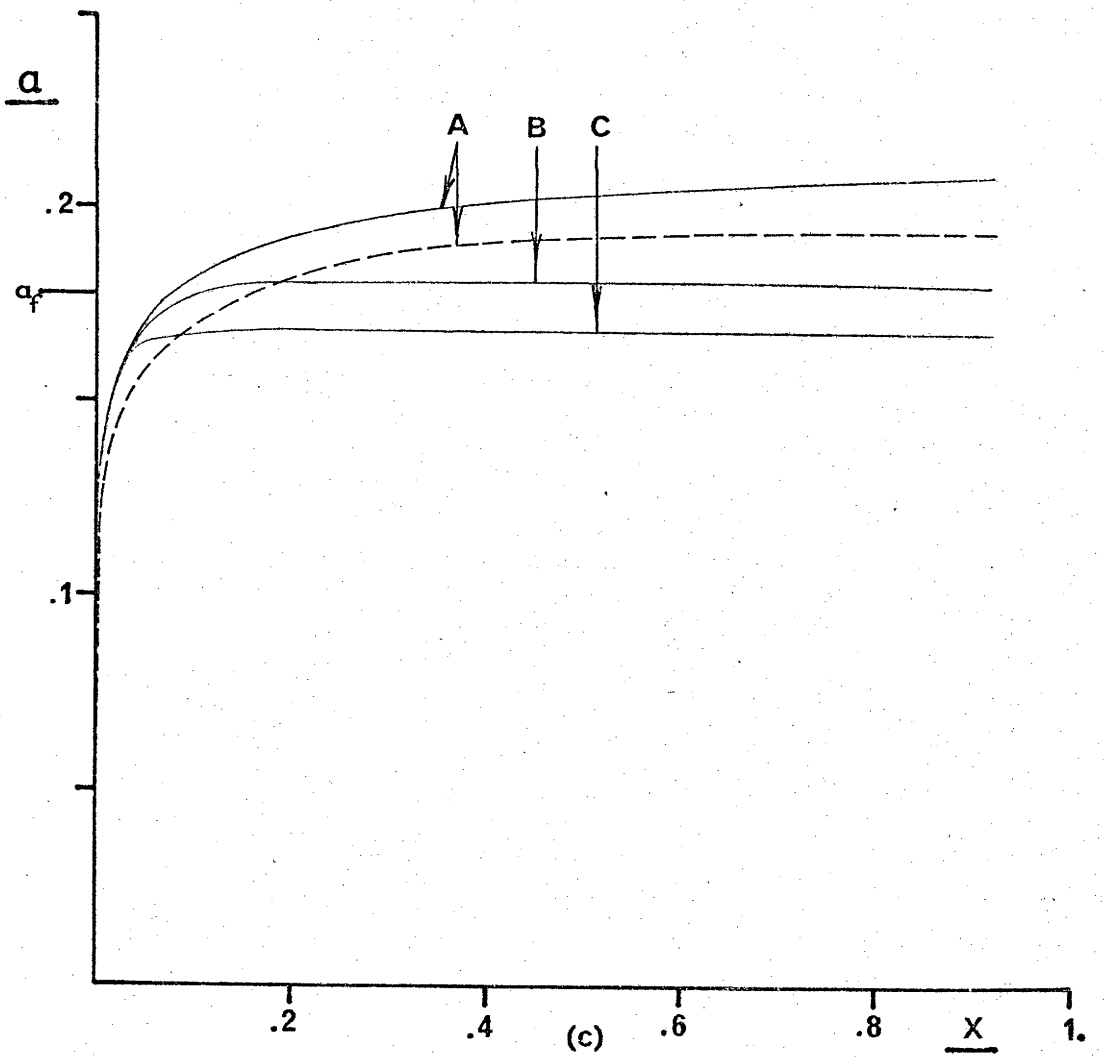
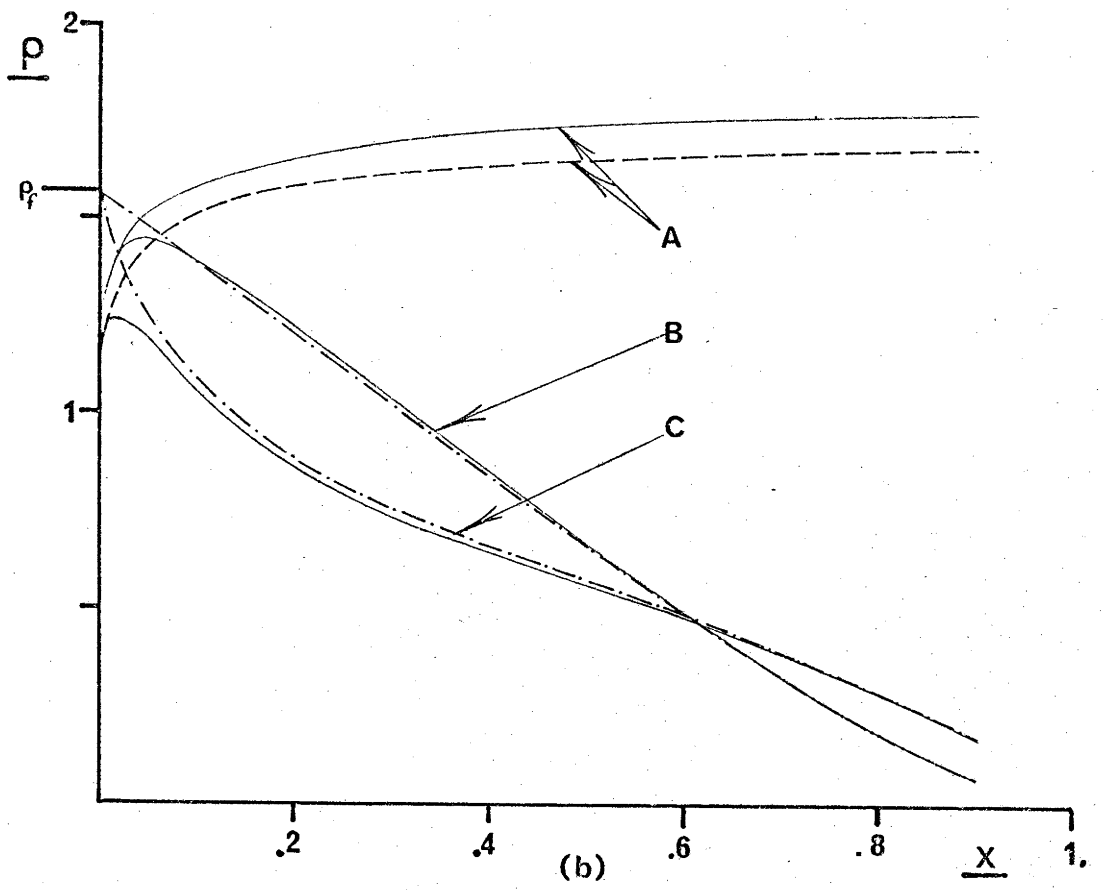


FIGURE 6 (cont.)

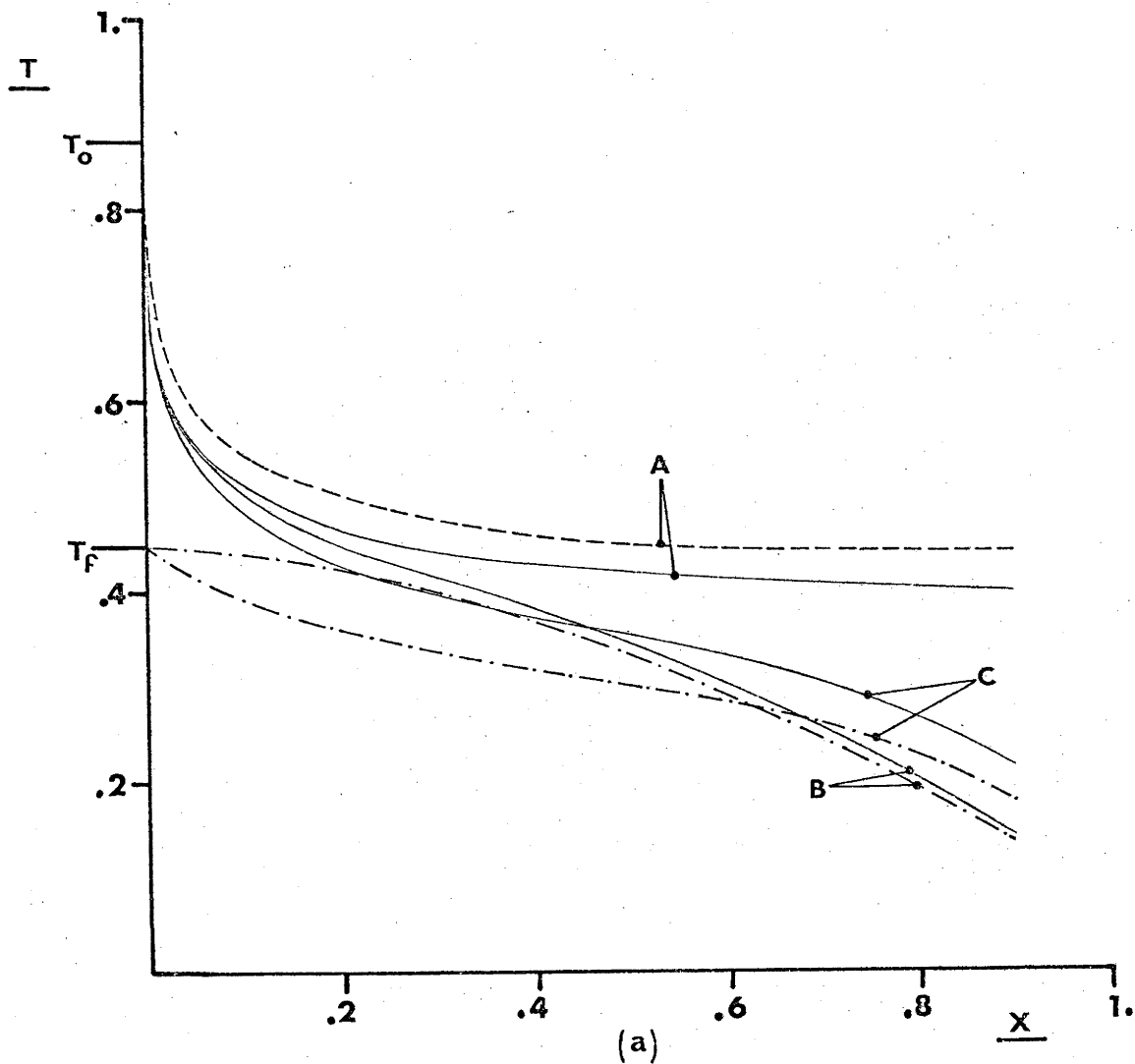


FIGURE 7

$\Lambda = 10^4$
 $\Phi = 1.2$
 $\alpha_0 = 0$
 $\eta = 0$
 $\epsilon = 1/8$
 $a = 5$

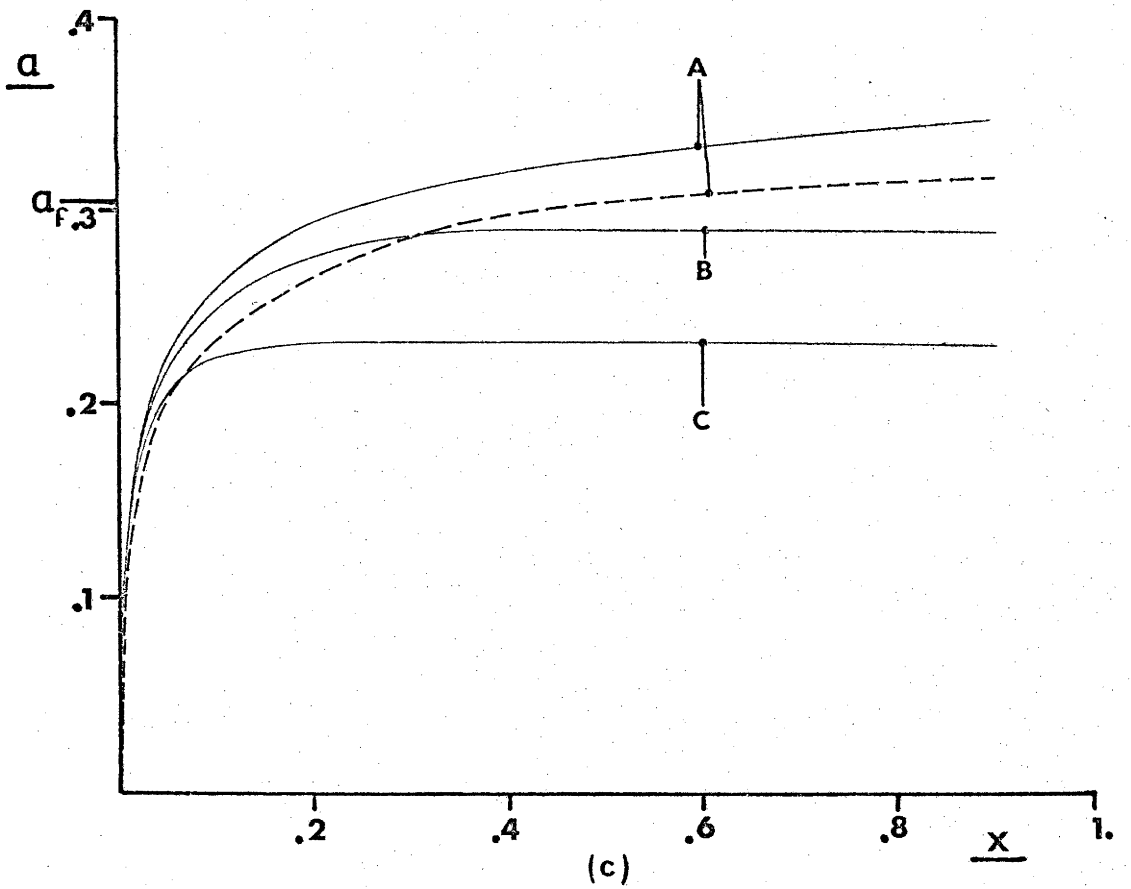
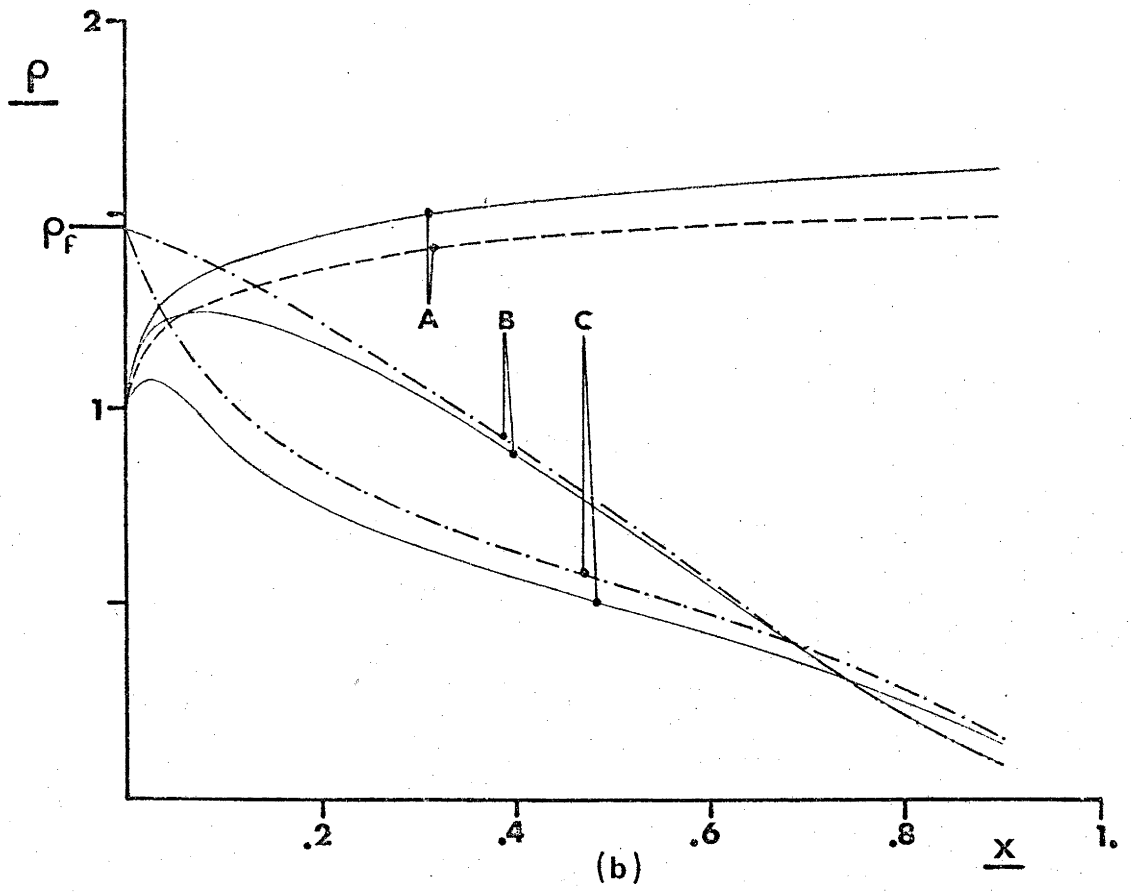


FIGURE 7 (cont.)

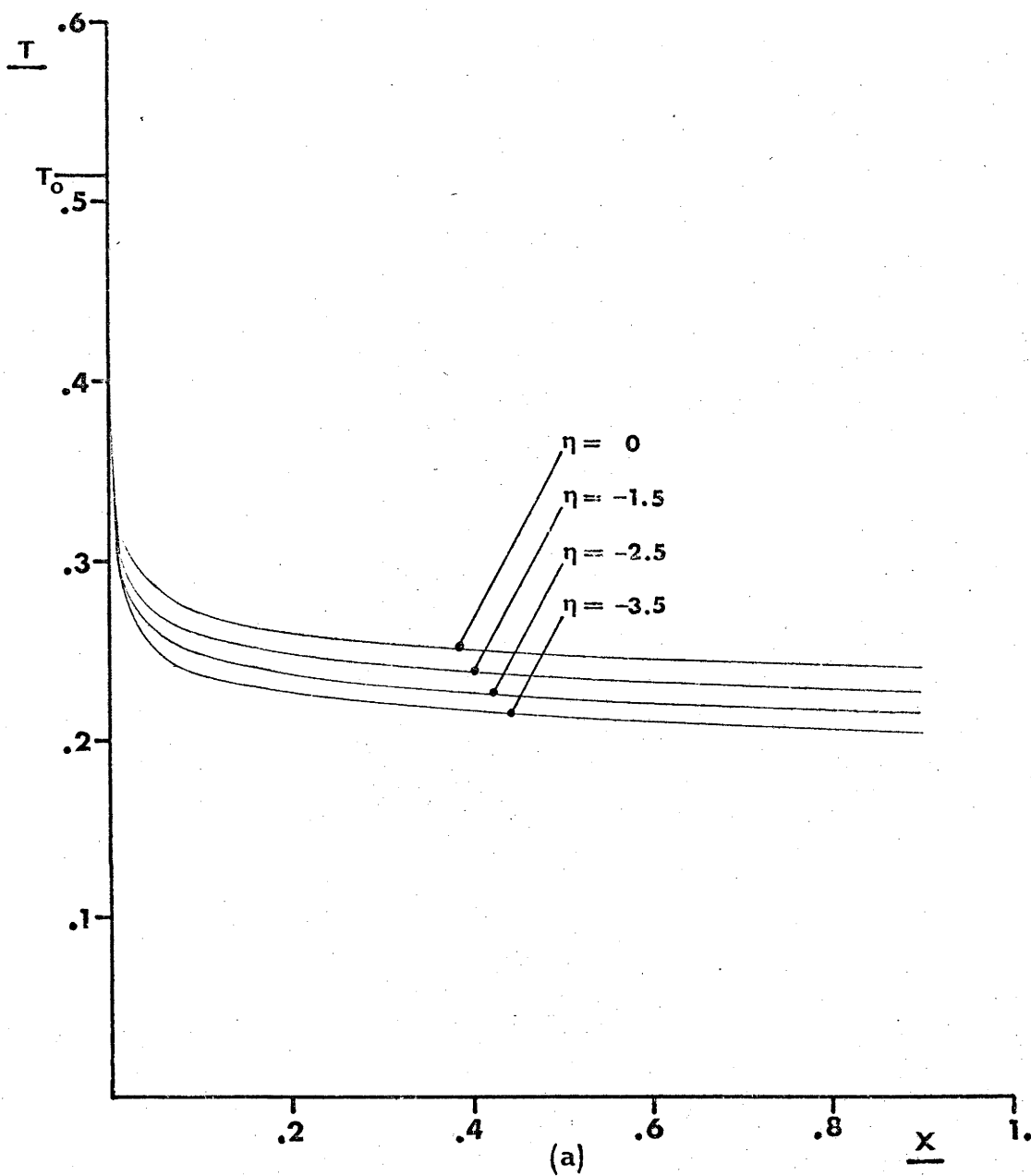


FIGURE 8

The effect of η on a computed solution.

Zero pressure gradient.

$$\Lambda = 10^7$$

$$\Phi = .8$$

$$a_0 = 0$$

$$\epsilon = 1/8$$

$$a = 5$$

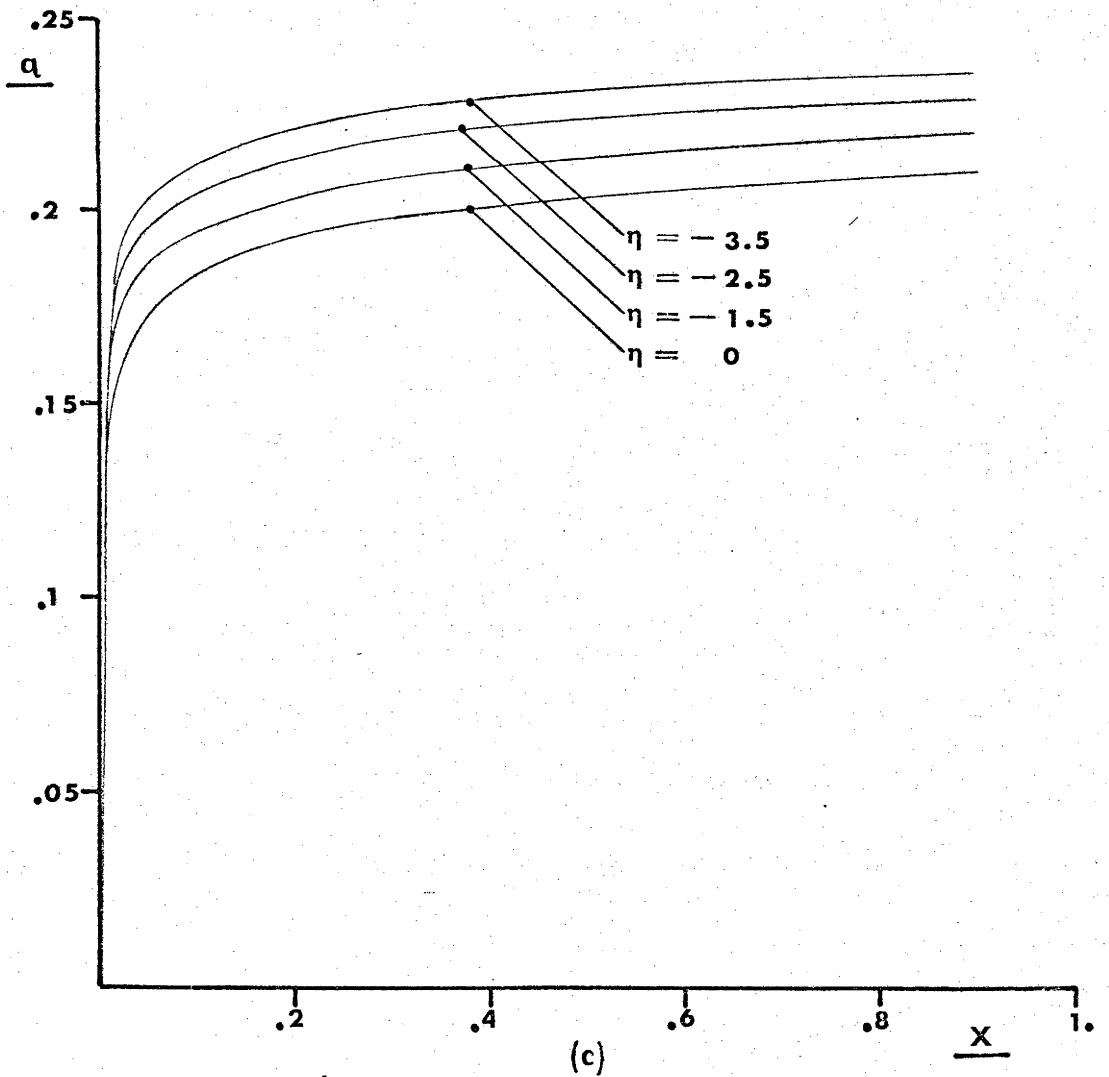
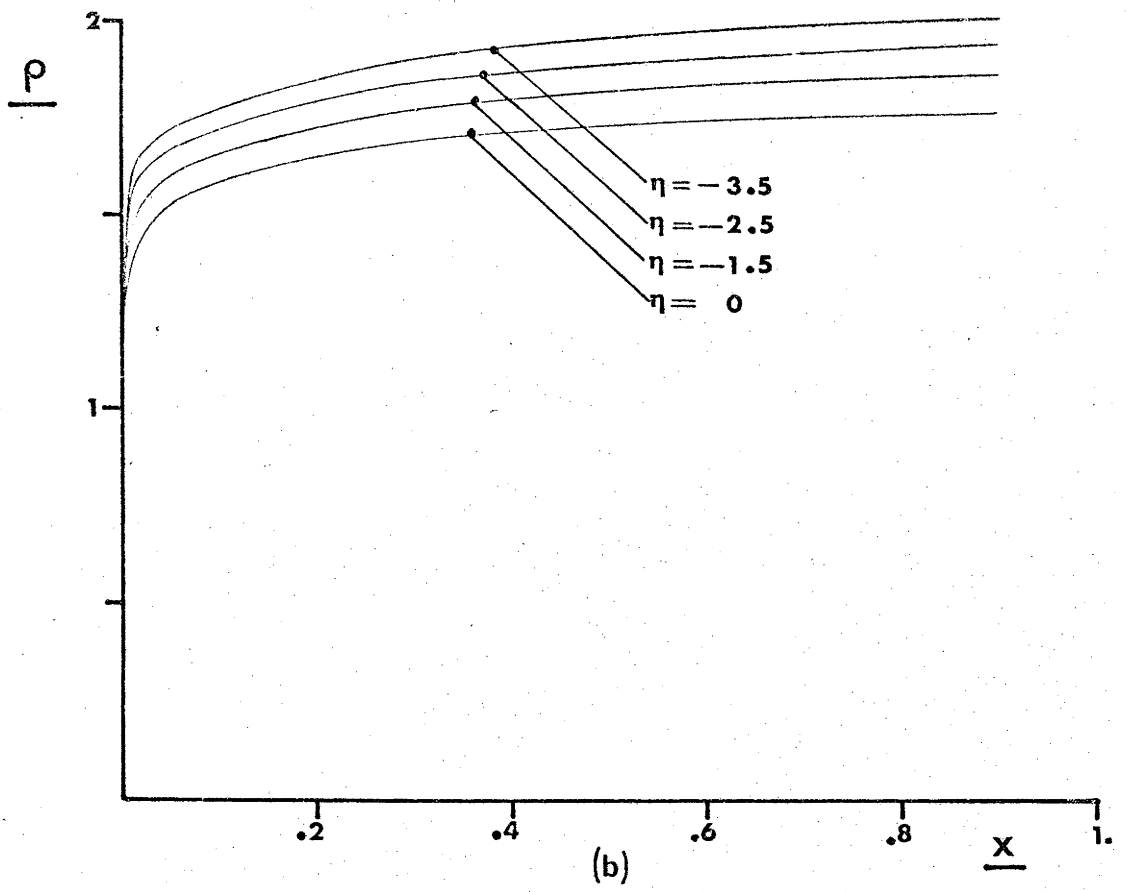


FIGURE 8 (cont.)

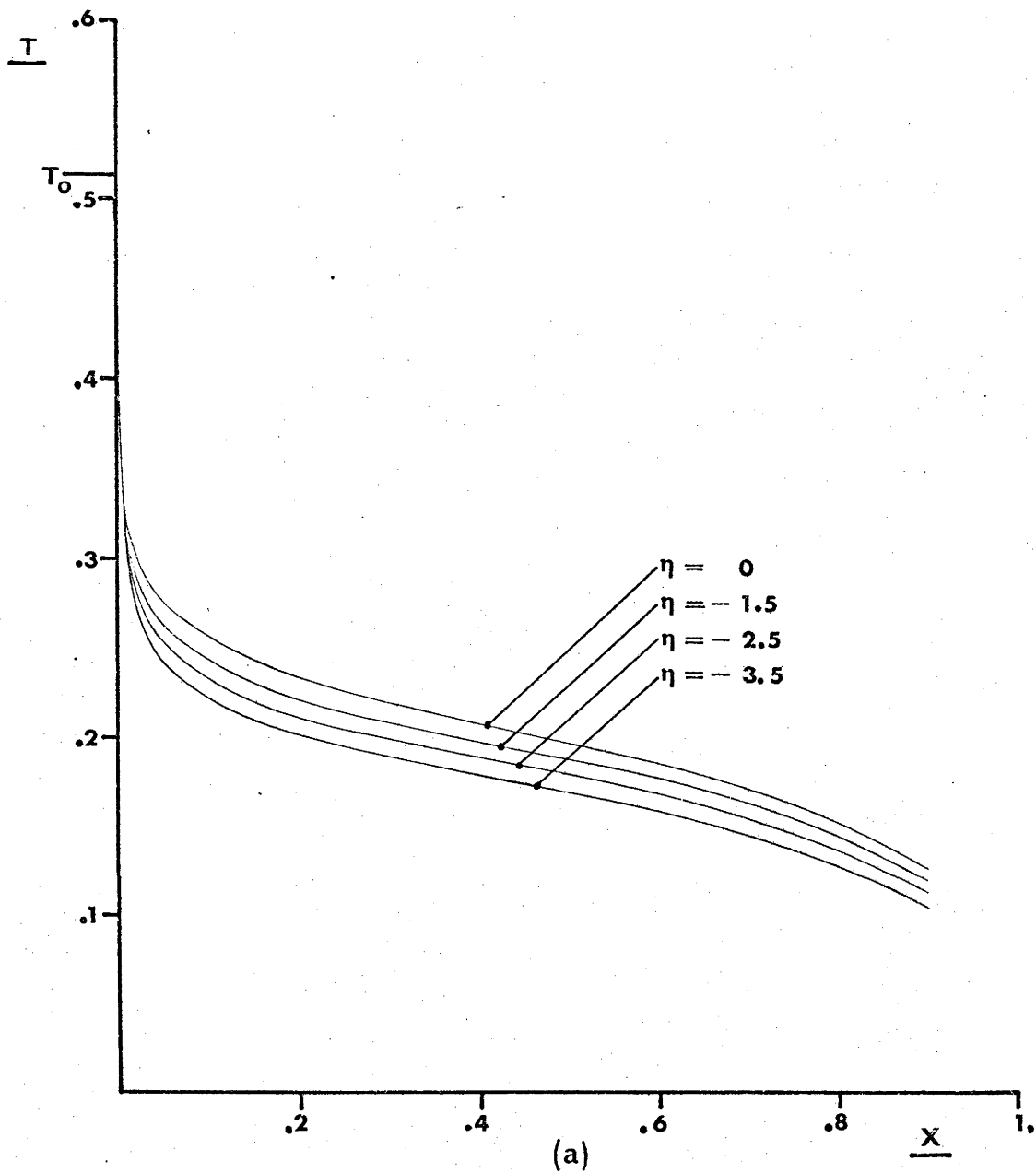


FIGURE 9

The effect of η on a computed solution.
 Pressure gradient given by equation 39.

$$\Lambda = 10^7$$

$$\Phi = .8$$

$$\alpha_0 = 0$$

$$\epsilon = 0$$

$$a = 1/8$$

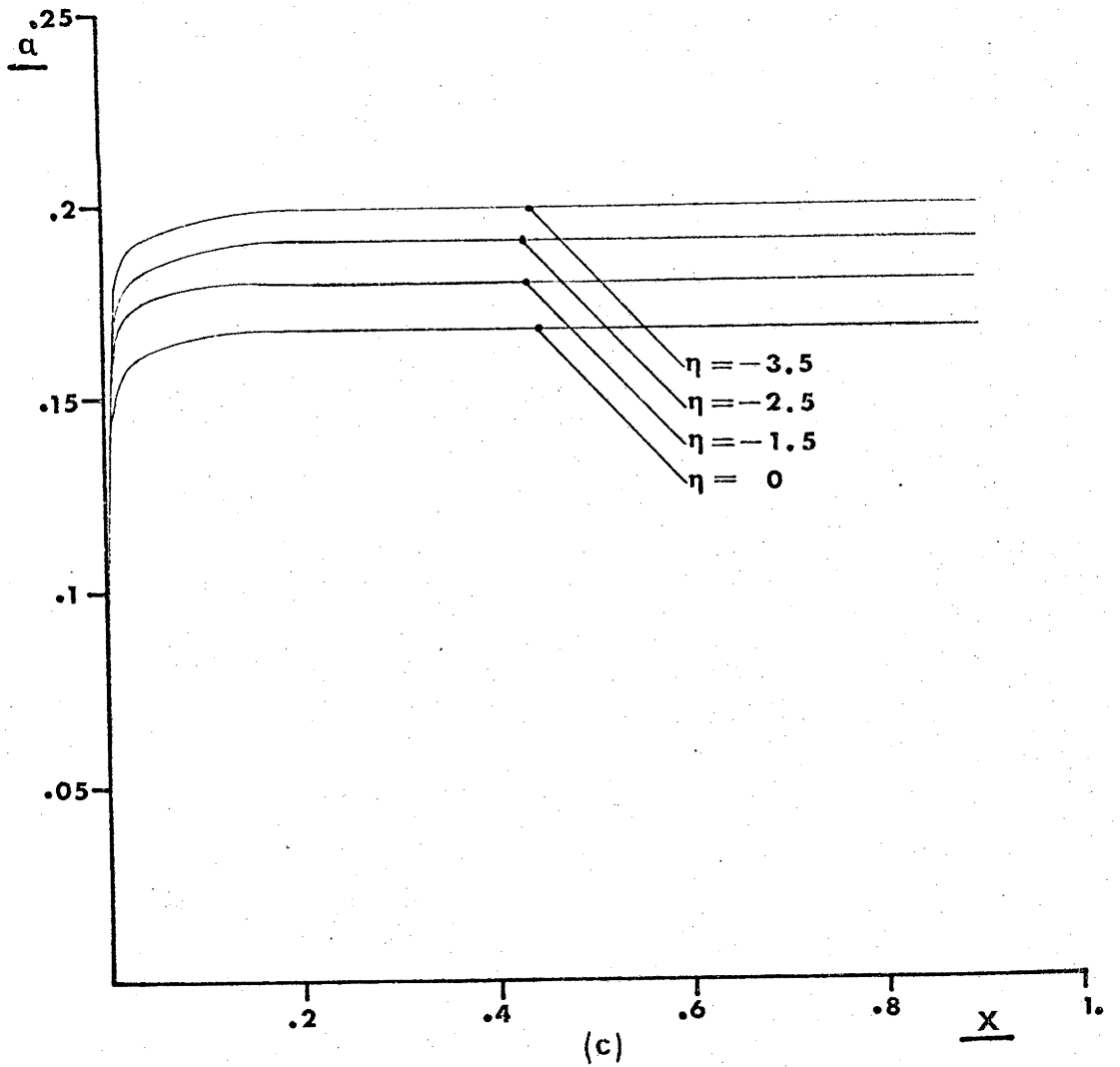
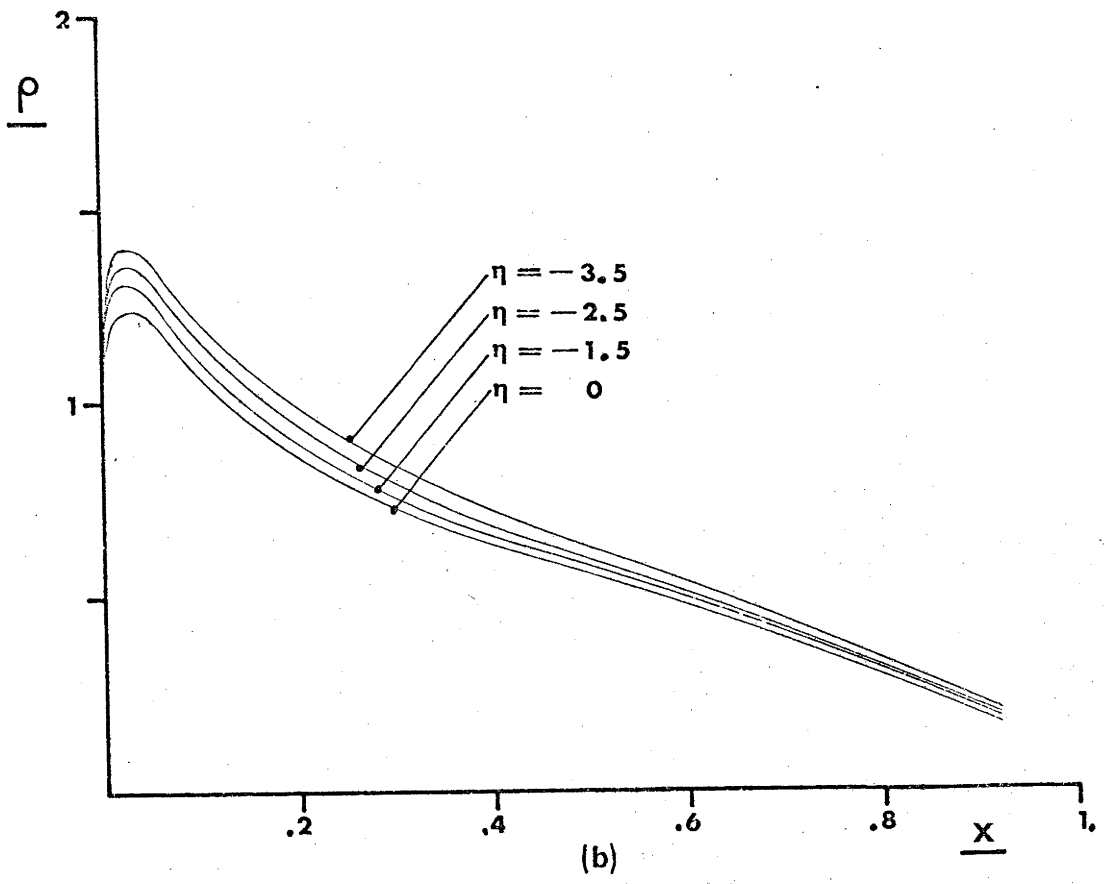


FIGURE 9 (cont.)

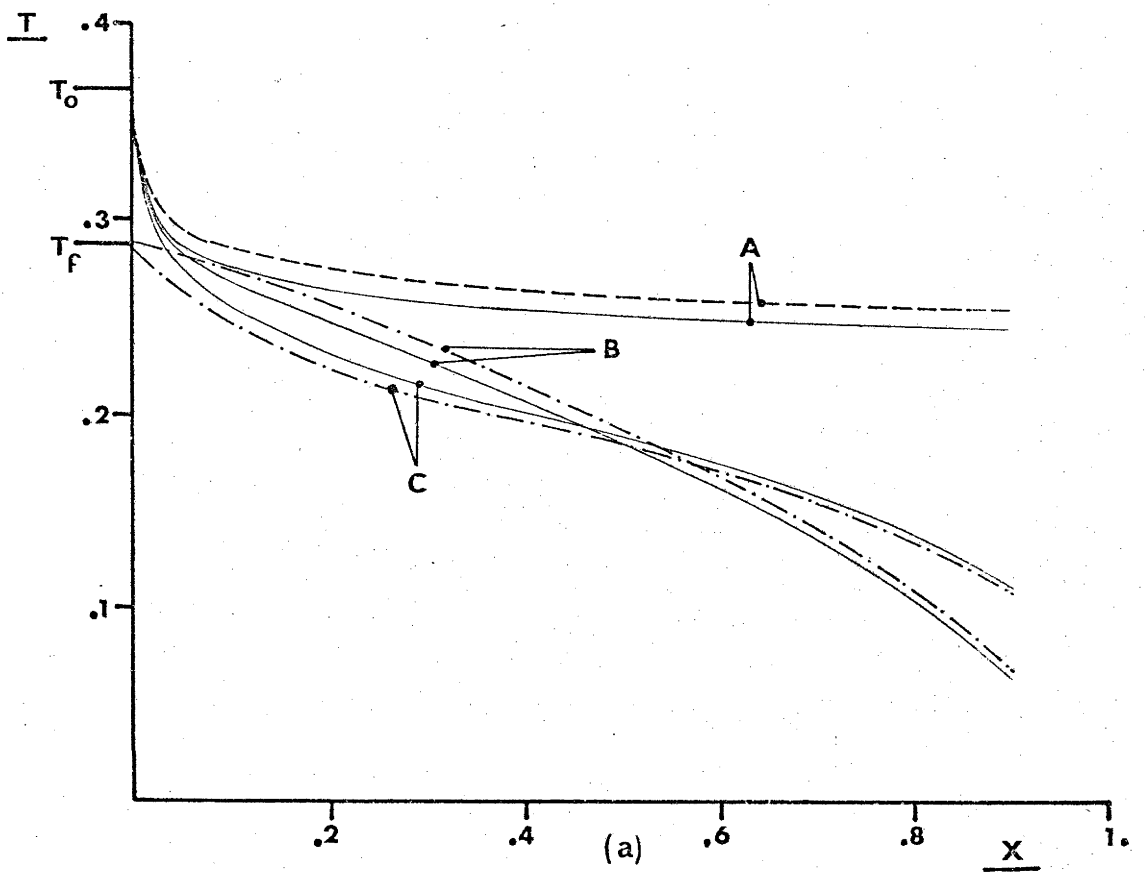


FIGURE 10

$$\Lambda = 10^7$$

$$\Phi = .8$$

$$\alpha_0 = .4$$

$$\eta = 0$$

$$\epsilon = 1/8$$

$$a = 5$$

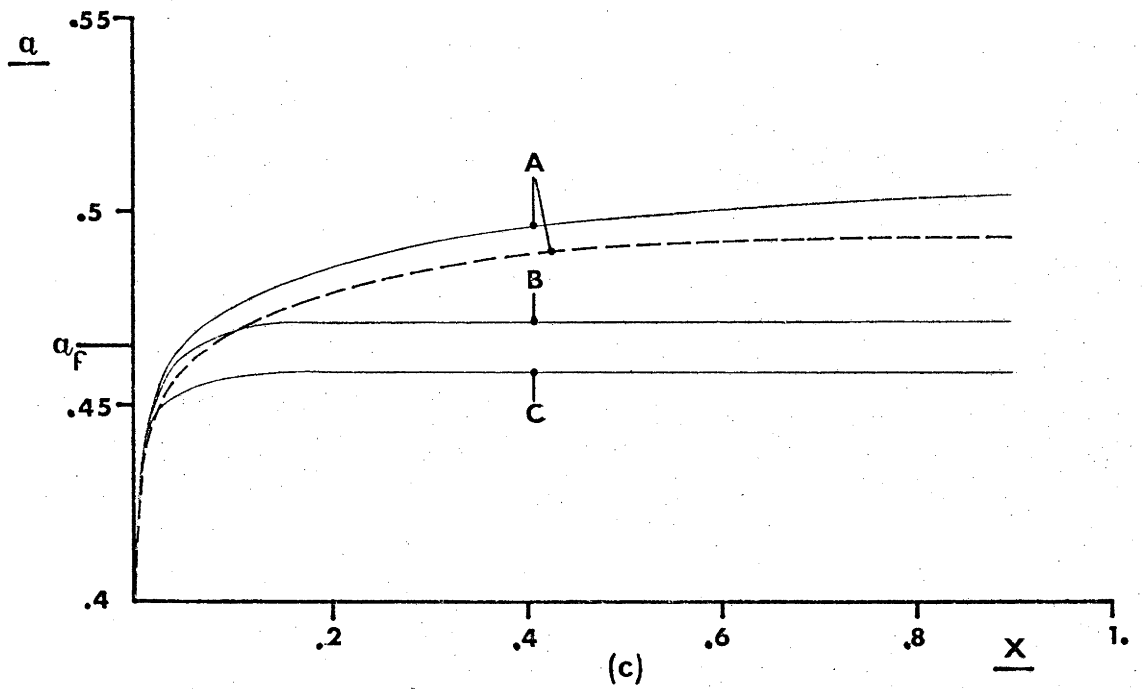
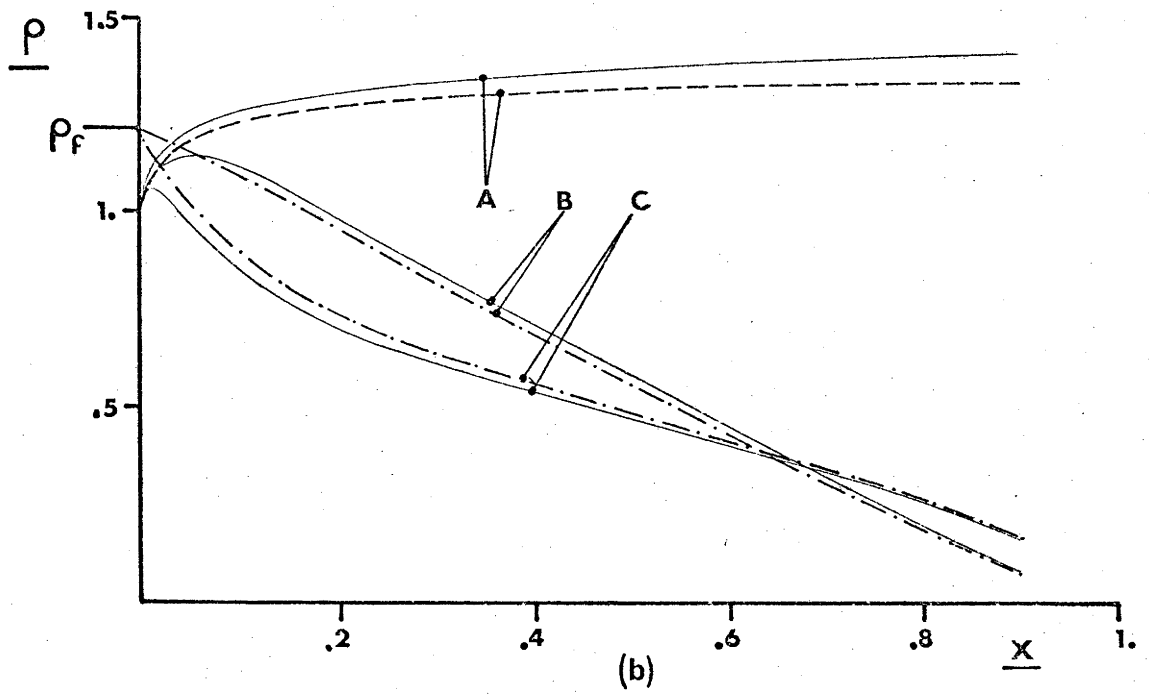


FIGURE 10 (cont.)

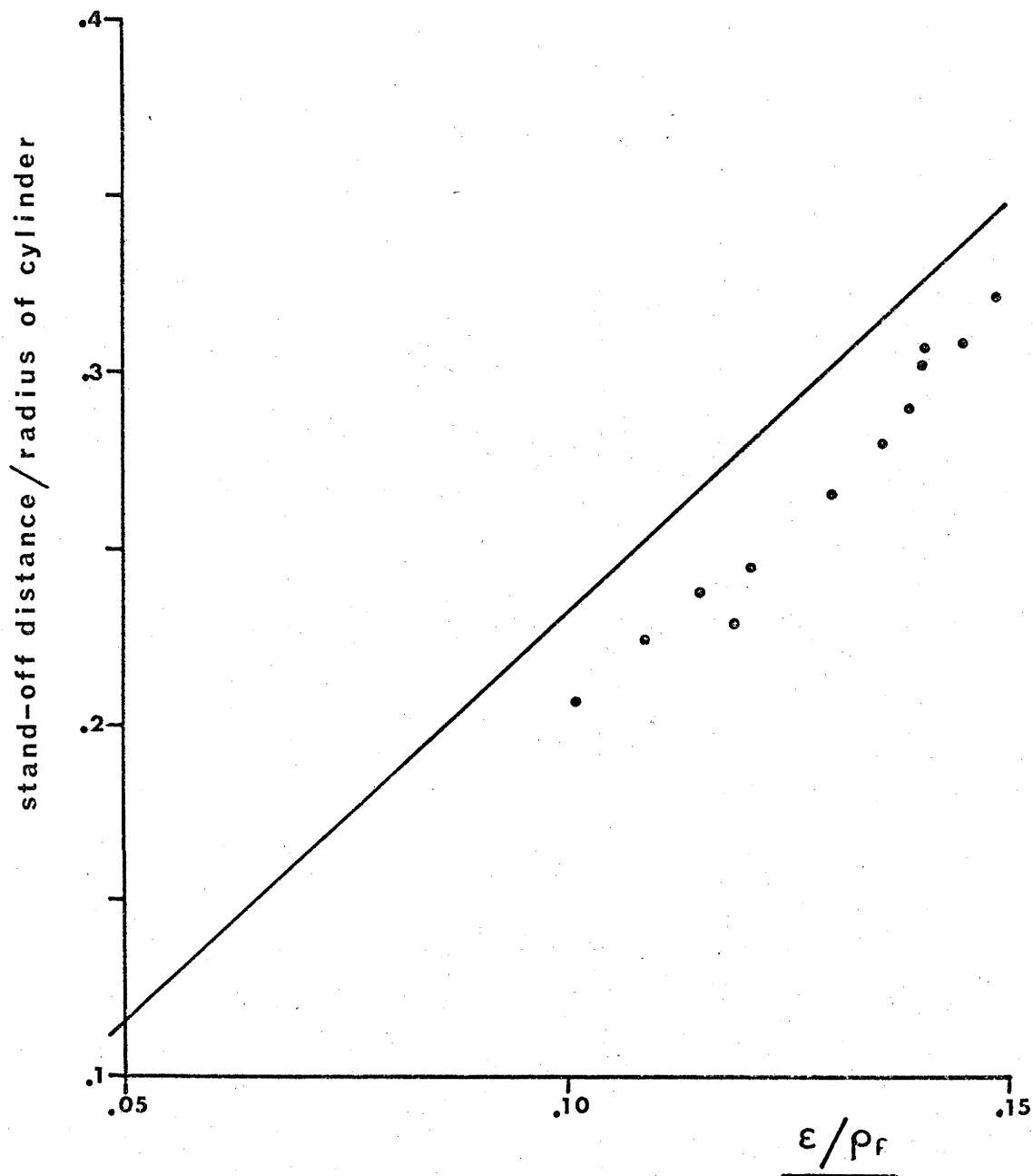


FIGURE 11

Correlation of computed shock stand-off distance for flow over a cylinder using normal shock relations to calculate ρ_F .

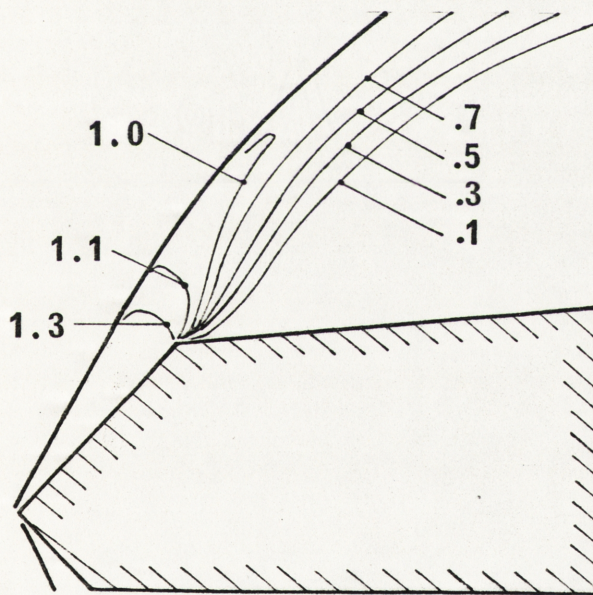
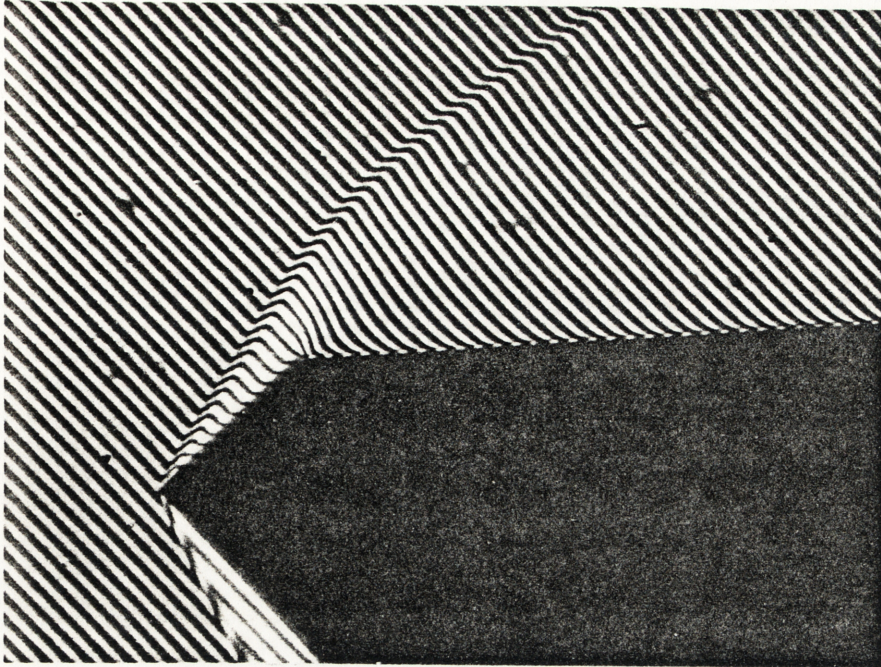


FIGURE 12

Interferogram and derived
fringe shift contours of flow
over a wedge with expansion
corner.

$d = 1.0 \text{ cm.}$

$P_r = 6 \text{ in. Hg.}$

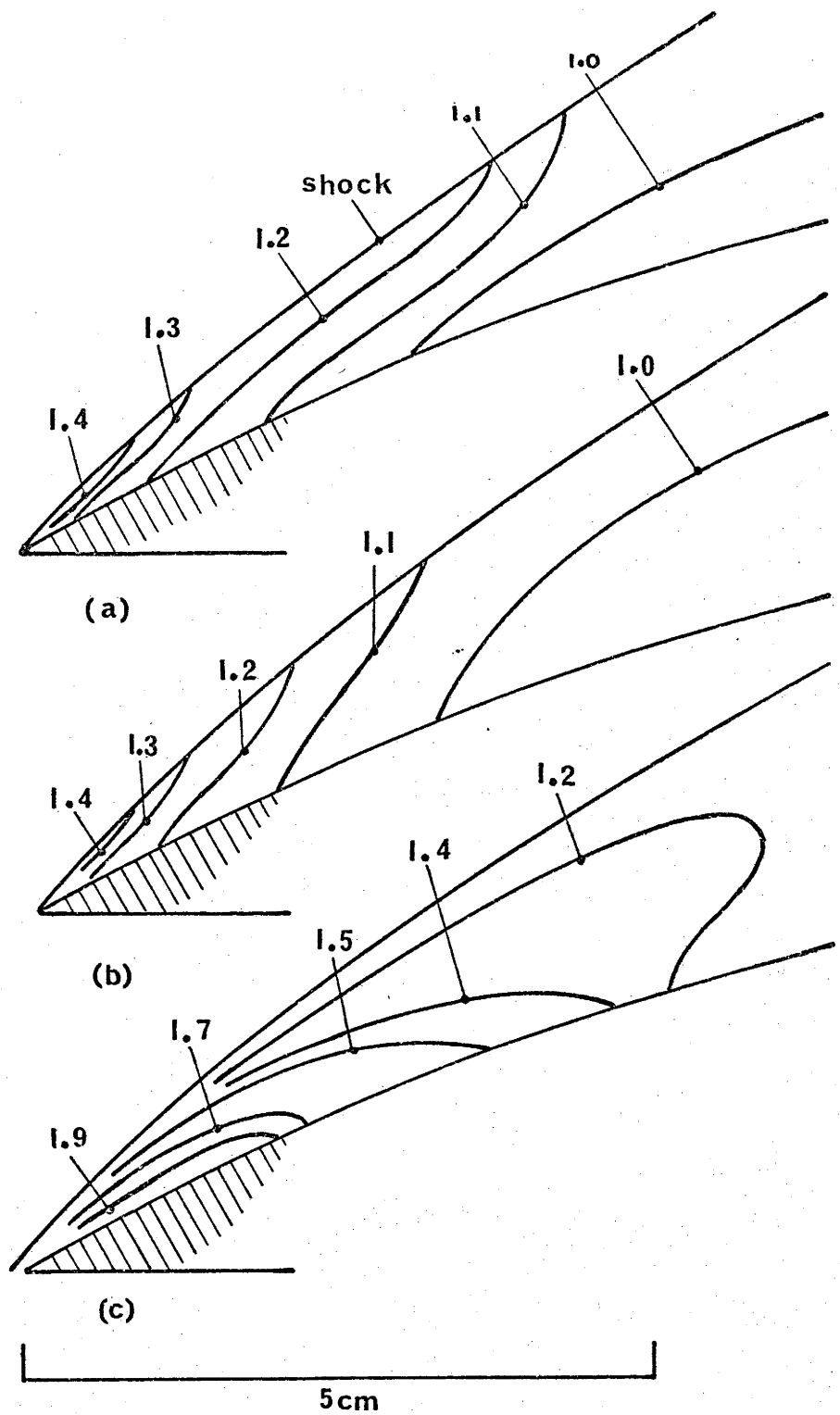


FIGURE 13

Constant fringe contours from interferograms of flow over a wedge with a constant curvature of 1 ft.

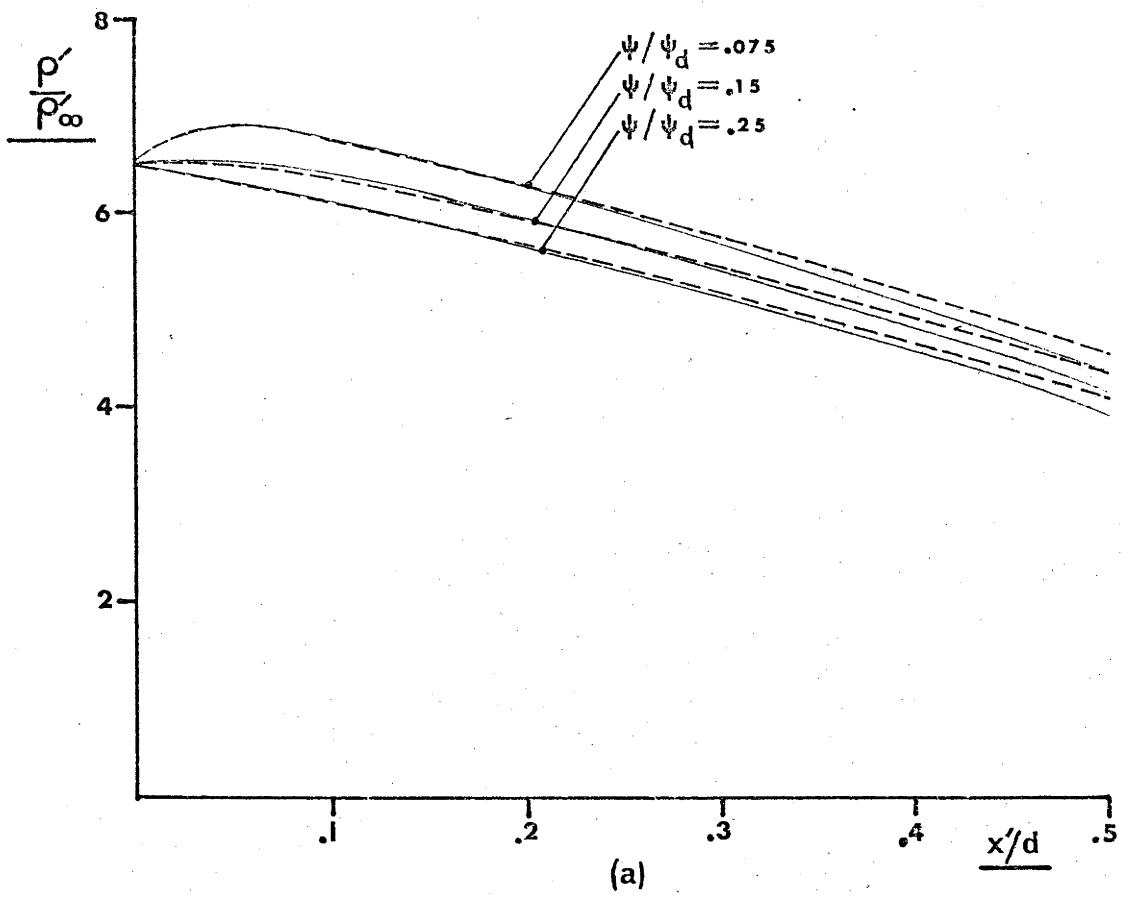
$p_R = 6 \text{ in. Hg.}$

Initial angle of incidence
 = (a) 43° (b) 46° (c) 49° .

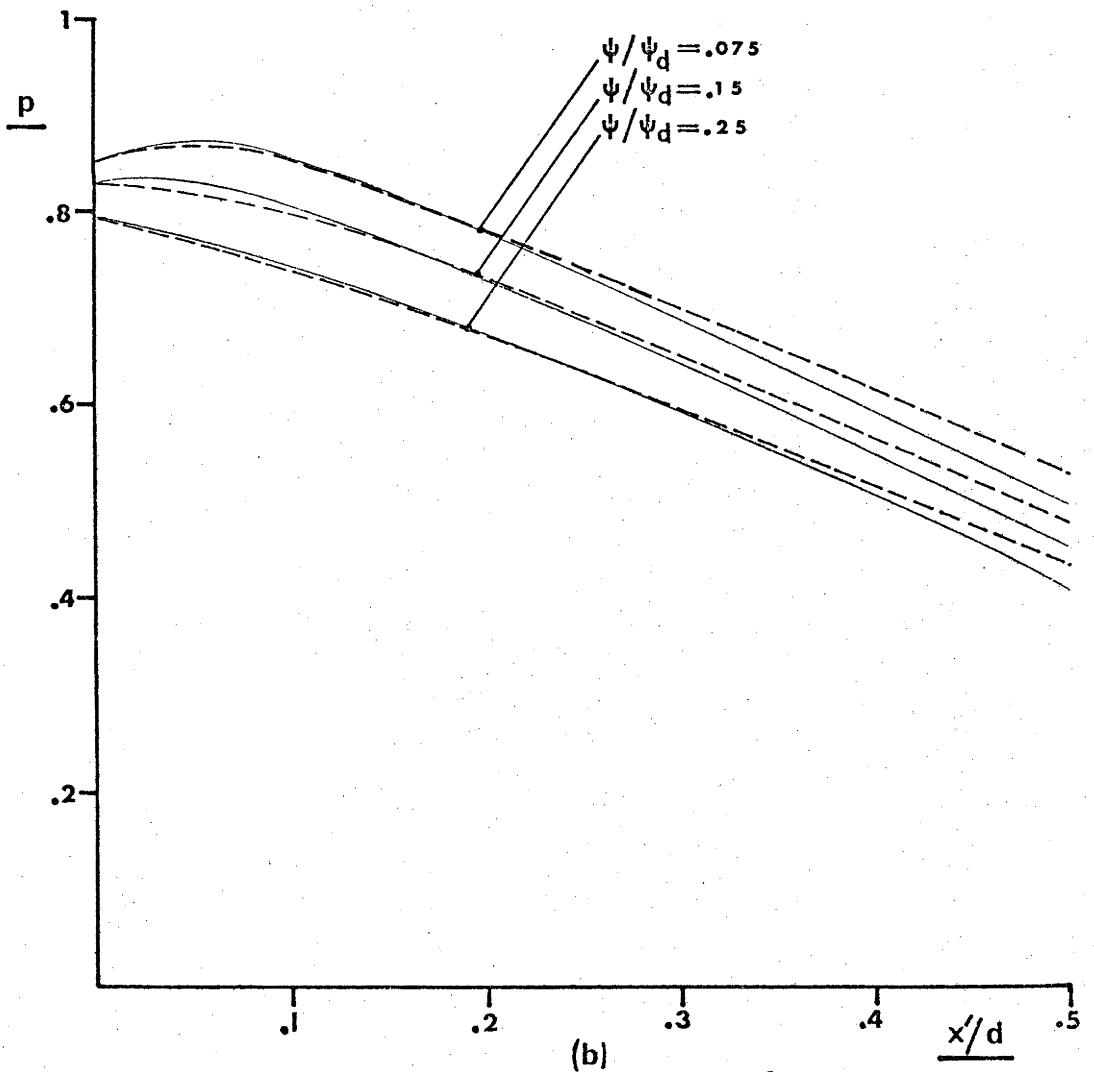
LEGEND TO FIGURE 14

examining the effect of reaction rate on streamline position relative to the density and pressure field calculated with a given reaction rate.

- flow parameter calculated along a streamline with the cylinder diameter (d) as specified.
- flow parameter measured along a streamline shape calculated with $d = 1$ cm, superimposed over the flow field as calculated with the cylinder diameter equal to d .



(a)



(b)

FIGURE 14

(a), (b), $d = 2 \times 10^{-2}$ cm.

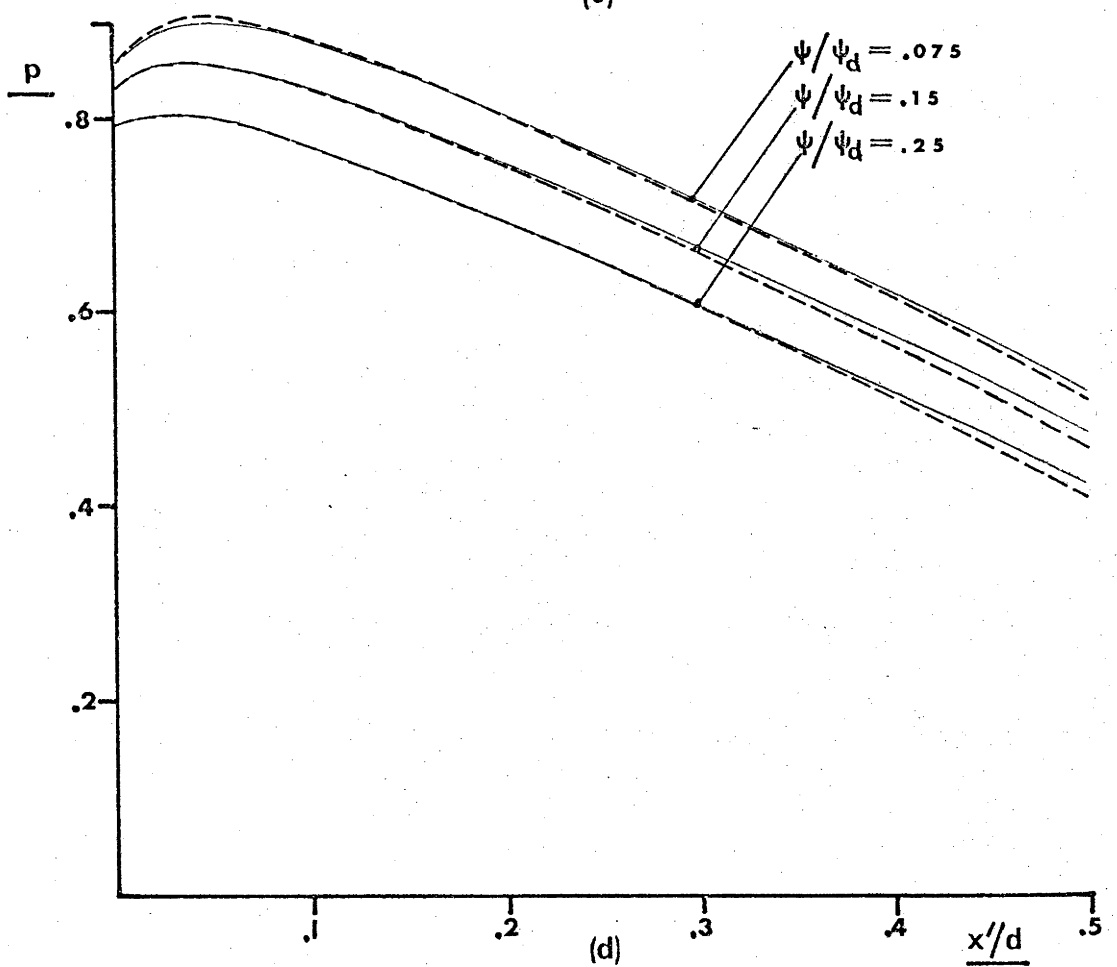
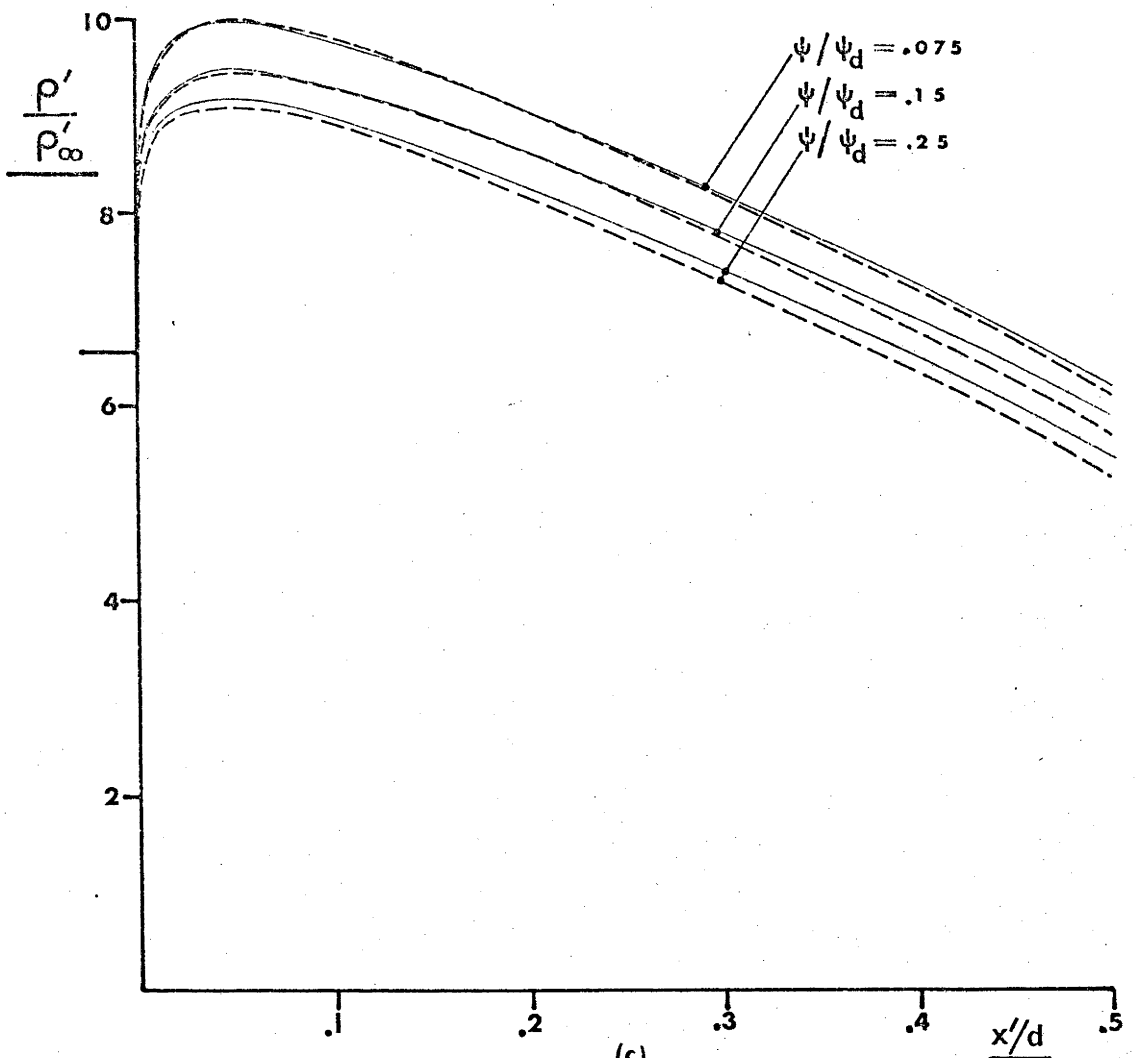
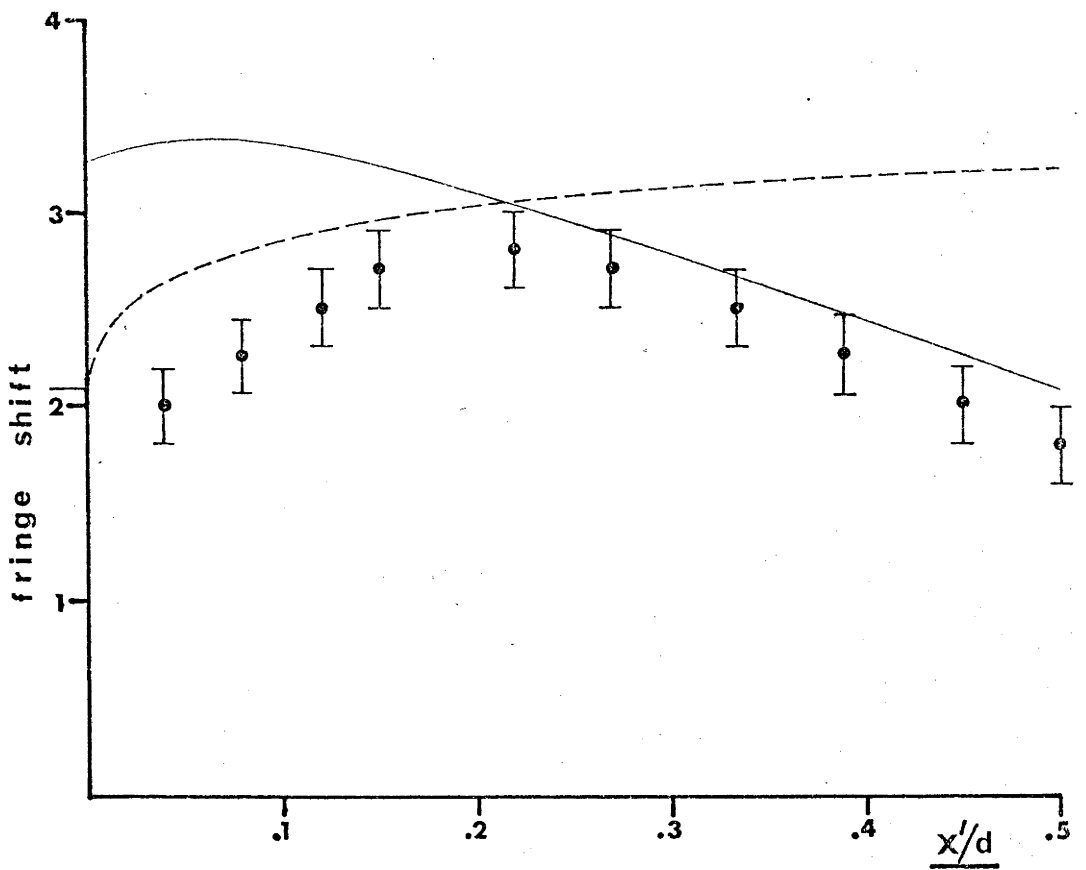


FIGURE 14 (cont.) (c), (d), $d = 20$ cm.

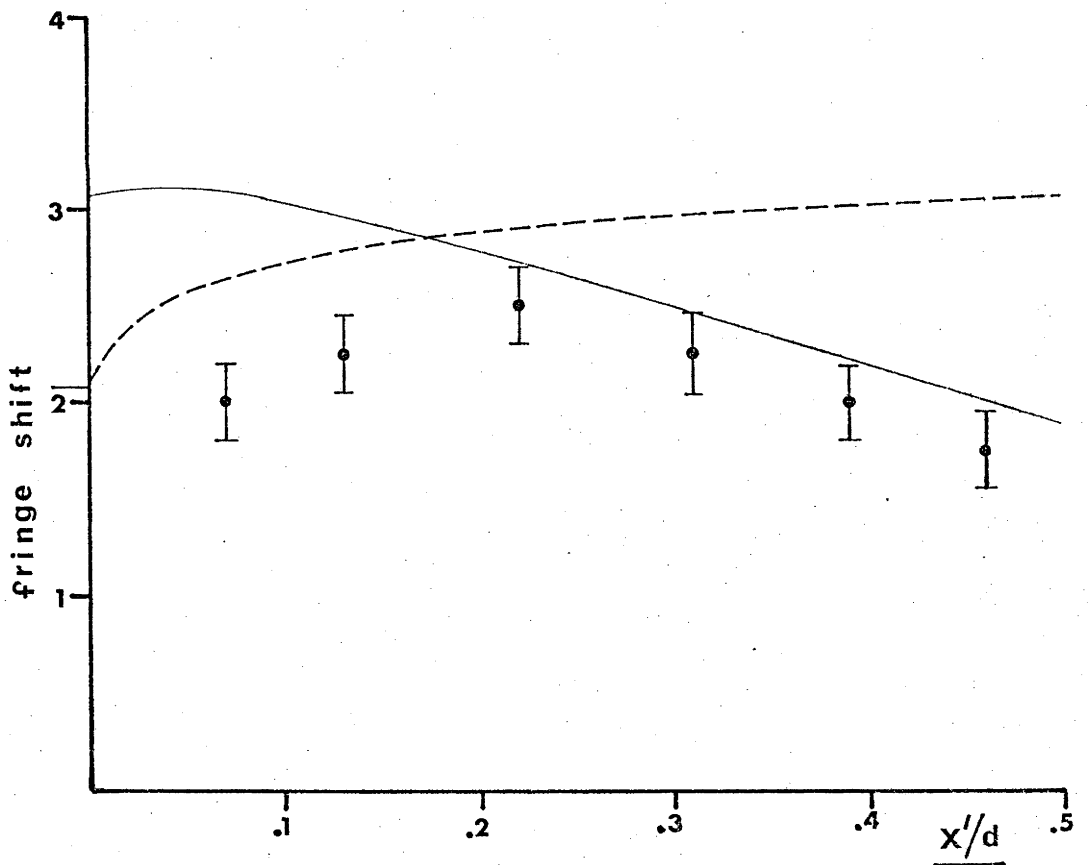
LEGEND TO FIGURE 15

showing the comparison of experimental fringe shift relative to the freestream, along a streamline, to the initial and final solutions of sections 2.2 and 2.4.

- Initial reacting solution using the reaction rates of Appleton *et al.*⁵.
- Final frozen reaction perfect gas solution using the computed pressure gradient.
- ⊙ Experimental point.

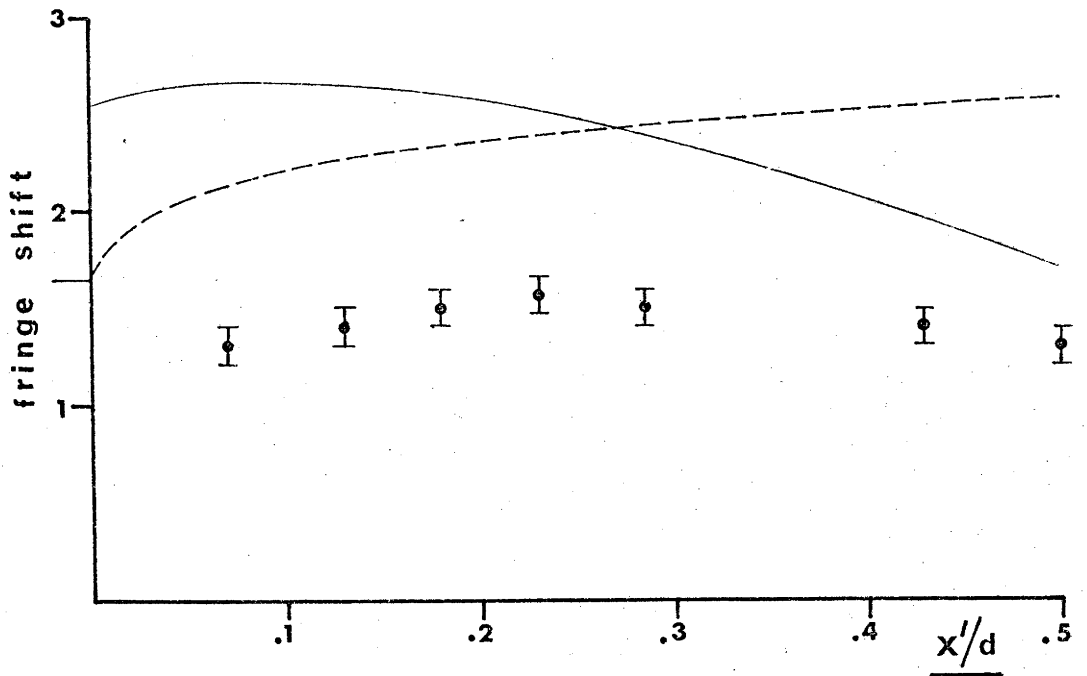


(a) $\psi/\psi_d = 0.05$, $p_R = 6$ in.Hg, $d = 1$ in., $a/\tau_0 = 7.4$.

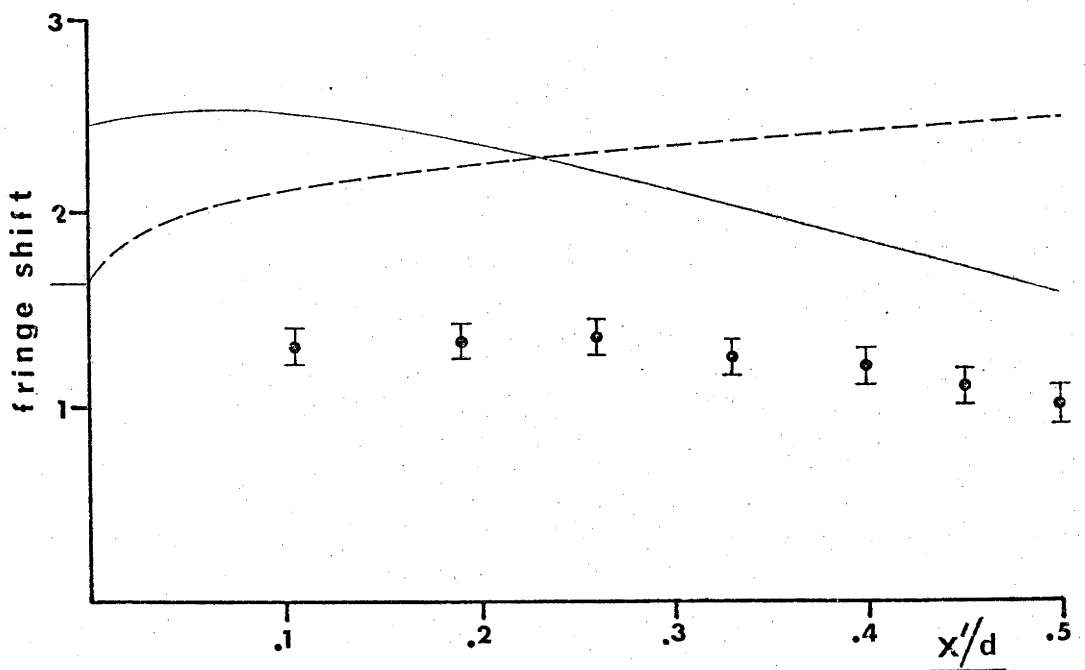


(b) $\psi/\psi_d = 0.15$, $p_R = 6$ in.Hg, $d = 1$ in., $a/\tau_0 = 7.4$.

FIGURE 15

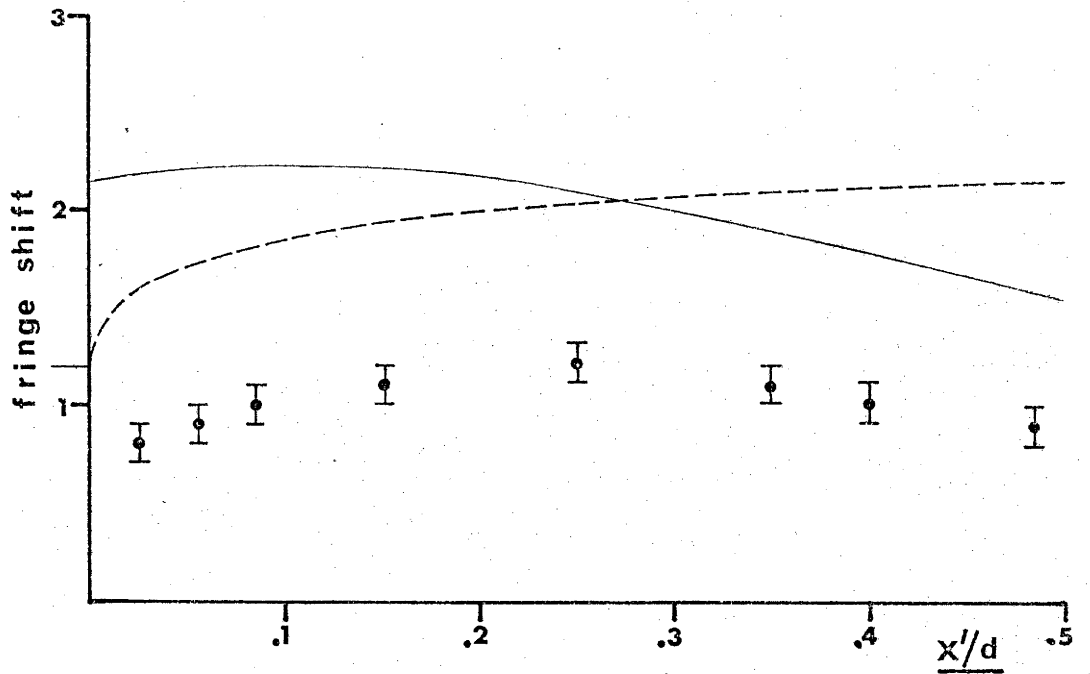


(e) $\psi/\psi_d = .05$, $p_R = 4$ in.Hg , $d = .5$ in. , $a/\tau_0 = 6.6$.

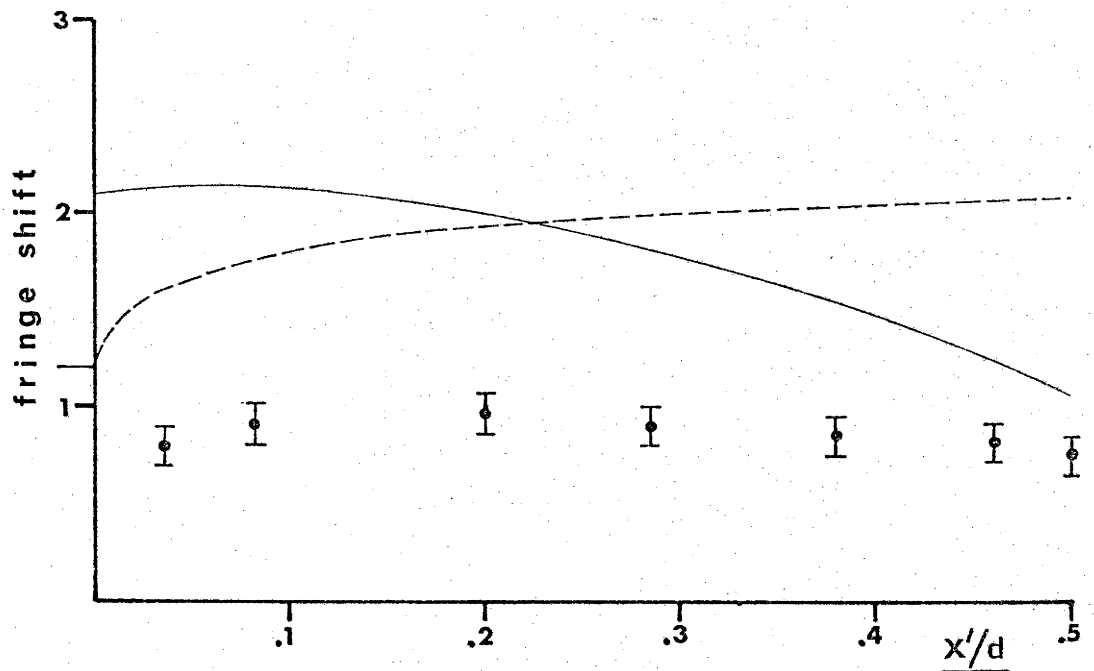


(f) $\psi/\psi_d = .15$, $p_R = 4$ in.Hg , $d = .5$ in. , $a/\tau_0 = 6.9$.

FIGURE 15 (cont)



(g) $\psi/\psi_d = .05$, $p_R = 2 \text{ in.Hg}$, $d = 1 \text{ in.}$, $a/T_0 = 5.5$,



(h) $\psi/\psi_d = .15$, $p_R = 2 \text{ in.Hg}$, $d = 1 \text{ in.}$, $a/T_0 = 5.6$,

FIGURE 15 (cont.)